Monitoring of Arduino-based PPG and GSR Signals through an Android Device

Abstract — the purpose of this project is to provide reliable heart rate readings and to monitor the influence of stress (as indicated by skin conductance) on the heart rate. The developed system monitors and processes Photoplethysmogram (PPG) and Galvanic Skin Response (GSR) signals. An Arduino microcontroller is paired with an Android device via a Bluetooth Low Energy (BLE) wireless connection, to monitor the signals received from the Arduino microcontroller. Such a system could be used in hospitals, for home-care, or by athletes, students, and people suffering from heart diseases. However, the primary audience is people who need a home-care system.

I. Problem Statement

Medical and engineering worlds are highly related nowadays. Most of the technologies used in hospitals are established by engineers. Developers have always been working to put Android and iOS devices into better use [1]. Health applications have become a stock feature in both Android and iOS devices, and some existing applications claim to measure heart rate [1]. Despite the large number of existing technologies and/or applications, estimating reliable heart rate readings has always been an issue in the medical world [2]. There are many technologies that have been developed to estimate heart rate, but they are rather expensive. Nonetheless, there are many factors that could affect someone's heart rate such as motion, emotions, and stress.

The problem at hand is to determine reliable heart rate readings and to monitor the influence of stress (as indicated by skin conductance) on the heart rate in an inexpensive manner. The aim of this project is to process Photoplethysmogram (PPG) and Galvanic Skin Response (GSR) signals, and then extract statistical parameters from the processed signals which can be analyzed to determine how changes in skin conductance would affect the heart rate of an individual. These goals will be achieved within a device for home-care systems that is low-cost and consumes low power (i.e. economical).

The developed system must provide reliable heart rate readings, as the accuracy of these readings is crucial to the life of patients. The developed system should also provide a reliable Bluetooth Low Energy (BLE) connection and reliable data collection. Such systems require relatively low power consumption; therefore, the components should minimize power consumption. Users would desire to see the status of their patient(s), detect any abnormal physiological conditions, and get alerted simultaneously. Thus, real-time monitoring of PPG and GSR readings is preferred. Portability is not always necessary in such a system. If the system is intended to monitor patients lying in bed, then there is no need to move any component of the system. However, if the system is intended for athletes to monitor themselves as they exercise, then there is a need to make all components of the system portable and movable. In terms of monitoring, any user should be able to realize and/or understand the displayed results of PPG and GSR. Thus, the application should provide a user-friendly Graphical User Interface (GUI).

II. PROPOSED Solution

The use of wearable sensors has made it possible to have the necessary treatment at home for patients suffering from heart attacks, sleep apnea, and Parkinson disease [3]. After an operation, patients usually go through a recovery or rehabilitation process where they must follow a strict routine [3]. All the physiological signals as well as physical activities of the patient could be monitored with the help of wearable sensors [3]. During the rehabilitation stage the wearable sensors may provide audio feedback, virtual reality images, or other rehabilitative services [3]. The system can be tuned to the requirements of an individual patient [3]. The whole activity can be monitored remotely by doctors, nurses, or caregivers [3]. Reliably detecting and alerting wearers and/or caregivers to abnormal physiological conditions with sufficiently high sensitivity will be critical in order to achieve a wider spread of adoption, and acceptance of semi-automated or closed-loop systems [2].

Recent studies have shown that changes in the levels of biological stress influence the heart rate [4]. In fact, the pumping process of the heart and in turn the blood flow throughout the body may be affected by changes in physiological stress [4]. One way to measure the heart rate of a person is through analyzing a PPG signal. PPG is a procedure that determines the change in blood volume pulse (usually in the soft tissues of the body) using the direct relationship between variations in volume and the absorption, reflection, and scattering of the light from a photo-emitter and then recorded by the photo-receptor [4]. The changes in the pulsatile flow of the arterial blood are then represented in a PPG waveform, which can then be used to extract useful information such as a person's heart rate. The modern way of estimating physiological stress is through the changes in skin conductance. GSR is a technique used to measure the changes in the

skin conductance, usually to indicate an estimate of the level of biological stress [5]. Both PPG and GSR sensors can be used to indicate how stress affects the heart rate by a simultaneous analysis of their corresponding waveforms.

With regards to our proposed solution, a PPG sensor and a GSR sensor are interfacing with a 3.3/5 volts Arduino microcontroller to acquire the required signals. The GSR sensor is used for detecting the stress level, while the PPG sensor is used for estimating the heart rate. An Android (4.3+) application is developed to monitor the PPG and the GSR signals. The Arduino microcontroller interacts with the Android device through a wireless serial BLE connection. Standard algorithms for deriving parameters from PPG and GSR signals are available [6], [7]. These algorithms are adapted to the acquired signals, and converted into the Android application. The derived parameters can be used to help in finding a correlation between PPG and GSR signals. Appendix A at the end of this report contains details about the used algorithms.

III. Impact

Every year, over 15 million people worldwide suffer from heart attacks, and nearly 6 million people die [8]. A heart attack can also lead to disabilities such as paralysis, and loss of speech. [8]. Globally, heart attacks are the second leading cause of death in people above the age of 60 years old, and the fifth leading cause of death in people aged 15 to 59 years old [8]. On the other hand, heart attacks are less common in people under 40 years old, although it does occur [8]. It would be very helpful if those people's heart rate could be monitored on a daily basis. If stress is left unmanaged, it can lead to emotional, psychological, physical problems, heart disease, high blood pressure, chest pains, or irregular heartbeats [9]. The general motivation of this project is to estimate heart rate variability in conjunction with stress levels as indicated by skin conductance. Nonetheless, most medical devices are very expensive and not affordable by a group of people in our community [10]. The developed system facilitates medical attention, care, and support to the vulnerable population of elderly and/or disabled people, monitors heart rate variability, and irregular heartbeats (i.e. Arrhythmia). The developed system helps in the early detection of heart diseases' symptoms, and post heart attack or stroke recovery.

IV. Project Development

The following is a list of the project's milestones:

- Requirements Elicitation and Analysis
  - Brainstorming
  - Researching and Reading
- System Design
  - Block Diagram
  - Circuit Diagram
  - UML Diagrams
- Implementation and Development:
  - Develop a working circuit using Arduino, a PPG sensor, a GSR sensor, and a BLE module
  - Create an Arduino sketch/code(s) to link with the Arduino board
  - Adapt the Arduino sketch/code(s) to identify the on board pins properly (wiring code in C)
  - Acquire PPG and GSR signals from the Arduino board
  - Write algorithms to process the acquired PPG and GSR signals (processing code in C)
  - Extract parameters from the PPG and GSR signals and analyse them to find any possible correlation between the acquired signals
  - Create an Arduino sketch/code to send the acquired signals via BLE
  - Establish a BLE connection between Arduino and an Android device (client-Server application in Java)
  - Develop an Android application to monitor the acquired signals and extracted parameters (GUI in XML, and functionality in Java)
  - Modify the application to invoke a notification for irregular heart rates
  - Add extra useful features to the application such as registering patient's profiles, and sharing information via SMS
- Testing and Verification of the system
  - Test the system on human subjects

The project is divided into two parts, the Arduino circuitry and the Android application. Hence, the system consists of two subsystems; the first subsystem is composed of an Arduino microcontroller and two sensors (i.e. PPG and GSR sensors), while the second subsystem is composed of an Android monitoring application. Generally speaking, all signal acquisition will be done within the Arduino microcontroller subsystem. Android (4.3+) is the platform used to develop the application, while the Android device is simply a receiver and a sender. It receives the PPG and GSR sensor readings along with the heart rate as it sends the start/stop command for the acquisition of each signal to the Arduino microcontroller. The Android application then plots the corresponding waveforms, and processes them to extract related parameters. The inter-communication between the Arduino microcontroller and the Android device is established through

a BLE connection. The two sensors are connected to a Grove shield that is mounted on top of an Arduino microcontroller. The GSR sensor that is used has Grove connectors, thus a Grove shield is needed for pairing it with the Arduino microcontroller. The Grove shield identifies the corresponding pins of the Arduino microcontroller, and allows the connection of additional sensors and/or other shields. Please refer to the figures in Appendix B to see a higher-level diagram, and a block diagram of the developed system.

The team was able to accomplish all of the proposed milestones. A working circuit consisting of an Arduino UNO microcontroller, a PPG sensor, a GSR sensor, and a BLE module was developed. The GUI of the Android application was developed, and the application's functionalities were implemented. Also, both PPG and GSR signals were successfully displayed on the developed application. Application users would now be able to register multiple patients' profiles, connect to the Arduino microcontroller, monitor the PPG and GSR signals, and share information with a selected emergency contact (preferably a doctor). Furthermore, the team performed an analysis on the acquired signals by extracting statistical parameters and conducting various experiments for the verification and validation of the product. Appendices C and D at the end of this report further contain details regarding the developed prototype and the Android application, respectively.

V. Conclusions

In conclusion, the purpose of this project was to monitor the influence of biological stress (as indicated by skin conductance) on the heart rate. Such a project would have a great impact on society as it could improve the quality of healthcare in the medical field. Nowadays, there are many devices/technologies which use wearable sensors to perform standard medical monitoring. However, most of the existing devices are worn as wristwatches, and one's wrist might not be the most accurate place to measure a PPG signal [11]. The combination of PPG and GSR sensors is relatively new. Such a combination has been used for commercial purposes in wristwatches for athletic activities, but not for health-care monitoring purposes. Any person would feel that stress affects their heart, and recent studies have actually shown that changes in the levels of biological stress influence the heart rate. Unfortunately, stress is not a quantifiable measure. So in order to determine any correlation between PPG and GSR a lot of research, testing, and analysis need to take place.

VI. References

[1] F. Wahab ,2014. *Are Heart Rate Monitoring Apps Really Accurate? We Put Them To The Test* [Online]. Available: http://www.addictivetips.com/ios/are-heart-rate-monitoring-apps-really-accurate-we-put-them-to-the-test/
[2] M. M. Rodgers, et al. (eds.), "Recent Advances in Wearable Sensors for Health Monitoring," in *IEEE Sensors Journal*, VOL. 15, NO. 6, June 2015.
[3] S. C. Mukhopadhyay, "Wearable Sensors for Human Activity Monitoring: A Review," in *IEEE Sensors Journal*, VOL. 15, NO. 3, March 2015.
[4] J. G. Webster and J. W. Clark, et al. (eds.), *Medical instrumentation: application and design*, 4th ed. Hoboken, NJ: John Wiley & Sons, 2010.
[5] M. V. Villarejo, et al. (eds.), "A Stress Sensor Based on Galvanic Skin Response (GSR) Controlled by ZigBee," in *Sensors Journal*, 2012, 6075-6101.
[6] Biopac, "Heart Rate Variability," in *Application Note 129* [Online]. Available: https://www.biopac.com/wp-content/uploads/app129.pdf.
[7] J. H.D.M. Westerink, et al. (eds.), "Computing Emotion Awareness through Galvanic Skin Response and Facial Electrography," in *Probing Experience*,149-162 [Online]. Available: http://eprints.eemcs.utwente.nl/20853/01/Westerink08-Computing_emotional_awareness.pdf.
[8] K. Skaarhoj, 2015. *Stroke - The global burden of stroke* [Online]. Available: http://www.world-heart-federation.org/cardiovascular-health/stroke/.
[9] M. C. Stöppler. *Heart Disease and Stress* [Online]. Available: http://www.medicinenet.com/stress_and_heart_disease/article.htm.
[10] J. Tozzi, 2014. *How Much Do Medical Devices Cost? Doctors Have No Idea* [Online]. Available: http://www.bloomberg.com/news/articles/2014-01-23/how-much-do-medical-devices-cost-doctors-have-no-idea.
[11] T. Tamura, et al. (eds.), "Wearable Photoplethysmographic Sensors—Past and Present," in *Electronics*, 2014, 3, 282-302; doi:10.3390/electronics3020282.
[12] "What is GSR (galvanic skin response) and how does it work?," in *Eye Tracking Software and Solutions - iMotions*, 2015. [Online]. Available: https://imotions.com/blog/gsr/.
[13] J. Bakker, et al. (eds.). *What's your current stress level? Detection of stress patterns from GSR sensor data* [Online]. Available: http://www.win.tue.nl/stressatwork/pdfs/stressdetection_hacdais11.pdf.
[14] B. Energy, "Bluetooth Low Energy | Android Developers," in *Developer.android.com*, 2016. [Online]. Available: http://developer.android.com/guide/topics/connectivity/bluetooth-le.html.
[15] *GraphicLoads. Heart beat 2 Icon* [Online]. Available: http://www.iconarchive.com/show/medical-health-icons-by-graphicloads/heart-beat-2-icon.html.
[16] *Heart Disease and Abnormal Heart Rhythm (Arrhythmia)* [Online]. Available: http://www.medicinenet.com/arrhythmia_irregular_heartbeat/article.htm.

APPENDIX A

To ensure synchronous transmission and minimize transmission delays, the rate at which the points were transmitted was made equal to the sampling rate of the analog data from the sensor. This was done using the same interrupt timer for both the sampling and transmission processes. The timer was set as such that it interrupted every 2ms (sampling period) to sample a PPG point and then send right away through the serial UART port to the application.

When dealing with the serial transmission of the points, each waveform point was sent followed by a heart rate value corresponding to an approximated number of points between the first and the second peak of the PPG signal (the distance between the peaks represents an inter-beat interval). An Arduino loop function was used to facilitate continuous transmission of data to the real-time monitoring system.

Moreover, to make the monitoring more informative and efficient, heart rate variability was also investigated using 5 common (HRV) parameters for normal R-R heartbeat (NN) intervals [6]. They are as follows:

- Mean of the NN intervals
- Standard deviation (SD) of the NN intervals
- The Coefficient of Variation (CV) of the NN intervals (the ratio of the standard deviation to the mean)

$$SDSD = \sqrt{\frac{\sum_{i=1}^{i=n-1}(D_i - D_{mean})^2}{n-1}}$$

Where:
i = interval index
n = number of total intervals
n- 1 = number of interval differences

- The Standard Deviation of Successive Differences (SDSD) of NN intervals [6]

$$RMSSD = \sqrt{\frac{\sum_{i=1}^{i=n-1} D_i^2}{n-1}}$$

Where i = interval index
n = number of total intervals
n - 1 = number of interval differences

- The Root Mean Square of Successive Differences (RMSSD) of NN intervals [6]

Unlike a PPG signal, a GSR signal is aperiodic and a number of factors can significantly affect the nature of the response, such as age, temperature, humidity, and health [12]. Figure 1 below defines a typical GSR response over time.

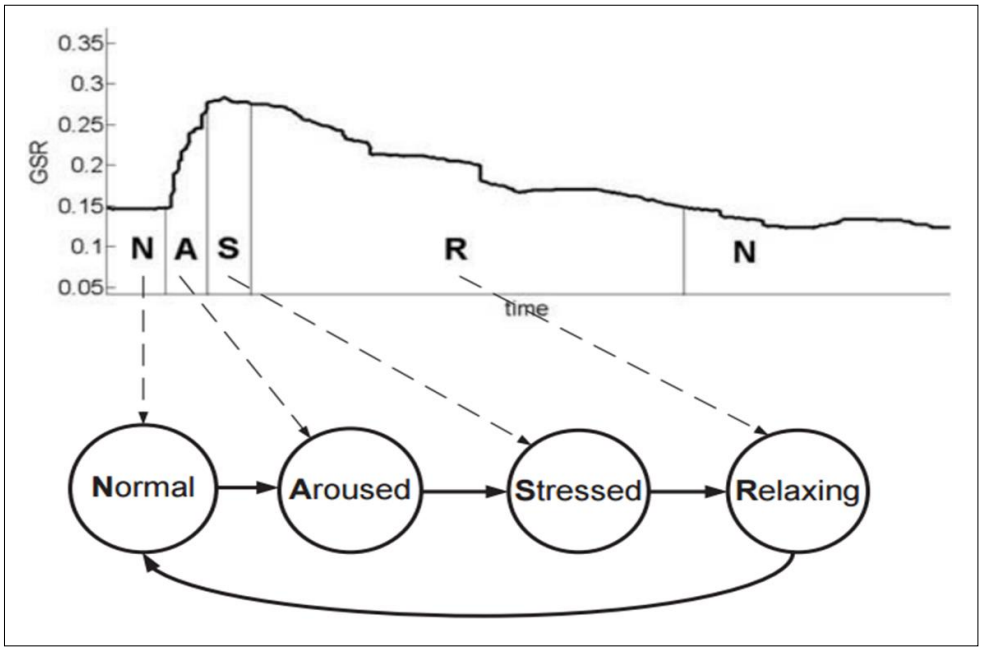

Figure 1: Typical GSR Signal [13]

For analysing the GSR signal, four parameters were used [7]:

- Mean
- Standard deviation
- Kurtosis
- Skewness

The mean of the signal represented its baseline. The standard deviation indicated changes in the signal relative to its baseline. Kurtosis, was used to measure the flatness of the signal relative to the normal distribution. Generally, a positive value for kurtosis indicates that the signal is Leptokurtic (more flat than the normal distribution) while a negative value means the signal is less flat than the normal distribution, or platykurtic. The implemented formula for Kurtosis is the following [7]:

$$Kurtosis(x_1 \ldots x_N) = \left\{ \frac{1}{N} \sum_{j=1}^{N} \left[\frac{x_j - \bar{x}}{\sigma} \right]^4 \right\} - 3,$$

Skewness was determined to indicate the symmetry of the GSR signal relative to its baseline. A positive skewness would indicate that the signal is skewed to the right while a negative skewness value would indicate that the signal is skewed to the left. The implemented formula for skewness is as follows [7]:

$$Skewness(x_1 \ldots x_N) = \frac{1}{N} \sum_{j=1}^{N} \left[\frac{x_j - \bar{x}}{\sigma} \right]^3$$

APPENDIX B

Figure 2 below shows a higher-level diagram of the system.

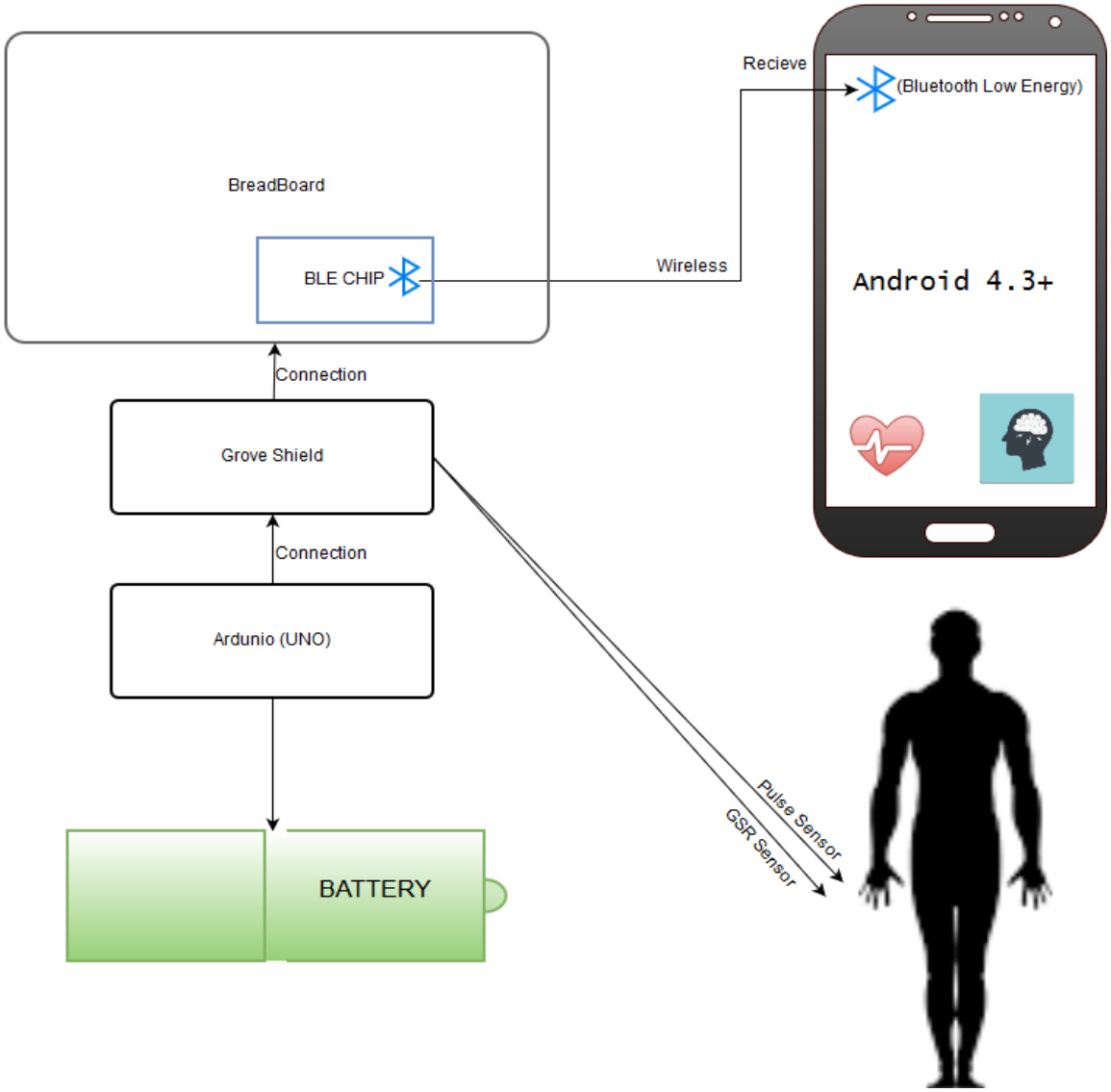

Figure 2: Higher-level Diagram of the System

Figure 3 below shows a block diagram of the system.

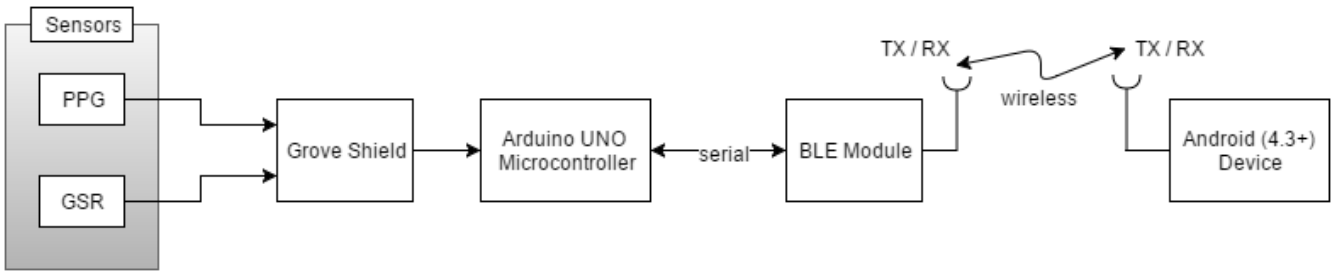

Figure 3: Block Diagram of the System

APPENDIX C

Figure 4 below shows a circuit diagram of the constructed circuit of the Arduino subsystem.

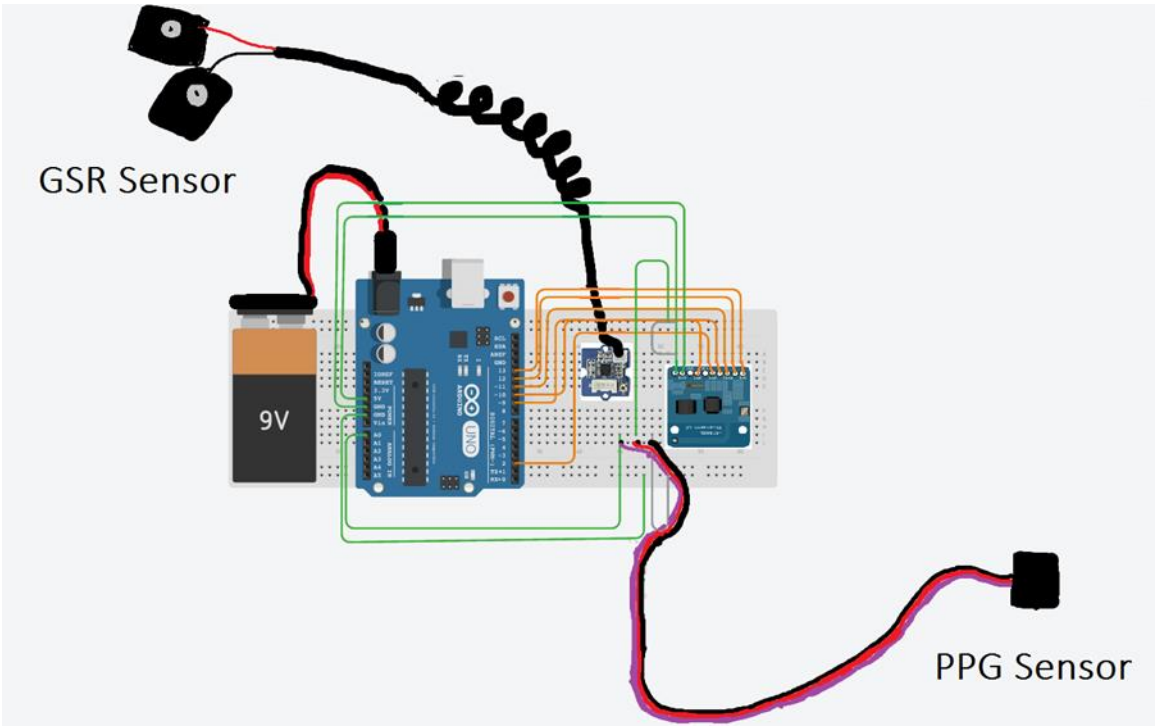

Figure 4: Circuit Diagram of the Arduino Subsystem

As shown in Figures 5-7, the developed circuit consists of two wearable biosensors, a BLE module, an Arduino UNO R3 microcontroller, a Basic Grove Shield, and a 9V battery. The first sensor is a PPG sensor (Pulse sensor AMPed), while the second sensor is a GSR sensor (Seeed Grove GSR sensor). Note that the Arduino microcontroller cannot be seen in some of the figures below as it is under the grove shield. The Basic Grove Shield has identical I/O pins as the Arduino UNO R3 microcontroller.

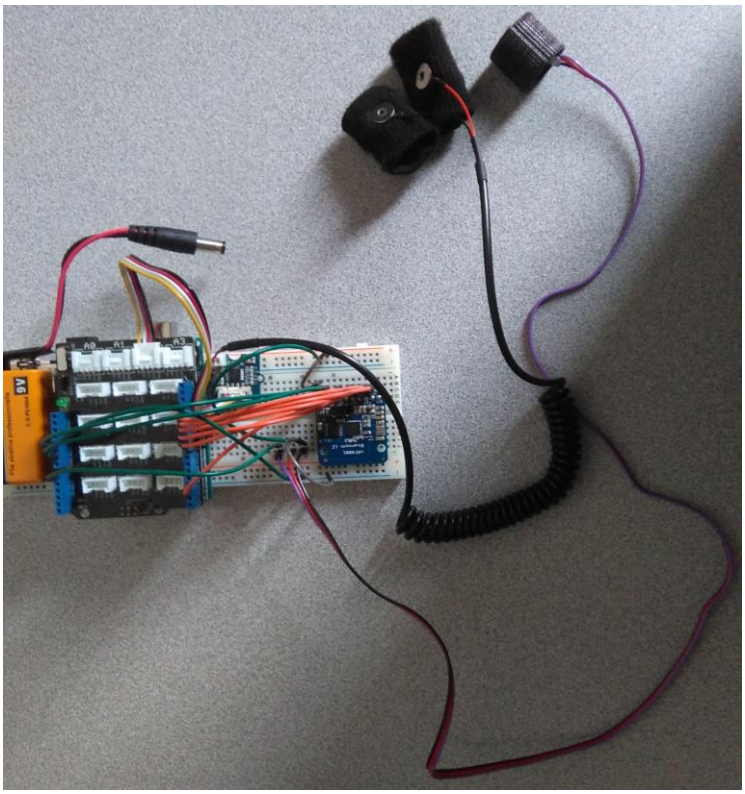

Figure 5: Arduino Circuitry – Battery OFF

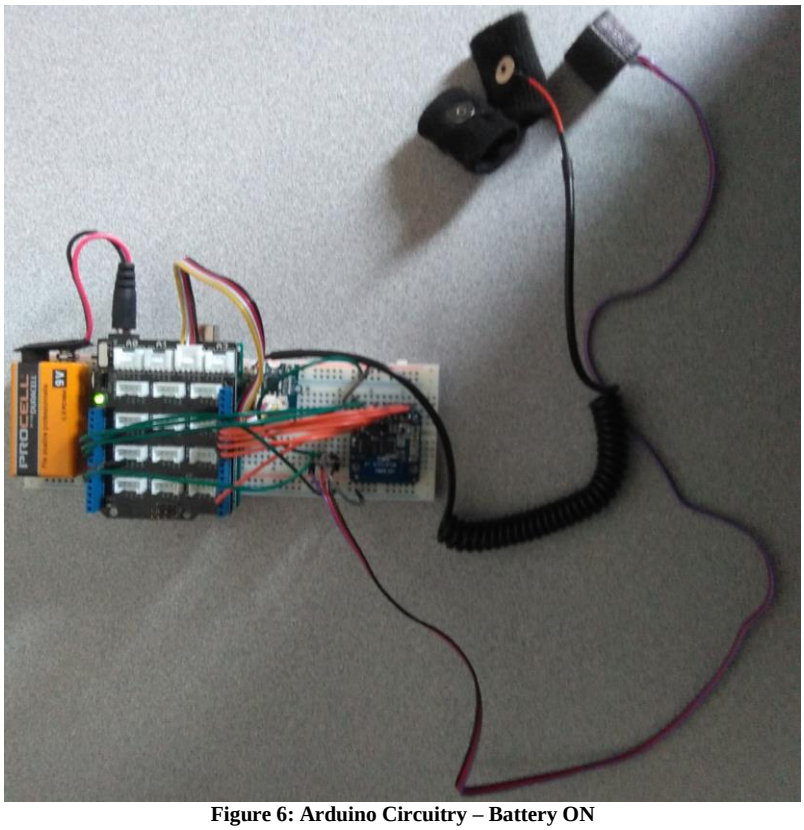

Figure 6: Arduino Circuitry – Battery ON

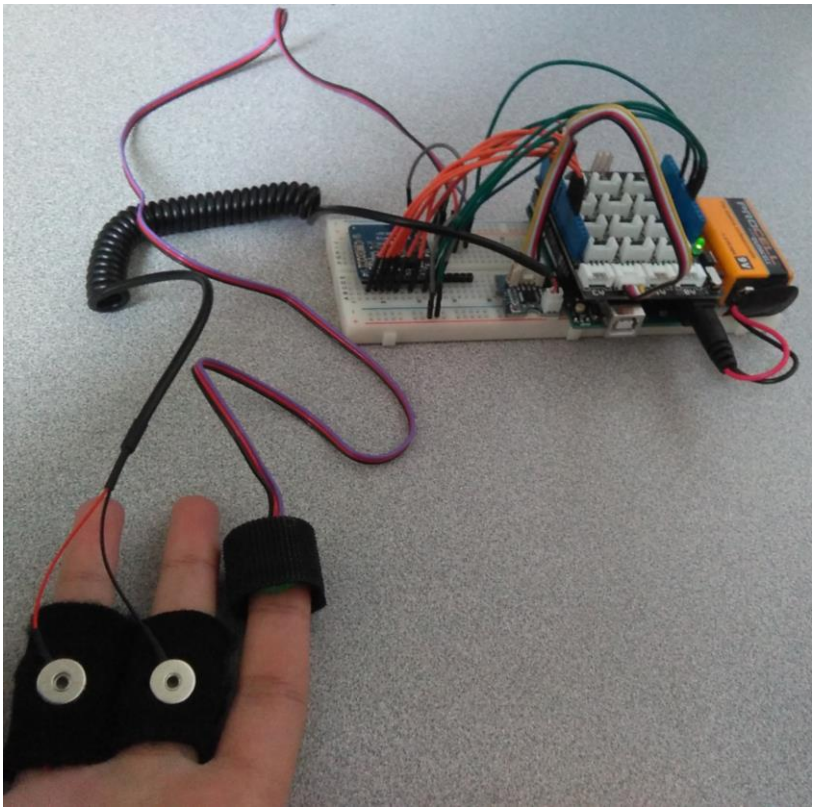

Figure 7: Arduino Circuitry – Monitoring

APPENDIX D

In general, Android devices are cheaper than iOS devices; so, Android is chosen as the platform for the developed application. In particular, Android (4.3+) is the platform used to develop the application. Android 4.3+ provides a wide range of Application Program Interfaces (APIs) that allow applications to discover devices, request services, and read/write characteristics [14]. They also have a built-in platform support for BLE [14]. With BLE, the Android device is capable of sending and receiving data up to 10 meters away from the Arduino microcontroller. Therefore, this allows Android applications to communicate with BLE devices that have low power requirements, such as heart rate monitors.

The developed application is named "AMIX", where the 'A' stands for Arduino/Android, 'M' stands for Monitoring, 'I' stands for Information, and 'X' stands for eXchange. To start, the name of the application consists of the first name initials of the group members. Secondly, it is descriptive of what the developed system actually does. The developed system is an Arduino/Android system that monitors the PPG and GSR information exchanged between the two, through a BLE wireless connection. Figure 8 below shows the icon of the application.

Figure 8: AMIX Logo [15]

The programming language for Android development is Java. Android Studio is the official IDE for the development of Android applications. In Android Studio, each page of the application is referred to as an Activity. Each Activity has an eXtensible Markup Language (XML) layout managing its GUI, and a Java class managing its functionalities.

When the user starts the application, he/she will be introduced with the 'Login' page. The 'Login' page allows users to either login, or register a new patient. Logging in requires a patient's profile to be read, while registration requires a profile to be written. When the user attempts to login to a patient's profile, the application will perform a lookup for such a file. If the patient has been previously registered, then the application will fetch the patient's information from his/her profile and the login process succeeds. Otherwise, the user will be asked to register the patient first. In order to register a patient, the user is required to fill a registration form about the patient. The registration form is set up by the 'Registration' page. The form asks the user for the patient's name, birth date, occupation, current address, medical condition and history, emergency contact, and other information. The other information field is optional for the user to include additional related information such as allergies. Figure 9 and 10 below show the 'Login' page and the 'Registration' page, respectively.

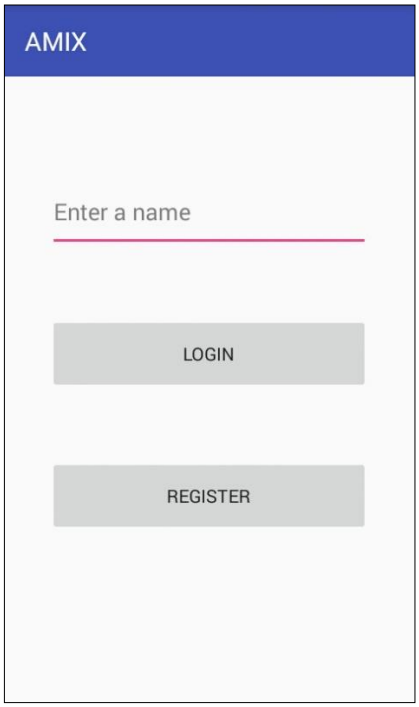

Figure 9: The 'Login' Page

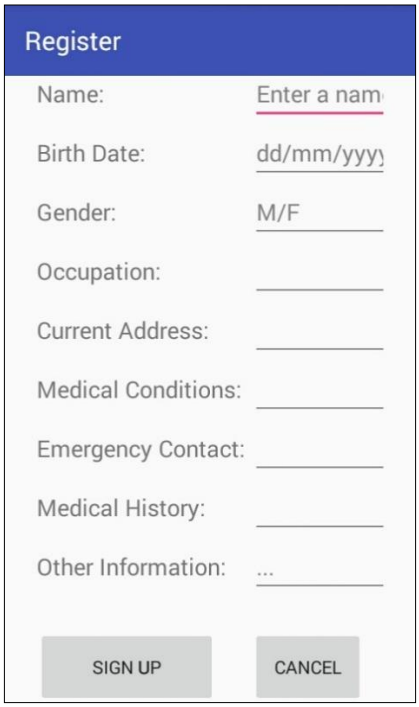

Figure 10: The 'Registration' Page

By registering patients, the application is capable of monitoring and keeping track of more than one patient as each patient has a separate profile. Android provides several options to save persistent application data. The selected option depends on specific needs such as data privacy, accessibility, and space requirements. For security reasons, the internal storage option is selected. The application saves patients' profiles directly on the internal storage of the Android device. Any files that are saved to the internal storage are private to the application; thus, other applications cannot access them nor can the user. Unless the user uninstalls the application, such files are permanent. If the user uninstalls the application, these files are removed.

Once logged in successfully, the user is directed to the 'Monitoring' page. First, the application requests to turn on Bluetooth. Figure 11 below shows the 'Monitoring' page upon start-up. If the user denies the request, the application does not allow the user to proceed further. Otherwise, the user can proceed normally. Figure 12 below shows the 'Monitoring' page when the user gets to proceed.

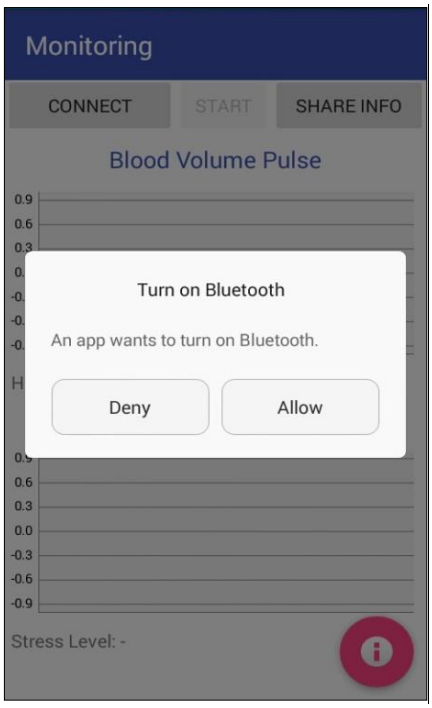

Figure 11: The 'Monitoring' Page (1)

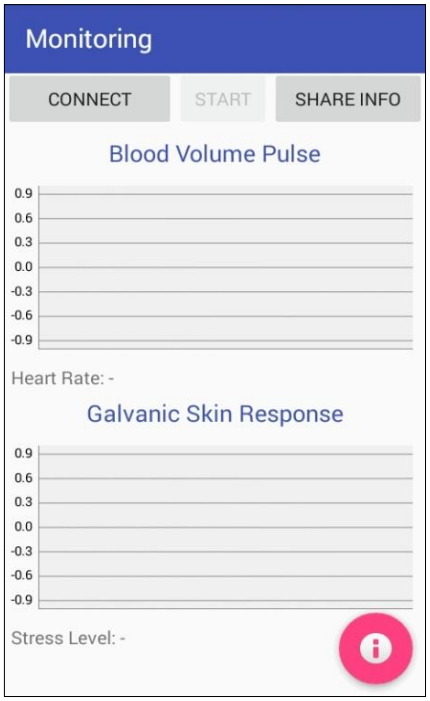

Figure 12: The 'Monitoring' Page (2)

As shown in Figure 12 above, the 'START' button is initially disabled because the user must connect to an available BLE device before starting the actual monitoring process. When the user presses on the 'CONNECT' button, the application will scan for available BLE devices in the area (for a period of 10 seconds). Figure 13 below shows the scanning dialogue. Once the user selects a device, the application initiates the connection. The application then allows the user to start the monitoring process, at any time, as long as the connection between the Arduino subsystem and the Android device is maintained.

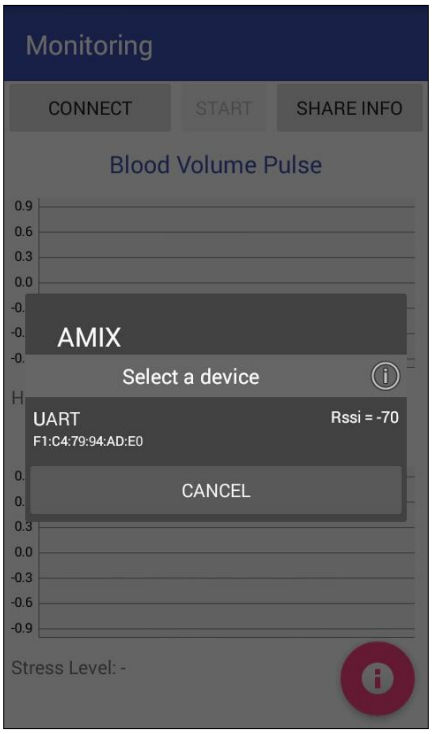

Figure 13: Scanning for BLE Devices

When the user starts the monitoring process by pressing the 'START' button, a "start" command will be sent to the Arduino subsystem to start sending data. The MPAndroidChart library provides functions that allowed the adjustment of the obtained PPG and GSR charts' features. Chart features involve scaling, zooming, selecting, and so on. The MPAndroidChart library is used for plotting the PPG and GSR signals from the received readings. The received readings consist of a PPG point, a GSR point, and the heart rate. Figure 14 below shows the 'Monitoring' page when the monitoring process has started. Note that the high heart rate is due to drinking coffee as the monitored subject drank coffee prior to the test.

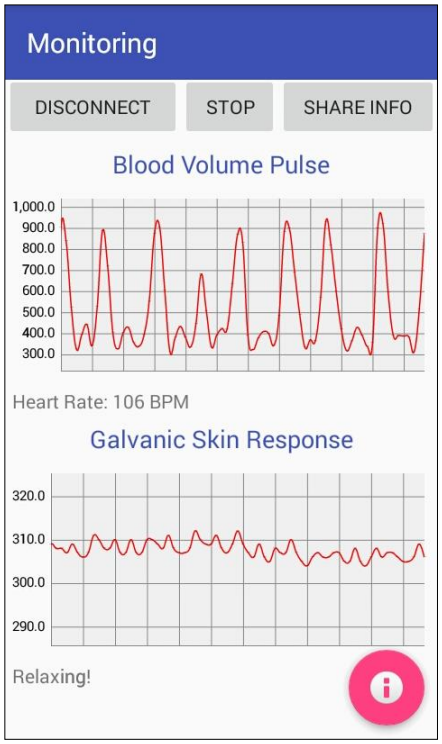

Figure 14: The 'Monitoring' Page (3)

The users can also view more information by pressing on the button at the bottom-right corner of the 'Monitoring' page. If the user presses on the button, the application will open a dialogue which includes 10 extracted parameters. The extracted parameters include the parameters discussed in Appendix A above. The application calculates the parameters using the readings received from the Arduino subsystem. Figure 15 below shows the extracted parameters dialogue.

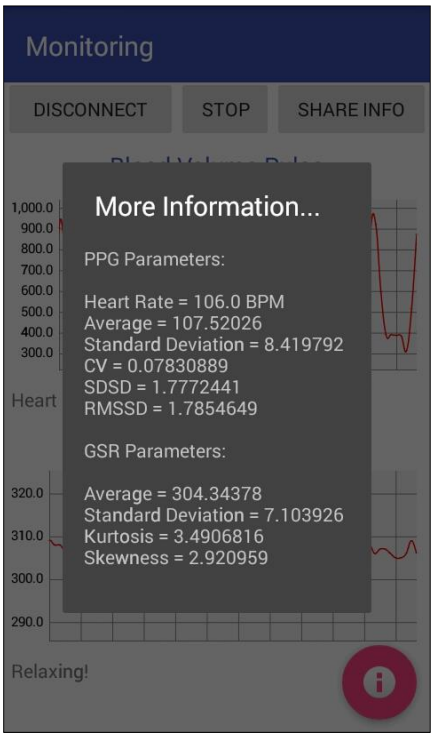

Figure 15: Extracted Parameters

A normal heart rate is 50 to 100 BPM; thus, anything lower than 50 BPM or higher than 100 BPM contributes irregular heartbeats (i.e. Arrhythmias) [16]. The application continuously checks the perceived heart rate for Arrhythmias. In case of an Arrhythmia, the application will dispatch a notification. If the heart rate goes back to normal within few seconds, the application would cancel the notification to avoid any false alarms. Figure 16 below shows a picture of the notification.

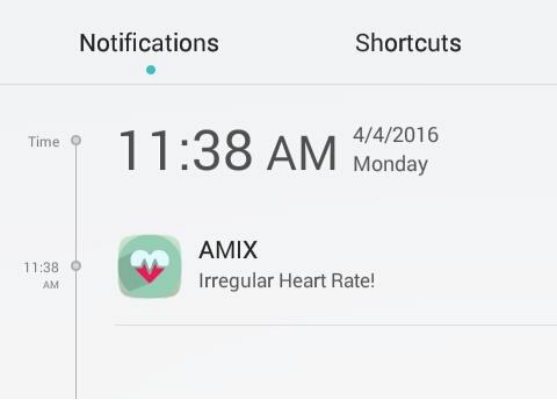

Figure 16: Irregular Heart Rate Notification via AMIX

When the user presses on the 'SHARE' button, the application directs the user to the 'Sharing' page. Through the 'Sharing' page, the user can send an SMS message to their emergency contact. For instance, this feature would provide the users with an easy way to contact their family doctor. A simple message contains the patient's personal information, extracted parameters, and a comment added by the user of the application. Figure 17 below shows the 'Sharing' page.

Figure 17: The 'Sharing' Page

CerebraLux

A Low Cost, Open Source, Wireless Device for Optogenetic Stimulation

Optogenetics is the utilization of specific wavelengths of light to activate neurons that are modified to express opsins. Wired systems severely restrict animal movement while wireless systems are expensive and inaccessible. In response, we have developed a low-cost, open source, wireless stimulator for mice behavioral models. With all of its components, the device weighs 2.8 grams and produces a range of light power from 0.1 to 1 mW. The efficacy of the stimulator was demonstrated by implanting into the right motor cortex of mice and inducing left turning behavior. The stimulator is designed to improve accessibility to optogenetics research.

I. PROBLEM STATEMENT

Optogenetics is a powerful new tool in the advancement of neuroscience research. It allows researchers to use light of specific wavelengths to selectively stimulate neurons that have been genetically modified to express opsins in their cell membranes. Opsins, the transducers at the heart of optogenetics, are a class of membrane ion channels that only open to allow ion flow when they receive light of a specific wavelength and of sufficient irradiance.[1] There are many subtypes that have been categorized based on function and the wavelength of light required for activation but the most commonly used class of opsin is Channelrhodopsin-2 (ChR2). ChR2 allows membrane conductance of cations like sodium, potassium, and calcium upon receiving light stimulation and in this way initiate action potentials.[2] The majority of Channelrhodopsins are stimulated with the application of blue light of wavelengths ranging from 465-473nm.[3] Because optogenetics utilizes light, it does not cause damage to neurons, as electrical stimulation does. Additionally, the genetic modification to introduce opsin expression can be cell-type specific if a site-specific recombination technology is incorporated. However, the field of optogenetics has yet to fully move beyond traditional wired systems that provided stimulation light in the early days of research. Wired systems consist of large external light sources connected via a long fiber optic cable to deliver light signals to the test animal's head, thus tethering it to the light source. This imposes severe restrictions on a test animal's movement, and therefore is not conducive to behavioral experiments. Wireless optogenetic stimulators are commercially available, but they are prohibitively expensive. One such system available is a head mounted, inductively powered wireless device for mice models offered by Cambridge Neurotech. It has a starting price of $9175 for the control unit and head mount, while each additional head mount costs $3000.[4] On the other hand, there are notable open-source designs that can be found in literature but require specialized manufacturing facilities. One such design is available from the Bruchas research group, which utilizes specialized Micro and Nano fabrication techniques and requires an average of 14 days to manufacture.[5] Another design by the Poon group utilizes radio-frequency (RF) power to wirelessly power and control a subcutaneously implanted light source, but requires manufacturing of a complex RF harvesting resonant cavity. Additionally, operation of the device is restricted to the 21 cm diameter of the RF chamber.[6] Therefore our device has to be small and wireless to remove restrictions on movement, easy to manufacture and assemble to reduce technical hurdles and finally cheap and open source to promote access to optogenetic research.

II. PROPOSED SOLUTION

To address these hurdles for cutting edge optogenetic neural research, we developed CerebraLux: a low cost, wireless optogenetic stimulator with accompanying signal transmitter. The device is designed to be simple to manufacture and assemble without the need for specialized facilities. CerebraLux is powered by a light rechargeable Lithium Polymer (LiPo) battery with sufficient capacity for full behavioral experiments. Most components of the device such as the fiber optic and electronic surface-mount devices (SMD) are cheap and commercially available, while custom parts like the printed circuit board (PCB) and the baseplate can be easily manufactured using consumer-grade machines or commissioned from widely available manufacturing services. Our baseplate was machined in-house in a consumer-grade table-top Othermill (Other Machine Company) out of white HDPE (High Density Polyethylene), while our PCB was manufactured by OSH Park. Both the stimulator and the signal transmitter can be constructed for a fraction of the cost of commercially available devices. In addition, CerebraLux is designed to be feasible for untrained research personnel to assemble and operate.

III. IMPACT

We built CerebraLux to solve the numerous drawbacks of current optogenetic stimulators. CerebraLux has the advantages of drastically decreased cost and effort to manufacture, while surpassing the function of the standard wired optogenetic stimulator. Any laboratories that are interested in optogenetic studies, regardless of their allotted budget are now able to overcome the hurdles to neural research using our wireless, open source, lightweight and inexpensive stimulator.

Manufacturing and assembly of CerebraLux requires a total of 3 hours once all the components are attained. Most of the components of our device are commercially available. We machined the baseplate in 1 hour using a low-cost, consumer-grade CNC mill. This drastically minimized the downtime in production. This is in stark contrast to the cellular-scale stimulator created by the Bruchas research group which requires specialized microfabrication facilities and a minimum production time of 2 weeks to complete.[4] This rapid turnaround time in manufacturing means that design iterations can be adjusted and tested immediately. Additionally, multiple devices can be assembled and implanted at the same time, thus increasing the number of optogenetic studies that a laboratory can conduct within a particular time frame.

The CerebraLux device is also designed so that researchers who do not have prior experience with electronics and manufacturing can easily assemble it. Step-by-step instructions detailing how to manufacture every component of the device will be posted on *openoptogenetics.org*, along with troubleshooting instructions. If users wish, they also may outsource the manufacture of certain components instead of constructing them. For example, the baseplate can be ordered from high-resolution 3D printing or laser sintering services like Protolabs.

CerebraLux alleviates the financial barriers to optogenetics technology with its open source design and low cost. Table 1 shows a price breakdown of all components used in our device, while Table 2 shows a cost analysis comparing our novel device with the current standards in the field of optogenetics. Our starting price of $108.10 comes out to be 84 times cheaper than our closest competitor Cambridge Neurotech's device [4], and 100 times cheaper than the RF resonant cavity proposed by the Poon group.[6] Furthermore, when comparing additional costs for our device (head stage and implant) with that of Cambridge Neurotech's, our device comes out to be about 31 times cheaper. Please note that this cost analysis does not include the cost of a CNC mill, as it is a standard machine in most universities and research campuses. However, even if the one-time investment of purchasing an Othermill at $2200 is included, our device is still much cheaper than competitors.

By lowering the financial barrier to this type of technology, researchers now have the capability to pinpoint and stimulate loci that are integral to behaviors of interest, such as actions induced by fear, anxiety, and addiction. Before, we have only been able to define regions containing multiple loci, but with the specificity afforded through optogenetics, the role of cell to cell interactions in behavior can be defined. With our device, laboratories can begin to conduct optogenetic studies on behaviors of interest with greater precision and for a much lower price than the current status quo allows.

Future directions for our device include reducing the fiber optic diameter, and introducing light focusing elements into the device. A smaller fiber optic diameter minimizes the area of stimulation in the brain, allowing for greater specificity in stimulation. Implementing lenses and condensers to focus light from the LED before transmission through the fiber optic would allow the device to be operated in experimental setups with varying light power needs.

Future iterations of our device will also aim to maximize efficiency of the optics assembly by manufacturing a baseplate with higher precision and tolerance to rectify any misalignment between the diode and fiber optic to further improve light power transmission, so that the LED can be driven at lower duty cycles to prolong battery life.

HDPE has been widely characterized to be biocompatible for in vivo applications and as such is an appropriate starting material for the baseplate.[7] Light leakage will be minimized by using black HDPE to absorb any light spill. Light leakage is a problem to be addressed as mice may react upon seeing light flashes and might confound results in studies of more complex behaviors.

IR communication was implemented in this preliminary system design. IR requires line-of-sight communication and is affected by ambient light sources, which may still place restrictions on the types of behavioral studies that can be done. The use of Bluetooth Low Energy 4.1 technology embedded in microcontrollers may provide a form of communication that can overcome these problems when moving forward.

Our baseplate design can also be altered to target different classes of opsins. By simply changing the location of the ferrule hole in the baseplate during milling, we can align the fiber optic with a different color diode on the LED. The LED used here has three color settings (red, green, blue) which can be programmed to allow for stimulation of a wider range of opsin subtypes.

IV. PROJECT DEVELOPMENT

Stimulator Light Output: ex vivo

We characterized the range of intensity output of our device when powered with the 20mAh battery. Based on the measurements shown in Figure 1, we observed a peak output of 1.29mW and minimum output of 0.08mW. With this information, one can extrapolate the pulse-width modulation setting required to deliver the power desired to stimulate the brain. However, it must be noted that our device utilizes direct butt-coupling between the diode and the waveguide,

with no optical focusing mechanism. Incorporating such focusing elements will improve the transmission efficiency, but also increase the weight and height profile of the device.

Battery Runtime

The stimulator runtime and light power output over time of our wireless stimulator are shown in Figure 2. In this trial, we measured the light power output of the on-board LED directly, with no fiber optic coupling. The 3.7V 20mAh battery supplied a total runtime of approximately 35 minutes. The device had a peak output of 8mW in the beginning, which eventually decayed to 5mW towards the end of the runtime.

IR Communication

Regarding the transmission of information, we successfully utilized infrared signaling as a medium of communication between the researcher and the stimulator. IR signaling is easy to implement using commercial off-the-shelf components such as IR LEDs and Arduino boards. Its ease of programmability was also demonstrated by sending signals with an Arduino Uno utilizing popular open source IR libraries. Transmission range was tested and found to be 1.8 meters from the transmitter LED which is less than the range of 4 meters for the Neurotech device [3] but was found to be sufficient for the behavioral studies of interest.

In vivo Testing

To demonstrate the effectiveness of our system in vivo, we implanted it into the motor cortex region of Ai32/CamKCre mice [8] as can be seen in Figure 3. The motor cortex was chosen as it provides a visually identifiable response in the form of the turning motion of the mouse. The whole system protrudes 25mm above the head of the mouse and allows unhindered free movement. The stimulator was designed to be used in mice, but is also compatible with other small animal models.

We were able to vary the light intensity provided by the device in vivo, thus demonstrating that our device can be fine-tuned to support a variety of experimental set ups. Our experiments in stimulating the motor cortex demonstrate a proof-of-concept that we are able to successfully target opsin-expressing cells in the brain with our low cost device. Table 3 shows a comparison of all relevant features with our closest competitors.

For the full realization of the open source concept, we will be uploading all of our materials, design specifications, Computer Aided Designs (CAD) and Computer Aided Manufacturing (CAM) files, PCB design, and programming protocols for the microcontroller (MCU), and infrared (IR) communication system to the optogenetics community wiki website *openoptogenetics.org*. We will also upload detailed instructions for device assembly and troubleshooting on this website. We hope that the neuroscience community will use the designs as they see fit, and continue to improve upon them to better suit their experiment needs.

V. CONCLUSIONS

Here we have presented a complete system design for optogenetic stimulation that has been validated in mice models. Our primary objective was to make our device cheap and completely open source. We have successfully kept the cost of manufacturing a fully functional and lightweight optogenetic stimulator under $200. We will also provide our designs and assembly instructions online for the neuroscience community to use and improve upon. Our optogenetic stimulator strikes a balance between cost, ease of manufacture, and functionality to improve accessibility to the optogenetics toolkit and advance neuroscience research. By ensuring an extremely low start-up cost and an easy-to-assemble design, we hope to lower the barrier of access to optogenetics technology.

References

1. Deisseroth, K. (2015) Historical Commentary Optogenetics : 10 years of microbial opsins in neuroscience, *18*(9), 1213–1225.
2. Nagel, G. "Channelrhodopsin-1: A Light-Gated Proton Channel In Green Algae". *Science* 296.5577 (2002): 2395-2398. Web. 20 Feb. 2016.
3. Lin, John Y. et al. "ReaChR: A Red-Shifted Variant of Channelrhodopsin Enables Deep Transcranial Optogenetic Excitation." *Nature Neuroscience* 16.10 (2013): 1499–1508. *PMC*. Web. 18 Feb. 2016.
4. Rossi, M. A., Go, V., Murphy, T., Fu, Q., Morizio, J., & Yin, H. H. (2015). A wirelessly controlled implantable LED system for deep brain optogenetic stimulation. *Frontiers in Integrative Neuroscience*, *9*, 8. http://doi.org/10.3389/fnint.2015.00008
5. Kim, T. -i., McCall, J. G., Jung, Y. H., Huang, X., Siuda, E. R., Bruchas, M. R. (2013). Injectable, Cellular-Scale Optoelectronics with Applications for Wireless Optogenetics. *Science*, *340*(6129), 211–216. http://doi.org/10.1126/science.1232437
6. Montgomery, KL, Yeh, AJ, Ho, JS, Tsao, V, Iyer, SM, Grosenick, L, Ferenczi, EA, Tanabe, Y, Deisseroth, K, Delp, SL, Poon, ASY. Wirelessly powered, fully internal optogenetics for brain, spinal and peripheral circuits in mice. Nature Methods. 12(10):969-974.
7. Wang G, Zhu S, Tan G, Zhou K, Huang S, Zhao Y, Li Z, Huang B.(2008). Study on biocompatibility of hydroxyapatite/high density polyethylene (HA/HDPE) nano-composites artificial ossicle. Sheng Wu Yi Xue Gong Cheng Xue Za Zhi. 25(3):607-10. http://www.ncbi.nlm.nih.gov/pubmed/18693441
8. Jackson Laboratories. Stock No 012569 Mouse Strain Datasheet. https://www.jax.org/strain/012569

APPENDIX

Component	Price
Fiber Optic + Fiber Optic Ferrule	$50.00
Magnets (8x)	$0.80
Baseplate + Baseplate Cover (machined)	$0.30
Stereotax Holder (3D printed)	$1.00
SMD LED	$2.50
Ultra-thin LiPo Battery	$8.50
Microcontroller	$4.00
Microcontroller Development Board	$5.00
Printed Circuit Board	$2.00
Arduino	$30.00
Resistor, Timing Crystal, Capacitor	$4.00
TOTAL:	$108.10

Table 1. Price breakdown of all components used in CerebraLux. Excluding the Arduino, the fiber optic and its ferrule holder, all other components are individually priced at under $10 each.

	Starting Price	Additional Costs
CerebraLux	$108.10 Aside from fiber optic and baseplate, all components reusable	$50.50 for each additional head stage (electronics) $52.50 for each additional implant (baseplate and fiber optic)
Cambridge Neurotech [3]	$9,175 Control unit, head stage, and implant.	$3,000 for each additional head stage $175 for each additional implant
RF Chamber [5]	$10,800 Signal Generator & power amplifier	--

Table 2. Cost analysis comparing CerebraLux with the field's current standards in optogenetic studies.

	CerebraLux	Cambridge Neurotech [3]	RF Chamber [5]
Size	0.95 cm3	1.19 cm3	10 - 25 mm3
Weight	2.8 g (Removable electronics = 2.5 g ; Permanently implanted optics = 0.3 g)	2.9 g	20 - 50 mg
Range	1.8 m	4 m	0.21 m (limited by RF chamber size)
Battery Time	35 min (rechargeable)	2 hr	None (RF scavenging)
Fabrication Time; Difficulty	< 2 hr; low difficulty	> 24 hr; medium difficulty (requires microscale surface mount soldering technique)	~ 11 - 14 days for fabrication; high difficulty (requires microscale surface mount soldering technique and machining of the resonant cavity)

Starting Price	$108.10	$9,175	$10,800

Table 3. Comparison of CerebraLux and its closest competitors. Note that only CerebraLux can be manufactured without specialized fabrication techniques. All parts of CerebraLux are available either off the shelf or easily reproducible using standard manufacturing tools accessible to most laboratories.

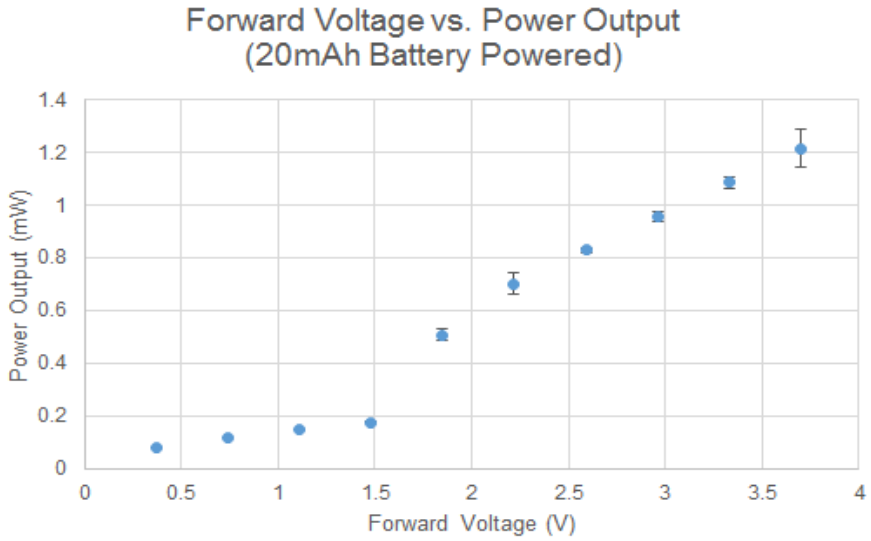

Figure 1. Effect of forward voltage from battery on resulting light output. Measurements taken at the tip of the fiber optic, from the LED when device is powered by a 20mAh battery. We observe a linear trend with a peak of 1.29mW at 100% full forward voltage, and a lower threshold of 0.08mW at 10% forward voltage. Error bars represent standard deviation.

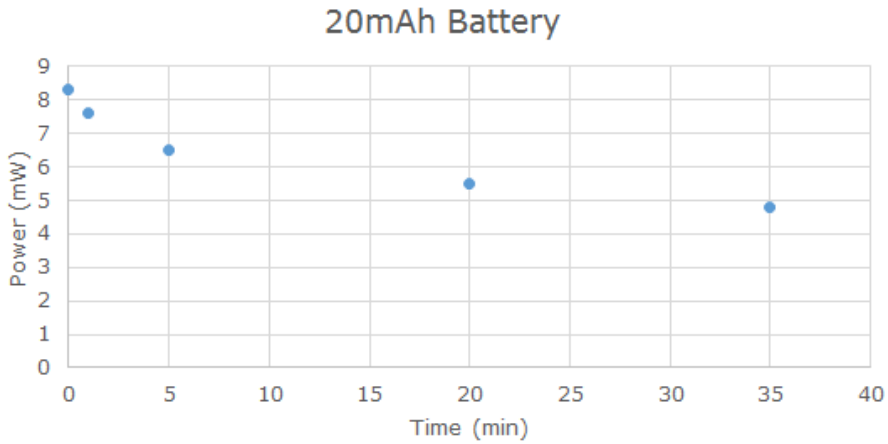

Figure 2. Effect of LED duty cycles on battery life and light intensity using a battery capacity of 20mAh. This figure shows the relationship between battery life and power intensity to provide insight on the best battery configuration and LED intensity based on the specifications of the experiment. Battery runtime lasted for about 30 minutes, while power output of the bare LED decreased to less than 5 mW in that time.

Figure 3. Implanted mouse model. We assembled and implanted our optogenetic device into the right motor cortex region of the brain

PRECIŚ VEINÉ

Non-invasive Low-Cost Vein Visualization Device

Abstract — Non-invasive detection of subcutaneous veins during intravenous (IV) procedure can be sometimes cumbersome, especially for pediatric and obese people. Vein detection using near-infrared (NIR) is amongst the latest techniques used to solve this issue. The technology being used here involves NIR rays to illuminate a vascular region, which is then observed using an infrared camera and the processed image is projected back onto the arm. The technology aims to improve the healthcare standards by reducing the stick count, which otherwise would result in rashes, nerve injury and bruises, while increasing the staff productivity and patient's satisfaction at the same time.

Keywords— Near-Infrared, Vascular Access Device, Venipuncture, Phlebotomy, Image Processing, Raspberry Pi

I. PROBLEM STATEMENT

Detection of veins in patients can be very difficult depending upon various factors, such as thin veins, fatty deposits, skin color or skin damage. In case of emergencies involving aforementioned patients, it sometimes becomes difficult to carry out an IV procedure in time, and the delay in treatment may become life-threatening. Procedures involving such cases call for a solution which can help the healthcare professionals in determining the exact location of a desired vein.

According to a locally conducted survey, it has been observed that at an average, two attempts are required for finding out a proper vein to carry out IV procedures. Multiple attempts or wrongly-administered injections might result in bruising, swelling of skin, nerve damage, and blood clotting.

To address this important issue, many strategies have been proposed. Some of these include i) Chemical paste on skin (It is not suitable for children, doesn't work on dark skin), (ii) Ultrasound (It needs expensive equipment and well trained staff), (iii) Secondary light sources (It requires dark room and may cause burns), (iv) Near Infrared Spectroscopy **[1]**.

Infrared imaging is one of the most promising areas in biomedical engineering which is least harmful to human tissues as compared to other wavelengths of electromagnetic spectrum and free from the above mentioned flaws. But the problem lies with their high cost. The currently available products are manufactured at quite a high cost of around $5000, and are generally not affordable by general practitioners who perform IV procedures regularly, especially in a developing country like Pakistan **[2]**. Few examples include (i) AccuVein **[3]** (It still demands a ribbon to be tied on arm), (ii) VeinViewer **[4]** (It's much bulky in size, so not easy to use and not portable), (iii) Vasculuminator **[5]** (Uses separate LCD to display veins instead of on the arm. This gives rise to potential chance of human error)

II. PROPOSED SOLUTION

Human eye is sensitive to the visible region of electromagnetic spectrum, which ranges from 390-700 nm. Other regions of electromagnetic spectrum are invisible to human eye and can be used for a variety of purposes. For example, X-Rays are being used in chest radiology but X-rays cannot be used in visualizing veins. However, near-infrared (NIR) spectroscopy has been found to solve the issue and can help in visualizing the veins.

The most important characteristics of infrared wavelengths exploited for the development of vein visualization device are:

- Infrared rays can penetrate into the human tissues up to a depth of about 5 mm before scattering and deviating from the initial direction [6].
- The deoxy-hemoglobin present in venous blood absorbs the infrared light and the surrounding tissues reflect back the light.
- The reflected light is captured using an infrared (night-vision) camera and processed in real-time.

Therefore, when the required area is illuminated with the help of near infrared rays, they are absorbed by the blood in the veins and the rest of the light is reflected back. The image (in the form of reflected light) being captured by the camera contains some dark areas as compared to other, which indicates the fact that the light has been absorbed by those areas. These dark areas are actually the veins.

However, studies reveal that different IR wavelengths result in different level of vein illumination. Blood

consists of two different types of hemoglobin: oxy-hemoglobin and deoxy-hemoglobin. The main optical coefficient involved in this process is Absorption coefficient (α_a), which determines how far light can travel before losing its intensity while still in its original path. Both type of hemoglobin (oxy-hemoglobin and deoxy-hemoglobin) have different absorption coefficient for different wavelengths as shown in Figure 1. Recent literature states that in infrared region, the highest absorption in venous blood is achieved at a wavelength of 750 nm, which is best described by the Figure 1[7]. Hence, it is intended to use 750nm wavelength for visualizing veins.

III. IMPACT

The purpose of development of the device is to help the healthcare professional in performing the IV tasks in a risk-free way. This will not only increase the patient satisfaction but will also result in increased staff productivity. This will also reduce the cost incurred during each procedure. The targeted beneficiaries of the device are emergency wards of hospitals, operation theatres, blood donation centers, clinics, and around-the-corner dispensaries. A locally conducted survey from hospitals stated that approximately 300 intravenous procedures are carried out, in hospital wards alone, on daily basis. Approximately 1.5 million units of blood is transfused annually in Pakistan and more than 50 blood samples are collected daily from around 4000 testing laboratories in Pakistan [8].This further boosts the demand for such a device not only locally but also in the international market.

The development of the device can further other areas of related research. Infrared rays being the core part of the device, various imaging systems [9] can be developed that use infrared rays. For example, infrared rays can also be used in fever screening, blood pressure monitoring, detection of gastrointestinal cancer, and various other areas. The main idea behind all these applications is the absorption and reflection of infrared rays, in and from desired body areas. The device is intended to be a low-cost device as compared to its competitors, whereby providing the same functionality. The final design is proposed to have much better results as compared to the present stage prototype.

IV. PROJECT DEVELOPMENT

Here, we propose an extremely low cost, novel solution to the issue of vein visualization. The project is being developed in multiple stages and a working prototype has been achieved to this point. The main components of the prototype are:

- Near Infrared source (850nm)
- Raspberry Pi 2 Model B
- Raspberry Pi NoIR Camera
- Pocket Projector

In principle, we shall use illumination from NIR LED sources to illuminate the body surface and take live video feed using Raspberry Pi NoIR Camera. It is a simple camera with its infrared filter removed, and hence allowing the infrared light to pass through its lens. Raspberry Pi then performs real-time image processing and pico projector projects it back onto the region of interest.

The camera captures the live video feed of the desired area, frame-by-frame, and each frame is processed to achieve the desired results. Since the image contains some dark regions along with lighter areas, the darker regions are needed to be enhanced to make them darker and lighten out the lighter region. Contrast Limited Adaptive Histogram Equalization (CLAHE) [10] is a technique which is employed to enhance the contrast of the image. Histogram of an image describes the number of pixels in terms of pixel intensities, where numbers of pixels are plotted along y-axis and pixel intensities along x-axis. Hence, the application of CLAHE computes the histogram of each frame and then stretches the histograms over whole range of pixel intensities, in real-time. The output frames have dark regions darker and the lighter areas lighter. This processed video is then sent to the pocket projector so that the live processed video can be viewed in real-time on the arm. This is achieved by calibrating the projector in line with the camera, so that the image is projected back to exactly the same area from where it is taken. This calibration of camera and projector is done by taking image of region of interest and then doing pixel-to-pixel mapping of the captured image and projected image. This means that the four corners of projected image are exactly the same as that of captured image. For example, if four corners of projected image are named as (a,b,c,d), then the camera will capture image from the very same region having corners as (a,b,c,d).

IR beam illumination pattern is dependent on the number and power of LEDs and their positioning. For proper image quality, proper illumination is necessary. Current prototype consists of five 1Watt IR LEDs in a circle, soldered on a printed circuit board [PCB]. Each individual LED has a half angle of approximately 125 degrees which does not result in best absorption in the blood, as most of the IR wavelength is scattered in the air. To make absorption better in the blood, a 60-degree focusing lens is used to direct the IR wavelength to the arm. A major

problem was that the NoIR camera didn't block visible light, so it also captured the projected image, hence giving picture in picture. To counter this issue, floppy disk paper was placed behind the camera lens in front of CCD. This acted as a visible light filter to get proper image on the skin.

Currently, we are able to detect the veins of almost every 6 out of 10 sample of population. The current success rate is low because infrared LED having a wavelength of 850 nm is being used which has less absorption in blood and less penetration into the skin as compared to 750 nm which provides the best results in the infrared region. We are using 850nm for now because 750nm was not available locally.

V. CONCLUSION

The resultant device is stand mounted as shown in the Figure 2. It is very light-weight and user friendly device with obvious mobility and flexibility in use. It does not require any extensive training to operate, and works in real time on all skin color tones. The results are shown in the Figure 3, which are currently the best possible results, keeping in view that the wavelength being used is 850 nm. It can identify veins in first attempt that were not easily visible to the naked eye and required two to three attempts.

The results of experiment on 25 individuals as of now have been summarized in the Figure 4, which describes the success rate of the device as tested on the male and female population.

There are certain limitations specific to the equipment and setups used. For example, body region of interest must be placed at a specific distance from the projector in order to get proper calibrated results.

The success rates are anticipated to improve by incorporating the 750 nm infrared wavelength. Furthermore, we can make it adjustable for body regions at any distance from the projector by incorporating appropriate control systems. This will ensure auto-adjustment of projector and auto-focus of the camera. However, it will require expensive and precise components, resulting in overall higher product cost.

VI. REFRENCES

[1] Juric, S., & Zalik, B. (2014). "An innovative approach to near-infrared spectroscopy using a standard mobile device and its clinical application in the real-time visualization of peripheral veins". BMC medical informatics and decision making, 14(1), 1.

[2] Nundy, Koushik Kumar, and Shourjya Sanyal. "A low cost vein detection system using integrable mobile camera devices." India Conference (INDICON). 2010.

[3] AccuVein Website. URL: http://www.accuvein.com/. [accessed 2016-03-07]

[4] VeinViewer Vision Website. https://www.christiemed.com/. [accessed 2016-03-07]

[5] Cuper, N. J., de Graaff, J. C., Kalkman, C. J., & Verdaasdonk, R. M. (2010, February). "The VascuLuminator: effectiveness of a near-infrared vessel imaging system as a support in arterial puncture in children". In BiOS (pp. 75550U-75550U). International Society for Optics and Photonics.

[6] F. B. Chiao; F. Resta-Flarer; J. Lesser, J. Ng; A. Ganz; D. Pino-Luey; H. Bennett; C. Perkins Jr; B. Witek, "Vein visualization: patient characteristic factors and efficacy of a new infrared vein finder technology," *British Journal of Anaesthesia*, vol. 110, no. 6, pp. 966-971, 2013.

[7] Susan Wray; Mark Cope; David T. Delpy; John S. Wyatt; E. Osmund R. Reynolds, "Characterization of the near infrared absorption spectra of cytochrome aa_3 and haemoglobin for the non-invasive monitoring of cerebral oxygenation," *Biochimica et Biophysica Acta (BBA) – Bioenergetics*, vol. 933, no. 1, pp. 184-192, 1988.

[8] Pakistan Medical & Dental Council website. URL: http://www.pmdc.org.pk/Home/tabid/36/Default.aspx/ [accessed 2016-03-07]

[9] Lahiri, B. B., Bagavathiappan, S., Jayakumar, T., & Philip, J. (2012). "Medical applications of infrared thermography: a review. Infrared Physics & Technology", 55(4), 221-235.

[10] Djerouni, A., Hamada, H., Loukil, A., & Berrached, N. (2014). "Dorsal Hand Vein Image Contrast Enhancement Techniques".

APPENDIX

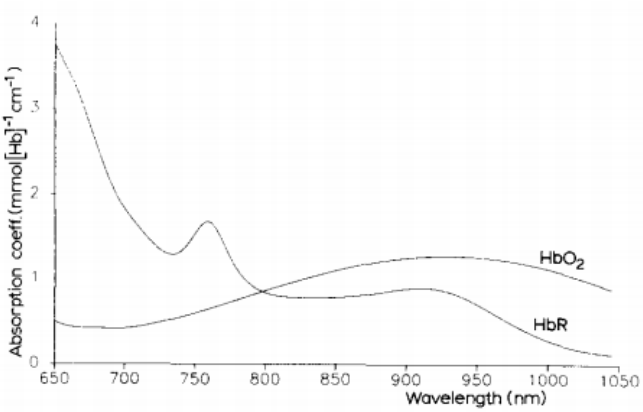

Figure 1. Absorption Coefficients of Oxy-Hemoglobin (HbO_2) and Deoxy-Hemoglobin (Hb)

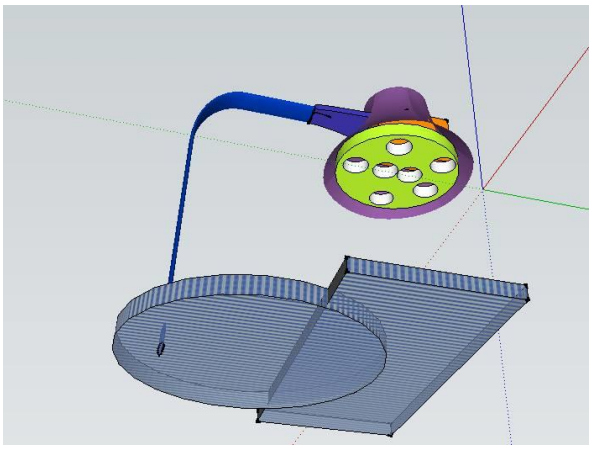

Figure 2. Concept of the Prototype

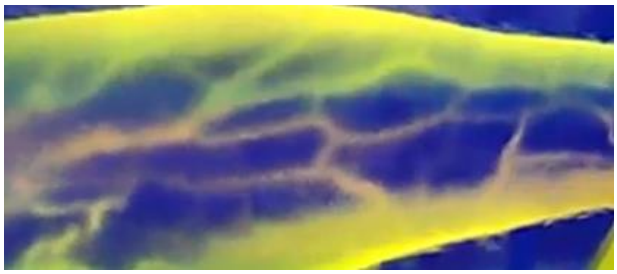

Figure 3. Working Prototype Results

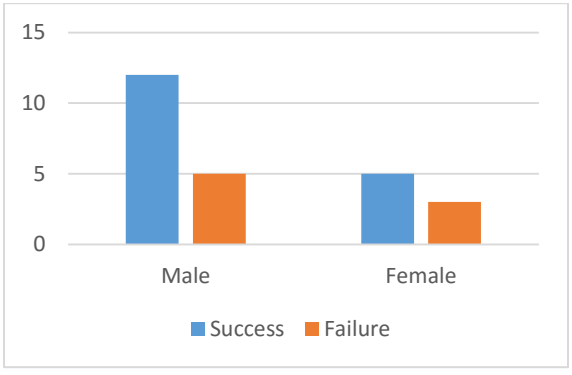

Figure 4. Device success rate with reference to population sample

IEEE Engineering in Medicine and Biology Society (**EMBS**) International Student Conference (**ISC**) 2016
Design Competition

Accessible Elevators

Making Elevators Accessible to Disabled Individuals

Electrical Engineering/Computer Engineering

Abstract – We have developed a design solution to allow disabled individuals to use elevators independently. Currently, many facilities like care homes and hospitals are multi-storied facilities that require residents to use elevators to travel to different floors. Disabled residents, like quadriplegics, are unable to interact with elevators, meaning that they must find someone else to push the elevator buttons for them. Currently, we have a Proof of Concept system showing the feasibility of using two Raspberry Pi computers with an infrared light emitting/detecting system to operate an elevator without manually pressing the elevator buttons, thereby providing enhanced independence.

I. PROBLEM STATEMENT

The following was determined as a problem statement:

> *Individuals with physical disabilities that prevent them from independently operating elevators need an on-demand, easy-to-use, safe, and inexpensive method to assist with elevator operation.*

This problem was discovered after speaking with an Occupational Therapist (OT) at a local prestigious care facility. She indicated that, of the facility's 265 residents, approximately 15 are completely unable to independently use the elevator. In addition, approximately 100 residents have difficulty using the elevator. Many of these residents are dependent on the elevator system to access services that the facility provides, like paying bills, using computer terminals, and participating in recreational activities.

When speaking with one resident he told of us a situation where he was on the first floor late at night and wanted to return to his room on the third floor. He ended up having to wait over and hour until someone could come operate the elevator for him. Currently, any disabled residents at the home must wait until an able-bodied person passing by can press the elevator buttons for them. In extreme cases, the resident enters the elevator and accidentally exits on the wrong floor, leading to confusion and frustration. Situations similar to this happen regularly at many facilities across the country and currently there is no solution known to aid them, other than waiting for other residents, visitors, or employees to press the buttons for them.

In terms of design requirements, we decided that a successful solution must satisfy three functions.

- The solution must identify the intent of the user to use the elevator.
- The solution must identify what floor the user would like to go to.
- The solution must relay the intent and floor selection of the user to the elevator control panel.

When designing a solution we adhered to 7 constraints that were identified in the design process. The requirements were:

- Cost – The solution must not cost more than $2,500 to the customer. This was chosen to ensure that the solution was accessible to as many facilities and users as possible and was based on a researched cost of approximately $25,000 to purchase an elevator (not including install and building material price).
- Safety – The solution must not interfere with or impair the safe use of the elevator, nor void any warranty or insurance associated with it. This was chosen to ensure that the high quality of safety associated with elevators was not infringed on.
- Independent operation – The solution must allow physically disabled individuals independent use of the elevator without external help. The focus of this design is to enable disabled individuals to have independent operation of elevators, and this function was therefore a requirement of the design.
- Current Functionality – Any added functions should not modify or eliminate current methods of interacting with an elevator for able-bodied people. We did not want to force able-bodied elevator users to relearn how to use elevators, or be confused when presented with an elevator equipped with the solution. Therefore, any design that forced a user to interact with the elevator in a new way was disqualified from consideration.
- Wait-time – The wait time must be no longer than 30 seconds to make a floor selection.
- Physical layout – The solution must not change the physical footprint of the elevator, or impede access to and from the elevator.
- Specific Floor – The solution must allow the user to select specific floors. Meaning the system cannot simply visit every floor one by one.

The design was then ranked by comparing its performance against ten objectives:

- Wait-time: The shorter the wait-time at the elevator, the better. If the wait-time is too long, the solution won't overcome the current inconvenience of operating an elevator.
- Cost: The less expensive the solution, the better. Low cost allows access of our product to a greater number of people.
- Adaptability: The more adaptable the solution is to people with varying physical limitations, the better. A solution that works for the majority of people that cannot operate elevators allows our solution to have the greatest effect.

- Training Time: The less training time required to use the solution, the better. We determined that teaching OTs to train the residents would be better than attempting to teach residents directly. To this end, we ranked this objective on how long it would take us to teach an OT.
- Daily Setup Time: If the solution requires too much setup the user will not use it and the problem will continue to go unsolved.
- Failure Rate: The less often the solution makes a wrong or unintentional selection, the better.
- Interference: The lower the chance of the solution interfering with day to day activities of the users and bystanders, the better.
- Durability: The longer the solution lasts without needing maintenance, the better.
- Ease of Installation: The easier the system is to implement in each situation the better.
- Design Risk: The more likely that our solution can be fully implemented, the better.

II. PROPOSED SOLUTION

We designed a system that solves the identified problem using two Raspberry PI computers, several Bluetooth relays, and an infrared (IR) sensing/emitting system. One common occurrence noted in the established user community is that they are able to move from one point to another on a single floor. We utilized this as an advantage, by designing the system to use a position-based sensing mechanism. In this way, users do not have to learn any complicated digital system, nor do they have to learn any new actions.

As noted, the system uses a position-based sensing mechanism. A number of zones, equal to one less than the number of floors in the facility, are identified on the floor in front of the elevator. For example, a four-story building would have three zones on the floor, corresponding with each floor other than the currently examined floor. These zones could be identified by modification of the floor tiles to display a floor number surrounded by an outline. The IR emitters are then placed above the zones, fixed to the ceiling. The Bluetooth relays would then be placed inside the elevator control panels, as indicated in Figure 1. One Raspberry Pi would be placed somewhere near the elevator, likely in a designated section of the wall. The user would then have one of the infrared sensor with a Bluetooth module on their person, likely on their shoulder or mobility device. A drawing of the system can be seen in Figure 2.

The Raspberry Pi in control of the system, labelled the “server” Pi, constantly rotates through the active IR emitters, keeping track of which emitter is currently active. At the same time, it is also listening on a Bluetooth socket for incoming transmissions. When it detects a transmission, it makes a floor selection based on the currently active IR emitter. This is done through the Bluetooth relay placed in the elevator. The sensor placed on the user is quite simple i.e. a simple IR diode with a Bluetooth module. When an incoming IR light is detected, it simply transmits a message to the server.

It should be noted here that due to time constraints with our GE 498 design class, there was insufficient time to gain permissions to test the system using the internal Bluetooth relay. Instead, as part of our proof of concept model, a module was designed to fit over the existing elevator buttons that included a motor drive circuit and motors to press the button. This module also still allowed able-bodied users to interact with the elevator, keeping the design within the current functionality constraint.

This method is clearly superior to the existing solution, as the users of the elevator no longer have to wait for others to use the elevators. Given the fact that users could wait hours for help, the solution is greatly beneficial. The disabled individuals increase their independence and gain unimpeded access to the equipped facility, while other residents are not impeded in any way.

III. IMPACT

Independence is something that many of us take for granted, whether it is walking to the grocery store or up a flight of stairs to get to class every day. For people with physical disabilities, these seemingly simple tasks can prove quite challenging. In recent years, there has been a big push in society to make buildings more accessible, from doors being outfitted with automatic door openers to ramps being built into buildings. One aspect of life that has not seen this accessibility push is elevators. Moving from one floor to another within a building can still prove challenging, if not impossible, for people that lack the ability to easily press the buttons on an elevator. This feeling of restriction and lack of control over one’s movements is a major problem not just at the local care facility, but at hospitals, care homes, and other buildings around the world.

The primary impact of the design is to the user and the independence gained. However, facilities like care homes and hospitals also benefit from the development of this technology as they become more accessible. Facilities equipped with this technology would be significantly more attractive to residents and visitors, increasing the client base for the facility, and increasing incoming traffic. In addition, elevator manufacturers have access to an entirely new market that was previously unavailable. Having access to this market means becoming a more attractive, positive company as the public would view them as forward thinking and having the best interests of their users in mind.

This device would benefit other areas where disabled individuals are unable to access facilities or make selections. The system can also be expanded to hold records of users, allowing the possibility of user-based floor permissions, customized interaction times for slower or faster users, and even tracking user travel patterns. One area for further work that we look forward to pursuing is verification that a user successfully arrived on the intended floor. If, for example, a resident using our system was to become stuck in the elevator, the system could notify an OT or nurse at the facility. Economically, the system would have little negative impact to the care facility as it is relatively inexpensive. In addition, the devices the users would wear would cost, at most, $20.

IV. PROJECT DEVELOPMENT

The solution is currently in the proof of concept phase. The system currently performs key functions and can be demonstrated outside of the elevator. Our internal button selection circuit has not been implemented due to the time constraints mentioned earlier. The next step is to optimize our design. We are looking to miniaturize our sensor as well as make it battery powered. Also, we will be working to implement our wireless button selector inside a functioning elevator. We will also be working to make the IR lights have a much longer range and more even distribution.

Due to the complicated nature of implementation, most testing was only able to be completed once all components arrived and the proof of concept was built. The coding was relatively simple, meaning that development of the software only took a few days. One advantage of the code development on the Raspberry PI is its modularity. Any tests that showed that the system was too slow was easily countered by adjusting the run time of the code. In a similar manner, any code section that seemed too fast was easily remedied. In terms of hardware, it was difficult to attain the correct range for IR transmission. Using the most luminescent LEDs available to us, the maximum range attained was approximately 30 cm. Given that the system is going to be placed on the ceiling, this was insufficient. The system was then redesigned to extend the range using higher current values, with shorter activation times. This extended the range to approximately six to eight feet, which allowed for correct operation of the system.

V. CONCLUSIONS

We have identified a real problem that affects many people across the country. Being unable to interact with elevators, especially at facilities like hospitals and care homes, robs residents and visitors of their independence. The use of this solution can give a portion of that independence back to its users. The system has clearly shown that it not only allows disabled individuals to use elevators, but it also retains the original method of interaction for able-bodied individuals. Adoption of this system can make facilities more accessible and attractive for residents and patrons, as well as introducing a new market area for elevator manufacturers. Given the innovative approach to a neglected problem of importance, as well as the inexpensive nature of the solution, and the large benefits provided to the users, Vertical Connection feels that they have a design worthy of further development and recognition.

APPENDIX

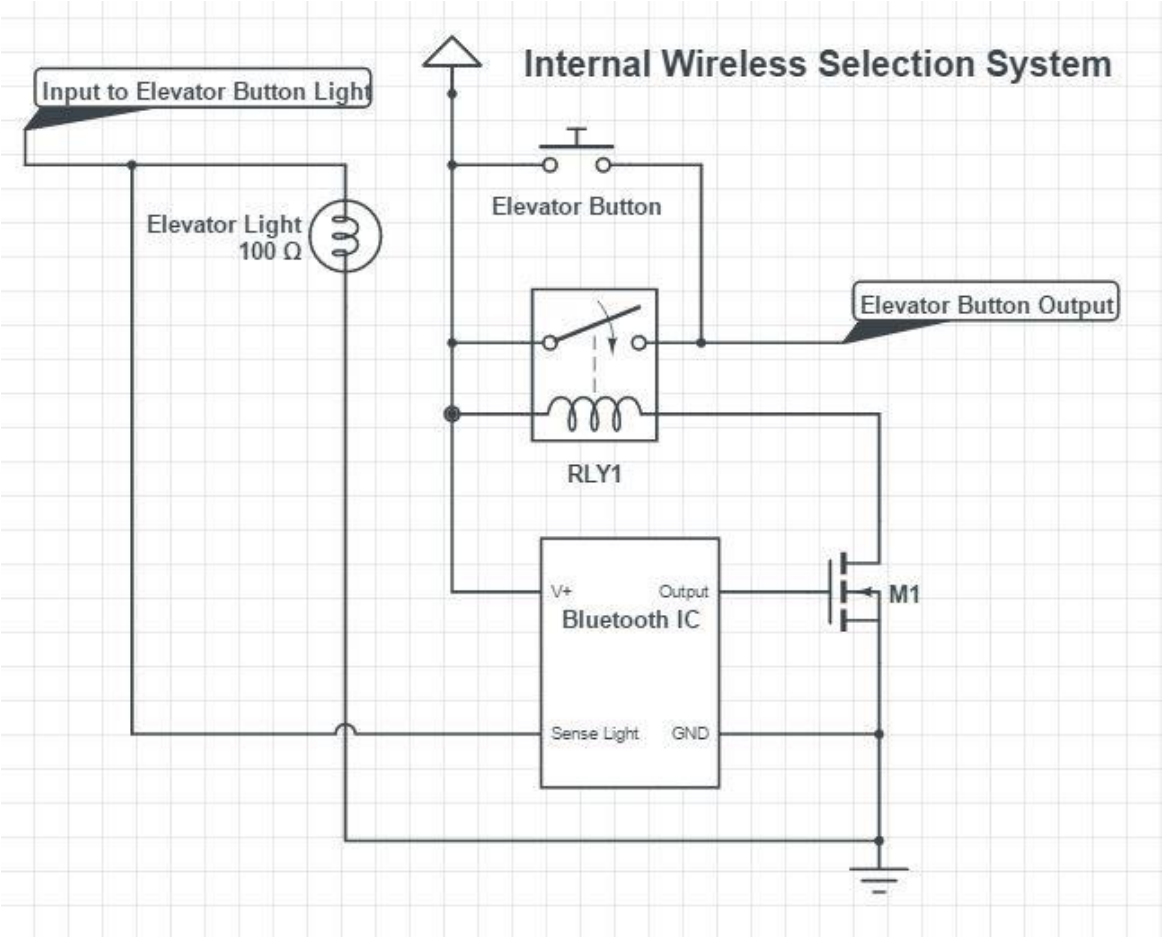

Figure 1 - Internal Bluetooth Button Selection

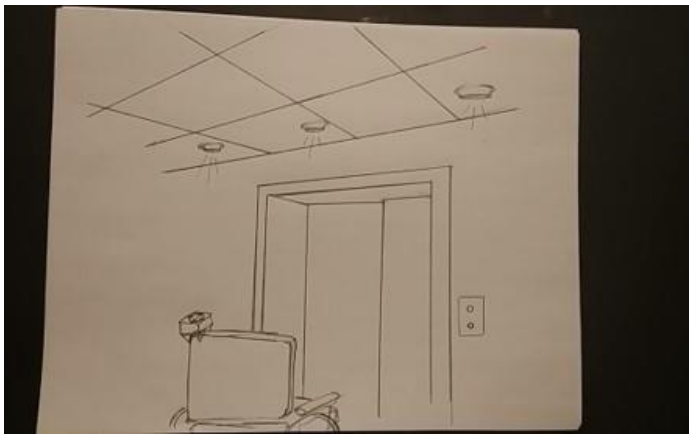

Figure 2- IR Emitter System Drawing

Electronic Swim Coach for Blind Athletes

The purpose of this project is to allow a visually impaired swimmer the ability to train without complete reliance on another individual. The final device prototype consists of a smartphone application that leverages the built in gyroscope and accelerometer of the smartphone, in order to track the visually impaired swimmer in a reliable manner and notify the swimmer if they have deviated to a side or if they are approaching the end of their lane. Machine vision is used to track a swimmer's position relative to the black "T" shaped lane guide on the bottom of a standard competitive swimming pool.

I. Problem Statement

Visually impaired competitive swimmers are presented with many unique challenges to overcome in their athletic pursuits. With the lack of the visual stimuli typically needed by competitive swimmers, the visually impaired swimmer has difficulty keeping track of their positioning within the lane. Knowing one's position is incredibly important for remaining straight in their lane and performing effective kick-turns, thus not knowing can hamper the swimmer's competitive performance significantly.

The current accepted solution to this problem is to have a coach at the end of the athlete's lane known as the tapper, as shown in Figure 1 [1]. The tapper is responsible for tapping the swimmer on the head with an object that consists of a tennis ball attached to the end of a stick, notifying the swimmer that they are approaching the wall. This solution is not ideal, given the reliance on a coach at all times for training and competition.

A solution with which the swimmer could have greater, if not total independence from a third party needs to be sought. Solutions to this problem proposed by other parties include the University of Notre Dame's solution known as the AdaptTap Lane-Gate System. This system eliminates the need for human tappers by using extending foam balls as markers, as shown in Figure 2 [2]. They are placed periodically from the lane dividers to mimic the backstroke flags. This design is functional, however, this design has two key issues. The AdaptTap has very poor portability and a very high setup time, leading to a large burden on the blind swimmer or the coach of the blind swimmer to setup and take down.

II. Proposed Solution

The objective of this project is to provide greater independence and autonomy to visually-impaired competitive swimmers through a smart phone application. The system design of the Electronic Swim Coach consists of a smartphone place in a waterproof case with the Electronic Swim Coach application running and attached to the waist of the swimmer. This application leverages the built in gyroscope and accelerometer of the smartphone, in order to track the visually impaired swimmer in a reliable manner and notify the swimmer by means of Bluetooth headphones if they have deviated to a side or if they are approaching the end of their lane. This notification will be in the form of a audio message generated by the application using Android's text-to-speech functionality. Machine vision is used to track a swimmer's position relative to the black "T" shaped lane guide, which is mandatory to be on the bottom of a standard regulated competitive swimming pool to adhere to the FINA (International Swimming Federation) RULES AND REGULATIONS illustrated in Figure 3 and Figure 4 [3]. Meanwhile the gyroscope and accelerometer are used to compensate for the roll, pitch, and yaw of the swimmer in real-time to allow for accurate tracking of the swimmer. The success of the application requires this standard black "T" shaped lane guide on the bottom of the swimmer's lane. It will additionally be able to collect data for the swimmer to produce stats regarding their performance for a particular session and progress over time. Other major features provided by the Electronic Swim Coach are:

- The application will be capable of tracking the swimmer's speed, position and lap-time.
- The application will be able to function with any swimming pose.
- The swimmer will be able to operate the application without external assistance.
- The application will be able to notify the swimmer of battery alerts.
- The application will be able to warn the swimmer should it fail to know the position of them within the pool.

III. IMPACT

Visually impaired competitive swimmers are presented with many unique challenges to overcome in their athletic pursuits. Swimming is the only existing sport that allows a visually impaired athlete to participate in with a full range of motion. For this reason, it is essential that swimming be an activity every visually impaired individual is given the opportunity to do.

All current solutions to this problem are not ideal, given the reliance on a coach at all times for leisure, training and competition. To promote greater independence and lesser reliance on coaches, the Electronic Swim Coach is intended to be operated solely by the swimmer themselves. This feature is non-existent to any current design and has the potential to revolutionize how visually impaired individuals exercise, whether the application usage be casual or competitive in nature.

There will always be a need for the advancements of assistive devices. This application has the potential to change the life of nearly every visually impaired individual desiring to exercise but are confined by their handicap. Whether it be for leisure, for fitness, for training, or for competition, this application has the potential to substantially increase the quality of life for many visually impaired individuals. With over 285 million visually impaired individuals worldwide, this application has the potential to affect millions of lives.

IV. PROJECT DEVELOPMENT

Methodology

The system design of the Electronic Swim Coach consists of a smartphone place in a waterproof case with the Electronic Swim Coach application running and attached to the waist of the swimmer. It can be attached anywhere along the persons waist so long as it is facing the bottom of the pool during their stroke, facilitating multiple different swimming strokes while still functioning properly.

The operational cycle of the electronic swim coach application is shown in Figure 5, and consists of five major steps that are constantly being repeated while the application is in operation. The operational cycle consists firstly of the image acquisition and the swimmer pose acquisition via the smartphone built-in camera and built-in gyroscope respectively. Extensive image processing is then done on the captured image in order to detect the lane guide. Next, pose compensation is done on the processed image using the gyroscope data (roll, pitch, and azimuth angles) of each frame to account for the roll, pitch, and azimuth that is present within each frame due to the moving hips of the swimmer, illustrated in Figure 6 [4]. Next, the side-to-side deviation is calculated based on the position of the swimmer relative to the lane guide. If this deviation results in the black lane guide to be found on the left or right extremity of the captured frame, as opposed to approximately centered in the frame, the swimmer is notified they have drifted to the respective side and may then correct their path. Finally end-of-lane detection is done by searching for the horizontal line in the processed image. If a horizontal line is found within the captured frame, the swimmer has reached the end of their lane and they are notified of this via Bluetooth headphones.

Results

As the Electronic Swim Coach has been progressing, various milestones have been completed along the way. Major milestones consists of designing the end-to-end system, static image data collection, development of a successful image processing algorithm, video and gyroscope data collection, successful image pose compensation, successful accessibility implementation, successful Bluetooth notification system, real-time human testing data collection, successful end-of-lane detection and side-to-side deviation detection. Static image data collection, video and gyroscope data collection, and real-time human testing were all completed in competitive swimming pool.

Static Image Data Collection and Results

Static image collection involved taking pictures of the bottom of the pool and using them to develop the image processing algorithm. Both clear and in motion images were recorded to test the algorithm under different conditions. The final image processing algorithm consists of the six major steps described below and illustrated in Figure 7.

1. Raw Image Captured: The raw frame is captured from the camera.

2. Grayscale: Grayscale the image solely on the blue color channel as this helps to remove unwanted interference from the pool floor.

3. Threshold: Threshold the image using Otsu's Method. Thresholding produces a binary image of the frame.

4. Edge Detection: A Canny Edge detector algorithm is used to determine the edges in the binary images.

5. Line Detection: From the edges, the lines in the images are identified using a Hough Line Transform.

6. End-of-lane: The end of lane can be determined by identifying horizontal lines in the image. Due to the thresholding and the gray-scaling of the image, the only horizontal lines that will be picked up are the ones marking the end of the lane.

Video and Gyroscope Data Collection and Results

The next testing stage involved using a modified version of the application to record video and corresponding gyroscope data for each frame of video. The two swimming techniques that were used in the recordings were the front crawl and the backstroke swimming techniques. In Table 1 and Table 2, a summary of the roll, pitch and azimuth data can be found. The focus was on fine-tuning the end-of-lane detection and pose compensation. Pose compensation refers to compensating for the roll, pitch and yaw of the swimmer that is obtained from polling the gyroscope of the smartphone, so that the post pose-compensated image appears as if the smartphone was perfectly flat and facing the bottom of the pool. From Figure 8, it is clear that using the gyroscope data, the position of the phone can be reconstructed for each frame and we can use this to predict if the image processing should be able to detect the line beneath the swimmer, and use the success or failure of this prediction to determine if the swimmer has drifted to the left or to the right in their lane. This pose compensation also required many mathematical calculations done by hand in order to confirm the accuracy of the pose compensation and rigorous dryland testing of the application to fine tune the pose compensation and ensure the accuracy of the pose compensation was acceptable. Once the accuracy of the pose compensation was nearly perfect, the real-time human testing of the application began.

Real-Time Human Testing and Results

Live human testing was the final testing stage that was completed for the electronic swim coach. The author's University Research Ethics Board clearance forms were submitted and accepted for this project before human testing was completed. Study participant were all formally contacted and gave complete consent for video recording of in-water testing and the use of their data for analysis and as an asset for the ongoing project development. The application was testing in real-life conditions by 3 test subjects. The application was tested under various conditions and for various strokes while attempting to find application failure cases. The heavily tested strokes consisted of the front crawl and the backstroke. The obtained results for the 3 test subjects, along with the results obtained by strapping the electronic swim coach to a floating boarding and swimming with it were very promising. These results can be found in Table 3 to Table 6. Based on all the sample data, the electronic swim coach has a 100% success rate on end-of-lane detection while containing no false positives, which is a rather remarkable accomplishment. We have attributed side-to-side deviation failures to the fact that the algorithm was too sensitive to pitch. This is a reasonable assumption as shown by the results in Table 6. These results were obtained by swimming with the electronic swim coach strapped to a floating board and obtained a side-to-side deviation success rate of 100%. The smartphone experienced substantial rolling, however it experienced minimal pitching, hence our reasoning for the failures in the human side-to-side deviation test cases. With a couple more rounds of human testing and fine-tuning of the application we believe the application will be ready to bring to market.

V. Conclusions

The idea of an electronic swim coach has been explored by several colleges and universities over North America, however substantial progress towards a prototype that is worn by the swimmer, allowing for maximum device portability and unique swimmer independence that has previously not been accomplished. There are many other qualities that set our electronic swim coach above other designs and the current solution to visually impaired swimming. This design is completely wearable and portable. It is fully accessible, meaning that the application is designed for an individual with visual impairment. The application functions with different swimming strokes. It grants independence to the visually impaired swimmer, and contains real-time image processing and pose compensation. The application is also inexpensive considering alternative designs, and has been human tested, achieving a 100% success rate on end-of-lane detection on all sample data. This application has the potential to heavily impact and increase the quality of life for many visually impaired individuals. Many visually impaired individuals would love a safe means of exercising, and with over 285 million visually impaired individuals worldwide, this application has the potential to affect millions of lives.

VI. References

[1] B. Briggs, "Wounded Warrior Seeks Glory Representing America in London," 15 June 2012. [Online]. Available: http://usnews.nbcnews.com/_news/2012/06/15/12227410-wounded-warrior-seeks-glory-representing-america-in-london?lite. [Accessed 27 09 2015].

[2] D. Krieger, "AdaptTap leveling the playing field for blind swimmers," 22 2 2008. [Online]. Available: http://masters.irishaquatics.net/usaswimming_adaptap.pdf. [Accessed 9 10 2015].

[3] FINA, "FINA Facilities Rules," [Online]. Available: http://archives.fina.org/H2O/docs/rules/2015/disciplines/FINAfacilities_rules_20152017.pdf. [Accessed 5 10 2015].

[4] MathWorks, "Android Sensor Support from MATLAB," [Online]. Available: http://www.mathworks.com/matlabcentral/fileexchange/40876-android-sensor-support-from-matlab--r2013a--r2013b-/content/sensorgroup/Examples/html/CapturingAzimuthRollPitchExample.html. [Accessed 10 12 2015].

APPENDIX

Figure 1: Accepted Tapper Solution

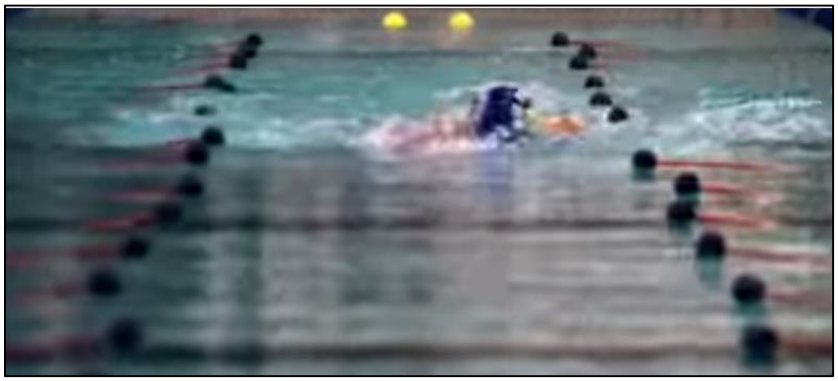

Figure 2: Notre Dame's AdaptTap

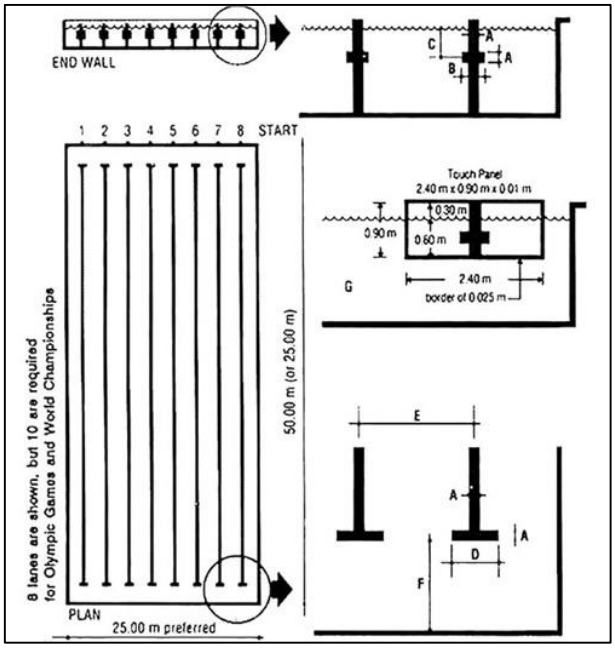

Figure 3: Lines required for Competitive Swimming Pools

WIDTH OF LANE MARKINGS, END LINES, TARGETS	A	0.25 m ± 0.05	FINA
LENGTH OF END WALL TARGETS	B	0.50 m	
DEPTH TO CENTRE OF END WALL TARGETS	C	0.30 m	
LENGTH OF LANE MARKER CROSS LINE	D	1.00 m	LANE
WIDTH OF RACING LANES	E	2.50 m	MARKINGS
DISTANCE FROM END OF LANE LINE TO END WALL	F	2.00 m	
TOUCH PAD	G	2.40 m x 0.90 m x 0.01 m	

Figure 4: Dimensions for Figure 3

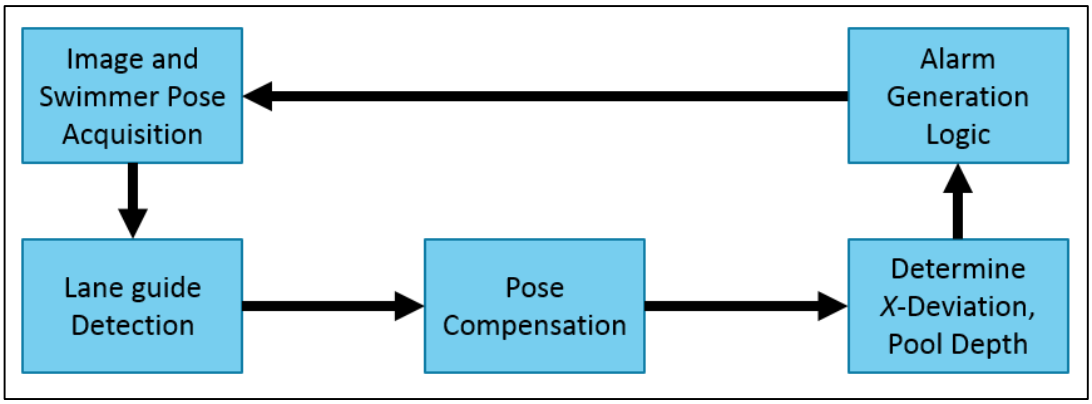

Figure 5: System overview of the electronic swim coach application

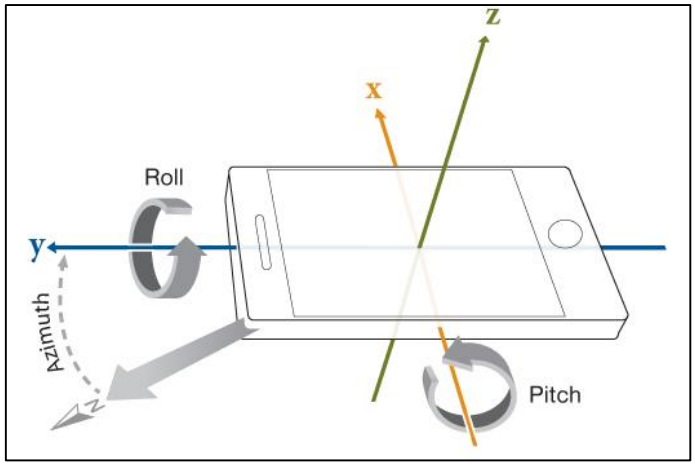

Figure 6: Visualization of roll, pitch and azimuth (yaw)

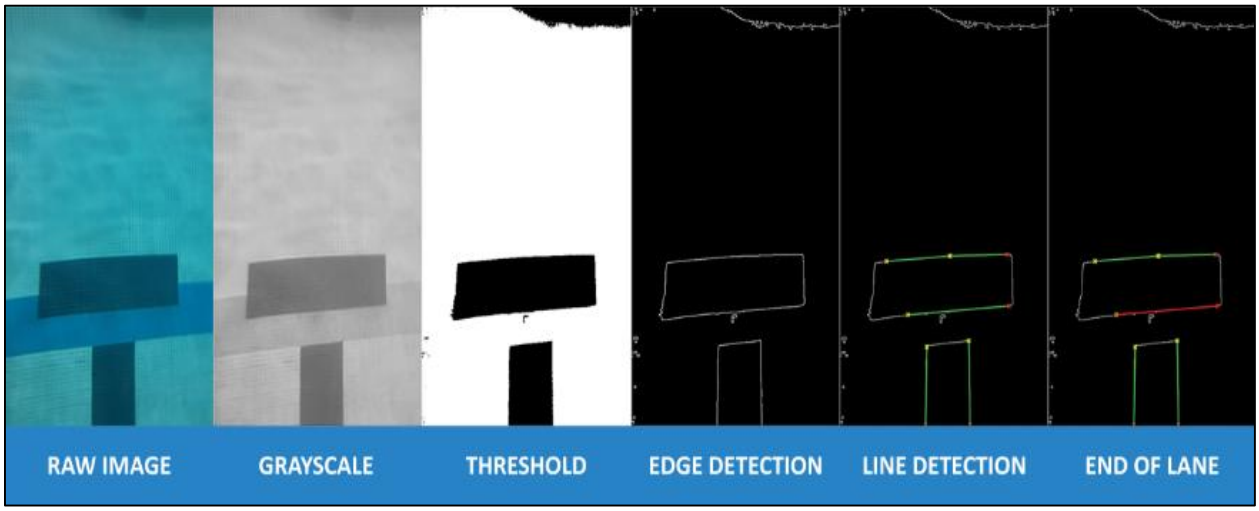

Figure 7: Major Image Processing Steps in the Electronic Swim Coach Line Detection Algorithm

Table 1: Front Crawl Gyroscope Testing Data

	Azimuth (degrees)	Pitch (degrees)	Roll (degrees)
Minimum	58.54	13.84	0.16
Maximum	132.96	40.18	42.46
Average	90.0	28.14	15.93

Table 2: Backstroke Gyroscope Testing Data

	Azimuth (degrees)	Pitch (degrees)	Roll (degrees)
Minimum	56.04	12.92	0.18
Maximum	134.57	39.01	45.95
Average	90.0	27.07	14.71

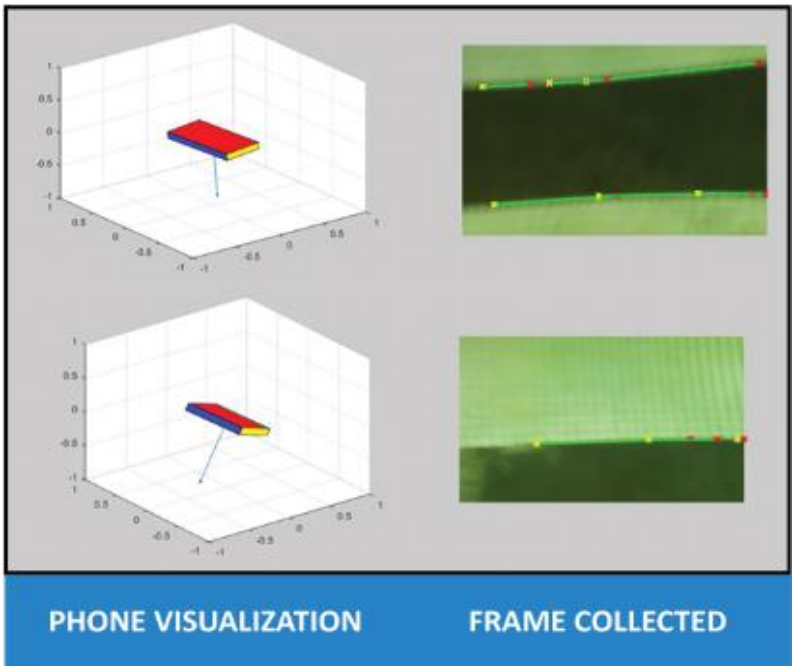

Figure 8: Phone position determined based on gyroscope data of the collected frame

Table 3: Volunteer 1 Real-Time Testing Results

Test Case	End of Lane Success	Left and Right Success	False Positives	Reason for Failures
Front Crawl (record)	3/4	6/8	0	Algorithm too sensitive to pitch
Backstroke	4/4	4/7	0	Algorithm too sensitive to pitch
Approach End of Lane	3/3	3/3	0	Algorithm too sensitive to pitch
Deviate Left	N/A	3/5	0	Algorithm too sensitive to pitch
Deviate Right	N/A	3/5	0	Algorithm too sensitive to pitch
Criss-cross lap	N/A	4/10	0	Algorithm too sensitive to pitch

Table 4: Volunteer 2 Real-Time Testing Results

Test Case	End of Lane Success	Left and Right Success	False Positives	Reason for Failures
Front Crawl (record)	2/2	2/3	0	Algorithm too sensitive to pitch
Backstroke	2/2	2/3	0	Algorithm too sensitive to pitch
Approach End of Lane	2/3	3/3	0	Algorithm too sensitive to pitch
Deviate Left	N/A	3/5	0	Algorithm too sensitive to pitch
Deviate Right	N/A	3/5	0	Algorithm too sensitive to pitch
Criss-cross lap	N/A	6/10	0	Algorithm too sensitive to pitch

Table 5: Volunteer 3 Real-Time Testing Results

Test Case	End of Lane Success	Left and Right Success	False Positives	Reason for Failures
Breaststroke (record)	1/2	2/5	0	Algorithm too sensitive to pitch
Backstroke	2/2	3/5	0	Algorithm too sensitive to pitch
Approach End of Lane	3/3	3/3	0	Algorithm too sensitive to pitch
Deviate Left	N/A	2/4	0	Algorithm too sensitive to pitch
Deviate Right	N/A	2/4	0	Algorithm too sensitive to pitch
Criss-cross lap	N/A	5/8	0	Algorithm too sensitive to pitch

Table 6: Flutter Board Real-Time Testing Results

Test Case	End of Lane Success	Left and Right Success	False Positives	Reason for Failures
Front Crawl (record)	4/4	5/5	0	None
Backstroke	4/4	5/5	0	None
Approach End of Lane	3/3	3/3	0	None
Deviate Left	N/A	5/5	0	None
Deviate Right	N/A	5/5	0	None
Criss-cross lap	N/A	10/10	0	None

IEEE Engineering in Medicine and Biology Society (**EMBS**) International Student Conference (**ISC**) 2016
Design Competition

OMNISTEP

A wearable technology to reduce falls in the elderly

Abstract— Falls affect one third of the elderly population and represent the seventh leading cause of death among seniors in the USA. Although tripping over obstacles causes 50-53% of falls, most current approaches to fall prevention tackle only intrinsic risk factors. Omnistep detects obstacles in the pathway and alerts the individual, preventing trips. Over-detection is avoided by ignoring tall obstacles and not alerting when the individual is motionless. Preliminary testing shows that our prototype has an accuracy of 75- 90% depending on the obstacle size. Omnistep can potentially reduce injuries and make elderly regain confidence in walking.

I. PROBLEM STATEM ENT

Falls threaten the independence of elderly people and cause a cascade of devastating individual and socioeconomic consequences. In the USA, falls are the leading cause of accidental death and the seventh leading cause of death in people over the age of 65 [1]. A combination of extrinsic, intrinsic, and situational factors put the elderly population at higher risk for falls, but the majority of falls are caused by environmental hazards [2]–[4]. Among them, tripping over obstacles is the leading reason for falls in the elderly, being reported as the cause for 50-53% of the falls [3]. Seniors are 76 times more likely to fall from trips when compared to young people [5].The problem is magnified in situations where the person is unable to see clearly, is hurrying, or is distracted and not looking to the front [2]. The increased risk of stumbling in the elderly is attributed to vision impairment associated with aging, slower reaction times when readjusting balance after tripping, and leg weakness which leads to inability to lift the foot enough during the swing phase of the gait [2]. In fact, a normal individual needs to react within 122ms after stumbling to prevent a fall, which is typically too quick for slower reacting seniors [6].

Current technologies targeting fall prevention are mainly concentrated on tackling the intrinsic risk factors for falls, such as balance disturbances [7]. Standard approaches such as grab bars, canes, walkers and even smartphone apps which gives feedback in response to gait patterns (in development) have minimal effect on environmental factors for falls, such as obstacles. Approaches that target environmental factors include anti-slip shoes, a robot that scans the environment for falling risks [7], and exercise to improve reaction times [6]. However, generally speaking these approaches are expensive, have little transference through different environments, and show limited efficacy. Thus, there is a clear need for better solutions that target environmental hazards for falls [7]. Our product aims to reduce falls and fall-associated injuries by addressing environmental obstacles, which is a major risk for falls among elderly people.

Our solution must not prevent users from carrying out their daily activities, meaning it needs to integrate seamlessly into the user's everyday life. The device should not cause additional burden; for example, a portable device would be clipped onto clothing. Moreover, the product will be lightweight and used outdoors as there are a lack of technologies addressing trips that occur outside the home. Lastly, the appearance should be stylish and can be worn with most attires.

II. PROPOSED SOLUTION

Although environmental factors are among the most common causes of falls in the elderly, there are currently very few solutions targeting this issue [7]. Omnistep addresses the major issues behind tripping associated falls, namely decrease in visual acuity with age and slower reaction time in the elderly [2]. The device compensates for the vision loss by scanning the environment for non-easily visible obstacles and it alerts the individual in advance, providing enough time for the person to react. Therefore, this addresses the issue of slower reactions times in the elderly population that makes it difficult for them to recover after tripping.

OmniStep is designed to detect obstacles in the user's path which may be difficult to see, then discretely alerts the individual to preventing trips. At the foot, a sonar sensor (*Figure 1*) detects obstacles up to 1.5m away, which is the necessary distance to stop walking after being alerted [8]. Moreover, we decided that the device should not be triggered when there is no threat of tripping, such as when the obstacle is too large and when the user is standing still. To address the first issue, an additional infrared (IR) sensor at a 45° with the sonar points obliquely upward to detect obstacles that are tall enough to be visible. Secondly, an accelerometer was incorporated to detect inactivity. Our devices uses vibration feedback to discretely alert the user in public situations.

To our best knowledge, the only wearable obstacle detector devices currently available is designed for visually impaired individuals [9]. These products are not suitable for our target population because of the excessive feedback they would provide. Instead, our device focuses on alerting only in the presence of small obstacles, which are difficult to see, thus preventing an excessive level of feedback.

OmniStep is designed to be a stylish and discrete wearable in order to prevent the stigma associated with aging while protecting the elderly from the devastating consequences of falls (*Figure 2*). The device can be incorporated into a variety of shoes, facilitating the adoption even by people wearing special or season-specific footwear. The device does not interfere with the current exercise-based therapy for fall prevention, but adds to current approaches by protecting the individual from environmental hazards. OmniStep can potentially increase users' confidence while walking, and therefore, prevent the vicious cycle between fear of falling and reduced physical activity, which results in a significant decline in walking performance and increased risk of falls [10]. Finally, as the device relies on affordable IR and sonar sensors, the cost of the device is projected

to be less than $100 USD, which will facilitate adoption.

III. Impact

Falls are one of the most devastating events that can happen to an elderly individual. Every year, over one third of elderly above the age of 65 fall, and 31% of these falls result in injuries requiring medical attention [11]. The frequency of falls rise with age and reach nearly 50% of the individuals over the age of 80 [11]. This corresponds to more than 150 million people around the world who suffer from falls every year [12]. Falls are not restricted to the elderly; individuals with stroke, Parkinson Disease and neuromuscular diseases also experience an increased risk, although there is a significant overlap between these populations.

Our design tackles a large extrinsic risk factor for falls: tripping over obstacles. Tripping is estimated to cause of 50.2% of falls in the elderly [3] and 20% of falls among stroke patients [13]. Preventing obstacle-related falls using our device can potentially avert 760,000 falls annually, leading to a cascade of socioeconomic and health improvements. Every year, 2.5 million older adults are treated in emergency rooms due to fall injuries, and over 700,000 end up hospitalized [14]. Approximately 10-15% of fallers suffer from fractures, 5% experience serious soft-tissue injuries or head trauma, and a smaller proportion die after a fall [11]. Long-term complications extend beyond injuries and include decreased physical function, fear of falling, and institutionalization. The scenario has become aggravated over the past few years and the number of unintentional fall deaths rose from 410,000 to 570,000 between 2004 and 2013 [14].

Moreover, falls incur a heavy financial burden and are currently among the top 20 most expensive medical conditions in the US [15]. The direct medical cost of treating fall injuries is positively associated with age, and due to the aging population, both the number of falls and the cost to treat accompanying injuries are likely to rise. In 2013, direct medical cost for falls in the US is $34 billion annually and expected to reach $68 billion by 2020 [16]. Each fall costs approximately $35,000 and the cost for treating falls increases with age [16]. Falls caused by stumbling over obstacles are among the most common causes of hospitalization, and incurs exceedingly high costs [5]. As tripping represents more than 50% of falls in the elderly, our design can potentially both reduce the number of falls and cut fall-related healthcare costs by half.

IV Project Development

This project was developed as part of BME498 Biomedical Engineering Capstone Design course under the supervision of Dr. Sabine Weyand.

Works-like prototype (*Figure 1*)

The first step in developing Omnistep was creating a works-like prototype. We started our prototype by verifying the usability of sonar sensors for noticing obstacles in front of the user's foot. The design constraint tackled by this sensor was preventing it from detecting the floor or the alternate leg as an obstacle. This issue was solved by defining a minimum range of detection at 60cm, which is greater than the step length of an elderly person [17]. We considered that detecting obstacles closer than 60cm from the foot would not bring any advantage, as the minimum necessary distance to stop a walking individual after an alert is 1m [8].

Next, we prevented the device from detecting tall obstacles. Since sonar sensors are unreliable at oblique angles, we started our tests by adding another sonar sensor at the knee level pointing to the front. As the sensors were not attached to the same case structure, it was challenging to ensure that they were pointing in the same direction and measurements were very unreliable. We proceeded with the incorporation of an IR sensor at the foot level, which produced reliable measurements when pointing obliquely to obstacles (*Figure 3B*). The sensor was placed on a 3D printed case pointing upwards at a 45° angle and the device was programmed not to alert the individual when both sensors detected the same obstacle. We presumed that when both sensors return the same perpendicular distance (calculated using trigonometry for measurements obtained from the oblique sensor) they are pointing to the same obstacle. Two IR sensors were incorporated to cover the full desired range of detection (0.2m – 5.0m) and the sensors are alternately turned on to prevent interference. The data from the sensors is digitally processed using a median filter.

Finally, an accelerometer was incorporated into our device to inhibit alerts when the individual is standing still.

Looks-like design (*Figure 2*)

The looks like design consists of two parts: an elastic case that goes around the shoe and an adhesive strap that fixates the device to the sole of the shoe (*Figure 2A*). The elastic case holds the sensors at the top of the shoe and contains an elastic band around the ankle that provides the vibratory feedback. This case can be effortlessly transferred between shoes, and the ankle band gets easily hidden under the pants (*Figure 2B*). The strap, on the other hand, is permanently fixated to the sole of each shoe and provides stability to the sensors, so that they can get reliable measurements.

Testing

The first cycle of tests evaluated the accuracy of the device's sensors working together. The device was placed at defined distances from a wall, and the actual distance was plotted against measured distance (*Figure 3*). The device obtained very accurate measurements and the regression analysis shows $R^2 = 0.9999$ and $R^2 = 0.9977$ for the perpendicular and oblique sensors, respectively.

The device's detection rate was tested by three different individuals with varying obstacle sizes (4, 12 and 32cm). Each tester started 2m away from the obstacle and walked at a steady pace (100 steps/minute) in a straight line towards the obstacle (*Figure 4*). The proportion of the trials in which the person was alerted early enough to stop before colliding with the object was recorded (*Figure 5*). Omnistep was 90 ± 9.5% (SE) accurate in detecting the 32cm obstacle, and 80 ± 8.9% and 75 ±

10.8% accurate in detecting the 12 cm and 4 cm obstacles, respectively. The device was able to detect objects as small as 2cm; additional structured tests need to be performed for these obstacles to assess replicability. OmniStep was also tested against a tall obstacle (a wall, 3m high) and the measured non-detection rate was 70 ± 14.5%. To our knowledge, the accuracy of the device is mainly affected by unreliable measurements coming from the sonar sensor when the obstacle in front of it is not precisely perpendicular to the sensor, so an IR sensor pointing to the front can potentially increase the device accuracy in the future.

The users' ability to stop after being alerted by OmniStep was also assessed. Two independent blindfolded testers walked at a steady pace (95 steps/minute) towards a 24cm obstacle. The users were instructed to stop after an auditory alert was provided by the prototype. In this series of tests, the users were able to stop before tripping in 96 ± 3% (SE) of the cases (n = 30).

V. Conclusions

Omnistep provides a novel approach that addresses an underexplored and major cause of falls in the elderly: tripping over obstacles. Our works-like prototype has confirmed the viability of using affordable sonar and IR sensors to detect obstacles while walking and validated the accuracy of these sensors, including the use of IR sensors to obtain precise oblique measurements. Our prototype has already reached 90 ± 9.5% accuracy for obstacles 32cm high and 75 ± 10.8% accuracy for small obstacles (4cm). The use of oblique and perpendicular sensors to differentiate tall obstacles from small obstacles was proved viable and currently has 70 ± 14.5% accuracy. We designed a looks-like model that matches all the design criteria, as it is discrete, transferable between shoes and allows the sensors to stay stable to get precise measurements. Finally, as our device tackles the major cause of falls among seniors, it has the potential to reduce falls up to 50%. Therefore, we believe that Omnistep will make elderly fall less and be safe and confident in their own shoes.

REFERENCES

[1] "Falls in the Elderly," *Merck Manuals Professional Edition*. [Online]. Available: http://www.merckmanuals.com/professional/geriatrics/falls-in-the-elderly/falls-in-the-elderly. [Accessed: 08-Apr-2016].

[2] W. P. Berg, H. M. Alessio, E. M. Mills, and C. Tong, "Circumstances and consequences of falls in independent community-dwelling older adults," *Age Ageing*, vol. 26, no. 4, pp. 261–268, 1997.

[3] A. Blake, K. Morgan, M. Bendall, H. Dallosso, S. Ebrahim, T. Arie, P. Fentem, and E. Bassey, "Falls by elderly people at home: prevalence and associated factors," *Age Ageing*, vol. 17, no. 6, pp. 365–372, 1988.

[4] T. Masud and R. O. Morris, "Epidemiology, of falls," *Age Ageing*, vol. 30, pp. 3–7, 2001.

[5] A. A. Ellis and R. B. Trent, "Do the Risks and Consequences of Hospitalized Fall Injuries Among Older Adults in California Vary by Type of Fall?," *J. Gerontol. A. Biol. Sci. Med. Sci.*, vol. 56, no. 11, pp. M686–M692, Nov. 2001.

[6] V. Weerdesteyn, H. Rijken, A. C. H. Geurts, B. C. M. Smits-Engelsman, T. Mulder, and J. Duysens, "A Five-Week Exercise Program Can Reduce Falls and Improve Obstacle Avoidance in the Elderly," *Gerontology*, vol. 52, no. 3, pp. 131–141, 2006.

[7] J. Hamm, A. G. Money, A. Atwal, and I. Paraskevopoulos, "Fall prevention intervention technologies: A conceptual framework and survey of the state of the art," *J. Biomed. Inform.*, vol. 59, pp. 319–345, Feb. 2016.

[8] M. Wood, T. Ayres, R. Kelkar, and R. Khatua, "Walking and Jogging: An Analysis of Pedestrian Stopping Times and Distances," *Proc. Hum. Factors Ergon. Soc. Annu. Meet.*, vol. 54, no. 19, pp. 1435–1439, Sep. 2010.

[9] B. Mustapha, A. Zayegh, and R. K. Begg, "Wireless obstacle detection system for the elderly and visually impaired people," 2013, pp. 1–5.

[10] V. Weerdesteyn, M. de Niet, H. J. Van Duijnhoven, A. Cho, and M. D. Geurts, "Falls in individuals with stroke," *differences*, vol. 33, p. 36, 2008.

[11] S. D. Berry and R. R. Miller, "Falls: epidemiology, pathophysiology, and relationship to fracture," *Curr. Osteoporos. Rep.*, vol. 6, no. 4, pp. 149–154, 2008.

[12] N. I. on Aging, "Humanity's Aging," *National Institute on Aging*, 26-Mar-2012. [Online]. Available: https://www.nia.nih.gov/research/publication/global-health-and-aging/humanitys-aging. [Accessed: 01-Apr-2016].

[13] A. A. Schmid, H. K. Yaggi, N. Burrus, V. McClain, C. Austin, J. Ferguson, C. Fragoso, J. J. Sico, E. J. Miech, M. S. Matthias, L. S. Williams, and D. M. Bravata, "Circumstances and consequences of falls among people with chronic stroke," *J. Rehabil. Res. Dev.*, vol. 50, no. 9, pp. 1277–86, 2013.

[14] "WISQARS (Web-based Injury Statistics Query and Reporting System)|Injury Center|CDC." [Online]. Available: http://www.cdc.gov/injury/wisqars/. [Accessed: 06-Apr-2016].

[15] N. V. Carroll, P. W. Slattum, and F. M. Cox, "The cost of falls among the community-dwelling elderly," *J. Manag. Care Pharm.*, vol. 11, no. 4, pp. 307–316, 2005.

[16] J. A. Stevens, P. S. Corso, E. A. Finkelstein, and T. R. Miller, "The costs of fatal and non-fatal falls among older adults," *Inj. Prev.*, vol. 12, no. 5, pp. 290–295, 2006.

[17] C. Rigas, "Spatial parameters of gait related to the position of the foot on the ground," *Prosthet. Orthot. Int.*, vol. 8, no. 3, pp. 130–134, 1984.

APPENDIX

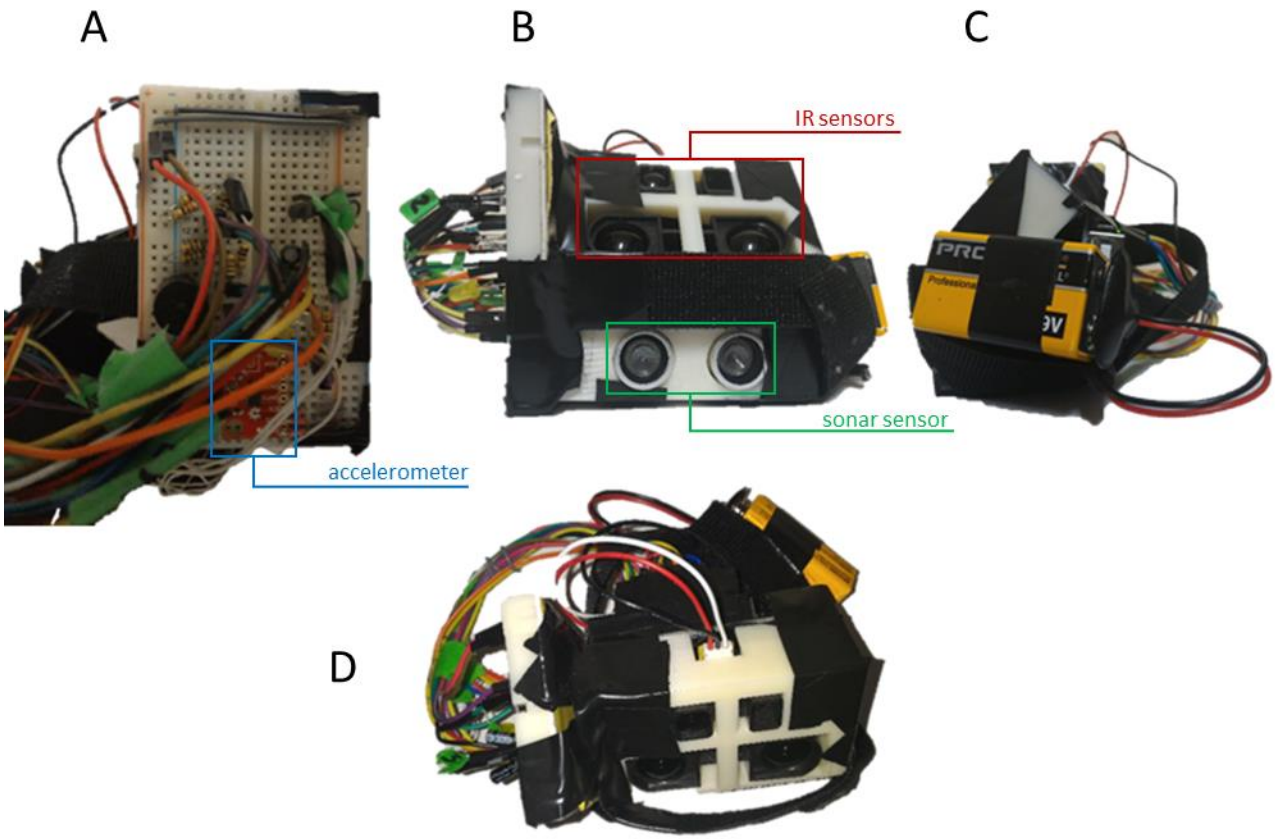

Figure 1. **Works-like prototype: A.** Left-side, **B.** Front, **C.** Right-side and **D.** Top views. The device contains an Arduino board, a 9V battery, two infrared sensors at 45°, a sonar sensor, an accelerometer, a buzzer and LEDs (the last two were used only for testing purposes). The vibration motor is not connected to this version of the prototype.

A B

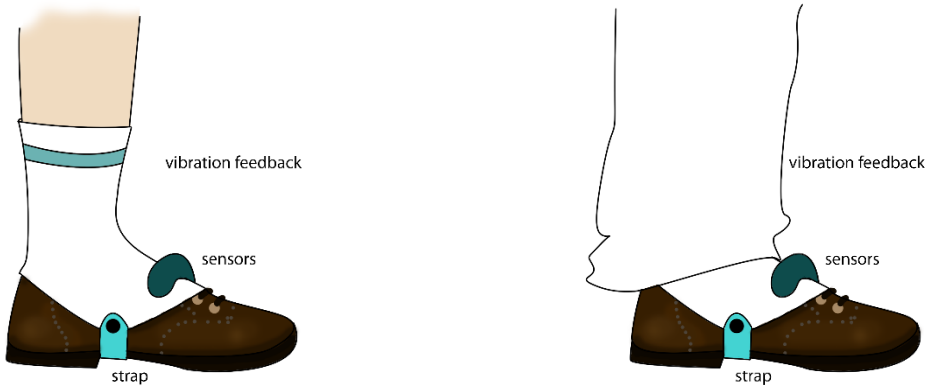

Figure 2. **Looks-like design: A.** The design consists in an elastic case around the shoes that fixates the vibratory band around the ankle and sensors pointing forward at the top of the shoes. An adhesive strap attaches the elastic case to the shoes. **B.** Pants can cover most of the case, making the wearable very discrete.

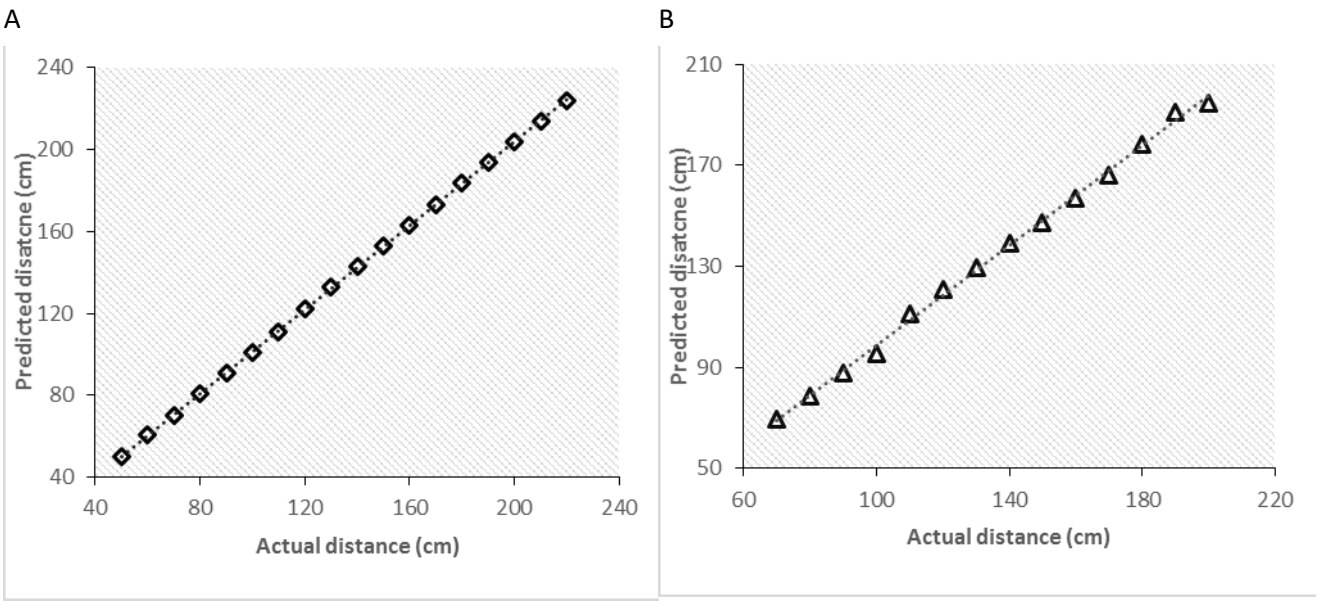

Figure 3. **Perpendicular sensor (A) and Oblique sensor (B) accuracy testing results:** the measured distances and the actual distances between the sensors and the obstacle was strongly positively correlated in the linear regression analysis ($R^2 = 0.9999$ for the perpendicular sensor and $R^2 = 0.9977$ for the oblique sensor).

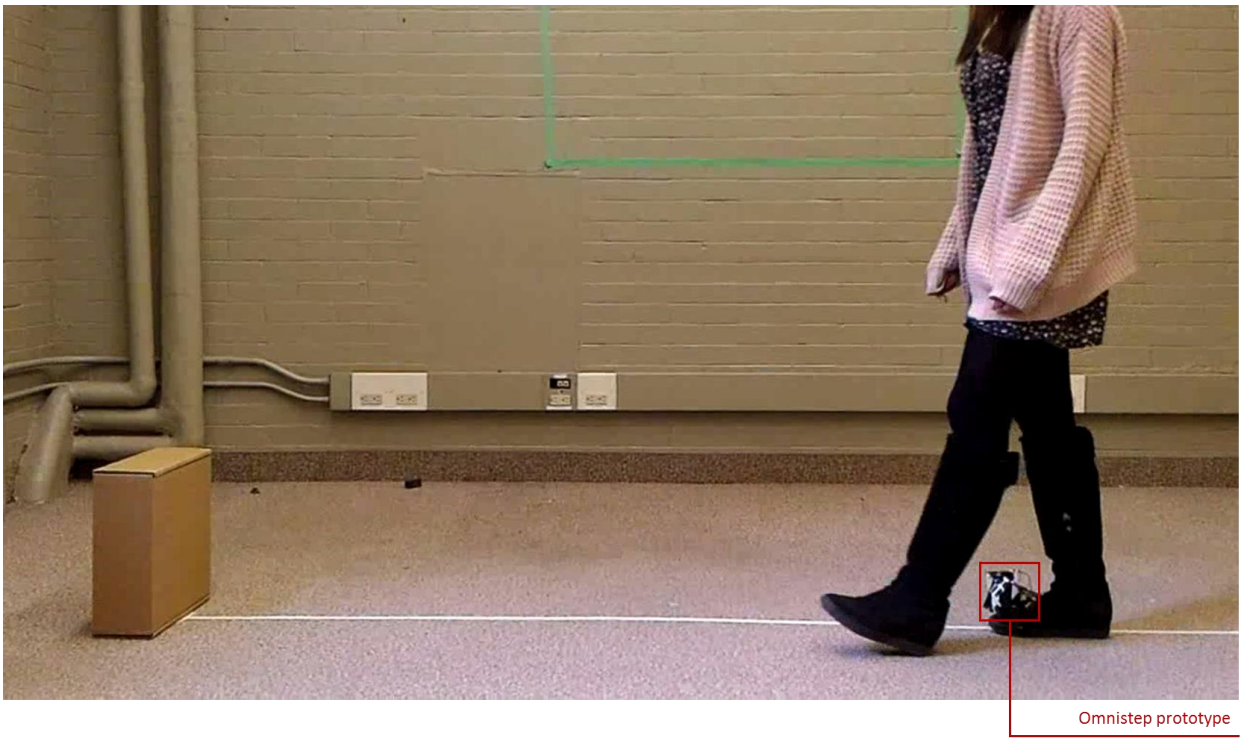

Figure 4. **Device accuracy tests:** the individual walked at a controlled speed (100 steps/min) towards the obstacle wearing the Omnistep prototype on the shoe. This picture depicts a test performed with the 30cm obstacle.

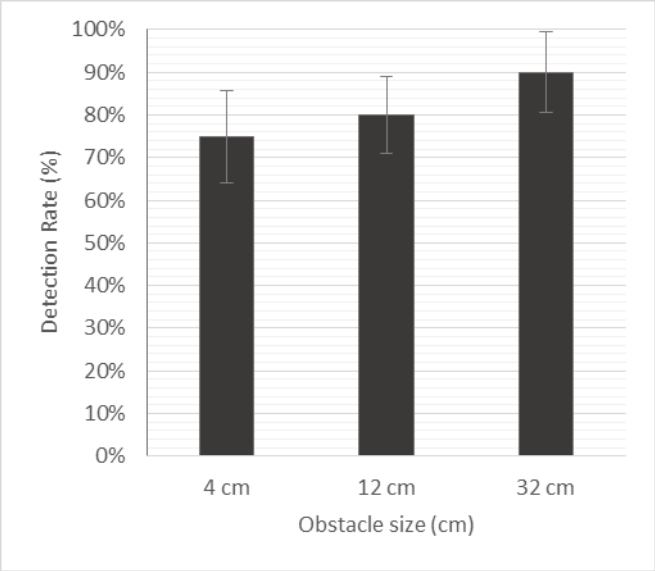

Figure 5. **Device detection rate:** the percentage of the tests in which the individual was alerted in time to stop before a collision with the obstacle happened. The tests were repeated 16, 20 and 10 times for the obstacles with 4, 12 and 30 cm, respectively.

A Better Prosthetic Hook

Extending the Mechanical and Sensory Capabilities of Body-Powered Prosthetic Hooks

Abstract — The commonly used upper-limb hook prosthesis operates with the force of rubber bands snapping the hook onto an object, resulting in the fear of a held object being crushed or slipping out of the hook. A solution has been generated to provide users with control over the hook's grip strength by locking the hook at an opened angle dependent on force readings in the hook (with a current mechanical model), and also to provide the user with sensation of the force exerted on an object through haptic feedback (with an electrical proof of concept).

I. Problem Statement

"Persons with a below-elbow, single arm amputation who use a body-powered prosthetic hook lack the ability to easily pick up objects of different geometries and weights without damaging them due to limited ability to perceive and control the grip strength of the hook."

Conventional body-powered prosthetics use the wearer's muscle force and upper arm movement to operate a metal hook terminal device (TD). The most common TDs are uniaxial, voluntary-open hooks (figure 1 in the appendix) which rest passively in a closed grip position [1] [2]. As seen in figure 2 in the appendix, these TDs are body-actuated by using shoulder movement to tension the cable assembly [3]. The hook's gripping strength is determined by the number of rubber bands that are wrapped around the base of the hook, and removing rubber bands is an arduous task. Furthermore, any attempted grip regulation requires the user to maintain some tension on the cable and this can be fatiguing. Users also have limited perception of how an object is being gripped with the hook since there is no direct feedback to the user for how strong of a grip the hook is exerting.

Current solutions to solve variable grip control and user grip perception exist in myoelectric prosthesis designs, denoting those prostheses which generally use electrical components for actuation [4]; however, no current solutions exist for hook prostheses even though they are the most commonly used. Analysing myoelectric solutions will help determine why they have not replaced the hooks completely. First, some myoelectric prostheses provide sensory feedback in order to determine how well they are gripping an object. If the user finds that their grip needs adjusting, they are able to do so themselves to prevent slipping/crushing. This method, however, is limited by the user's reaction speed and ability to understand the feedback signals [2] [4]. Second, some myoelectric prostheses have a closed loop feedback system which automatically adjusts grip on foreign objects without user input. These automatic control systems have found their way into Ottobock myoelectric prostheses [5], but the myoelectric prostheses are overly complicated and lose the robustness of the original hook.

There exists an opportunity here to add functionality to the hook prosthesis. Because it continues to be the most popular upper-limb prosthesis, research to improve the hook will translate into positively impacting the most amount of people.

II. Proposed Solution

The approach to solving the problem as described by the problem statement was divided into two functions:

A. *Control hook closure.* The design must improve how the hook closes onto an object. Currently, the rubber bands the hook uses for closing onto an object cause concern in users when the hook is used on household objects for fear of crushing or slipping.

B. *Provide grip perception.* The design must provide the user with information concerning the hook's grip on an object. Currently, users have difficulty using their hook intuitively as if it was a human hand because they lack perception of how an object is being held.

The functions listed above directly correlate with two subsystems. The function of "control hook closure" will be solved with a mechanical subsystem, and the "provide grip perception" function will be solved with an electrical subsystem.

Mechanical Subsystem:
The mechanical subsystem controls the amount of force exerted by the prosthesis by controlling the extent of hook closure. Closure is opposed through a locking mechanism with high spatial resolution, allowing for force control without significant power input (the rubber bands still do the work to hold an object). By controlling the locking mechanism based on force sensor readings taken from the hook end, the amount of force exerted on grasped objects is controlled, allowing users to grasp objects that would otherwise be dropped or crushed. The locking mechanism also has safety features, ensuring that the mechanical subsystem fails safely and that users can abort grips at any time. In addition to controlling force, the mechanical subsystem also takes advantage of damping in order to control the hook closure rate. This allows users to grasp a wider variety of objects and no longer requires them to be an arm's length away from an object that they would like to hold.

Electrical Subsystem:
The electrical subsystem provides grip perception to the user of the hook prosthesis by supplying haptic feedback correlated with the grip strength at the hook tips. Unintrusive sensors are placed at the hook's contact points, and a vibrational motor band is worn around the upper arm. As the user applies force onto an object with the hook, sensor readings will translate to drive motor vibrations where greater applied force equates to vibrations increasing in amplitude and frequency. In conjunction with the mechanical subsystem, once certain sensor values are met, the mechanical subsystem will lock the hook at the current angle and the haptic feedback will stop. The sensor values at which this occurs at can either be determined by an algorithmic threshold of force on an object, or by user input.

Vibrational feedback was chosen for the potential to tune motor frequencies to mechanoreceptors with certain frequency responses, providing more intuitive sensation to correlate with touch and grip strength. Compared with visual or audio feedback, vibrations correlate closest with a sense of touch which is a goal in advancing prosthetics. The electrical subsystem also has potential for very easy integration with the mechanical subsystem, in the sense that both the haptic feedback and locking mechanism can use the same force sensors, and the electrical subsystem only needs to send an on/off signal to actuate the mechanical locking.

III. Impact

Adding functionality to the popular conventional hook prosthesis must be done to provide for current users of below-elbow prostheses. While advancements in myoelectrics is a promising field, its unfavourably long timeline to market makes improving the existing solution very valuable for persons with transradial amputations who would benefit from additional grip control and grip perception now. For instance in Saskatchewan, the primary user group of below-elbow prostheses are farmers who use the hook at work since it is lightweight and robust, but generally will not use it in their home for fear of crushing more delicate objects [2]. Adding the proposed functionality will allow for these individuals to continue to use their prosthesis at home, and feel safe doing so.

The developments proposed for the hook are also very applicable to other areas of prosthetics research. First, the mechanical subsystem has design considerations to be fitted onto many voluntary-open hook prostheses. Second, the electrical subsystem has a direct haptic feedback system which can not only be added to hook prostheses, but the concepts can extend to myoelectric prostheses as well as to emerging open-source 3D printed designs whose mechanical actuation can benefit from a haptic interface. Work is also being done into detecting slip of objects which includes averaging filters and discrete time derivatives of raw sensor data. This data can be utilized by the mechanical subsystem in a closed-feedback loop to lock the hook an additional increment to correct for the slip. Finally, since both subsystems can be prototyped as attachments onto existing hooks, it holds promise to be used by many manufacturers.

IV. Project Development

Mechanical Subsystem:
The mechanical subsystem, as seen in figures 3, 4, and 5 in the appendix, is designed to control hook closure in order to deliver sufficient grip force, such that objects can be held without crushing or slipping. The subsystem's primary feature is a high-resolution locking mechanism, which consists of a compound ratchet gear, an 85:1 gear train, and a solenoid actuator. The design allows for the upper hook tine to be locked in increments of ~0.06 degrees, corresponding to ~0.1 mm of vertical displacement at the hook tip. This high resolution of the locking mechanism allows for a wide variety of objects to be held, with a large amount of control over the force exerted. During normal operation, the locking mechanism is controlled by the solenoid, based on force sensors readings taken at the hook.

However, the design also incorporates several safety features. In the event that power is lost, the locking mechanism is designed to use mechanical power in order to lock or remain locked, such that an object that is being held is not dropped or crushed. In addition, the user can abort a grip at any time, by extending their arm in the traditional mode of operation.

Pending the arrival of a few remaining parts, a proof of concept will be built for the mechanical subsystem based on figure 6 of the appendix. Physical testing will be used to verify the subsystem performance which has been predicted by analysis: specifically, the locking resolution, response time, and mechanical integrity of the system.

Electrical Subsystem:
For the electrical subsystem, a haptic feedback system has been built to prove the concept. The system uses two commercially available force-sensitive resistors (FSRs) which will eventually be placed on the hook's contact tips. As grip is applied, changes in FSR data are linearized through a microcontroller (Romeo-Arduino) and are converted to pulse-width modulate two vibrational motors. The vibrational motors are fitted into a velcro armband for the user to wrap around the upper arm. As greater force is applied to the FSRs, the motors alternatively vibrate faster and more intensely. Testing was done on the platform in figure 7 of the appendix.

To detect slip, primary trials were done by averaging and calculating derivatives of real-time FSR data. This method was used because setting down an object and an object slipping will both look like force being taken off of the FSRs. Analysis was done to understand data trends between setting down objects and objects slipping.

V. Conclusions

Current project development has produced a mechanical model to demonstrate a high-resolution locking mechanism to lock the hook at a specified opening angle provided by force feedback at the ends of the hook. This same force feedback, using FSRs, will correlate with vibrational motor pulsations on the skin to provide haptic feedback, and a proof of concept of this electrical subsystem was demonstrated on an electronics testbed based on Arduino. Early work to detect slip in the hook was also performed by averaging filters and discrete time derivatives of FSR data. The design was made such that the integration of the mechanical and electrical subsystems will done simply by a binary signal to actuate the locking mechanism.

VI. Works Cited

[1] J. Kraushaar and S. Wunder, Interviewees, *Physiatrists.* [Interview]. 9 November 2015.

[2] D. Nelson, Interviewee, *Certified Prosthetist.* [Interview]. 24 September 2015.

[3] M. Lusardi, M. Jorge and C. Nielson, Orthotics and Prosthetics in Rehabilitation, Saunders, 2012.

[4] D. D. Damian and e. al, "Slip Speed Feedback for Grip Force Control," *IEEE transactions on bio-medical engineering,* vol. 59, no. 8, pp. 2200-2210, 2012.

[5] Ottobock, "Myoelectric Prosthetics 101," Ottobock. [Online]. [Accessed 10 November 2015].

[6] M. Chorost, "A True Bionic Limb Remains Far Out of Reach," Wired, 2012. [Online]. [Accessed 24 November 2015].

[7] "Model 8X Medium Adult Size Hook," Amputee Supply. [Online]. [Accessed 24 November 2015].

VII. Appendix of Figures

Figure 1. Hook-Style End Effector [6]

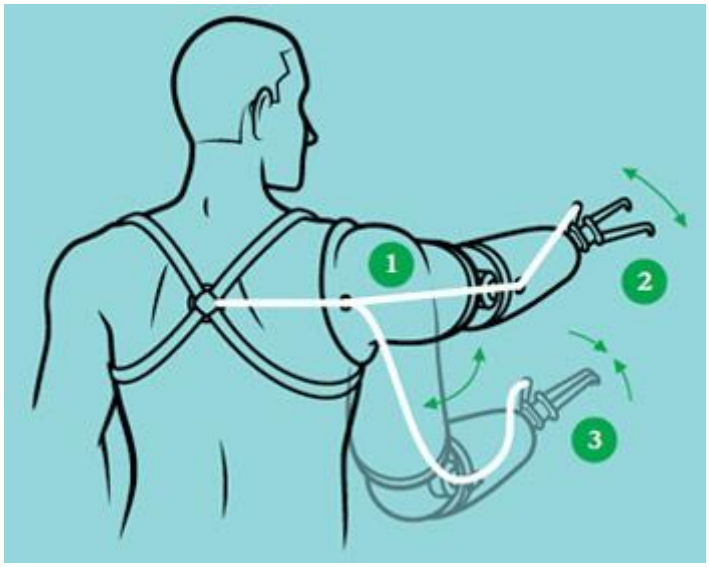

Figure 2. Operating Mode of Voluntary-Open Prosthesis [7]

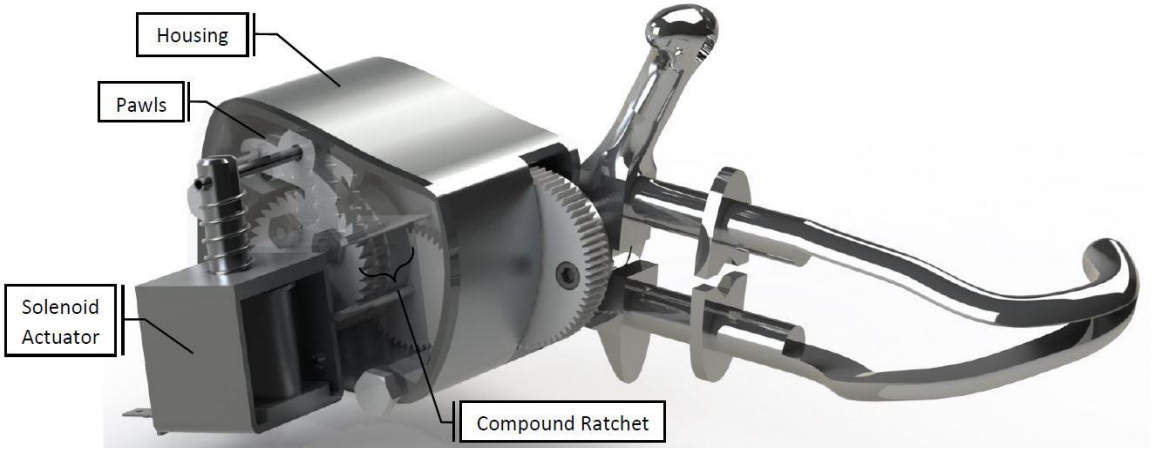

Figure 3. Mechanical Proof of Concept Render - Front View

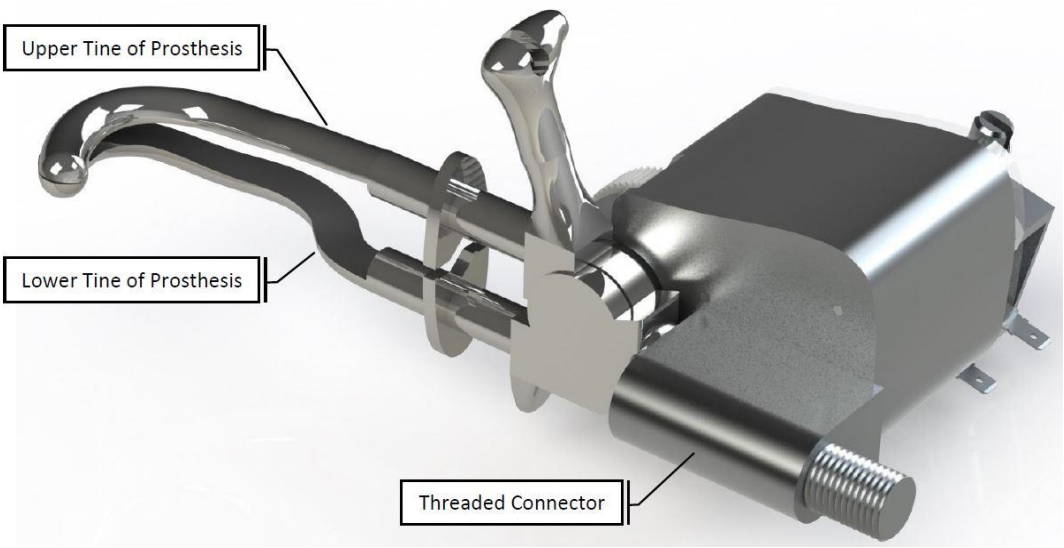

Figure 4. Mechanical Proof of Concept Render - Back View

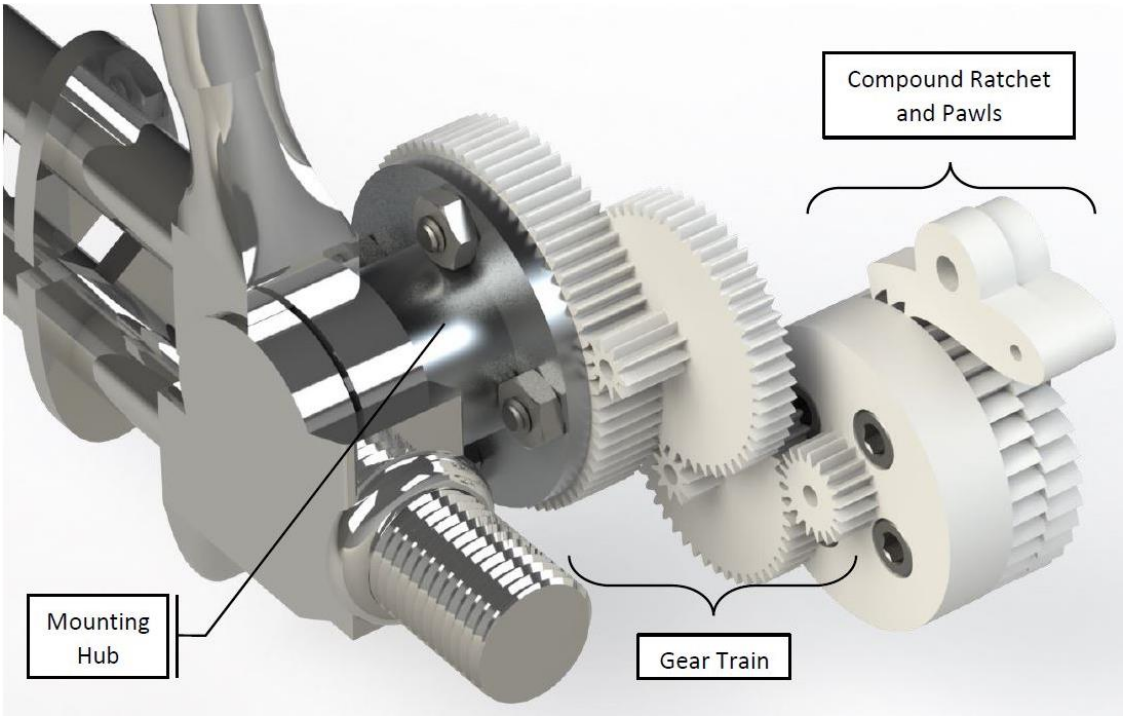

Figure 5. Mechanical Proof of Concept - Mounting Hub, Gear Train, and Compound Ratchet

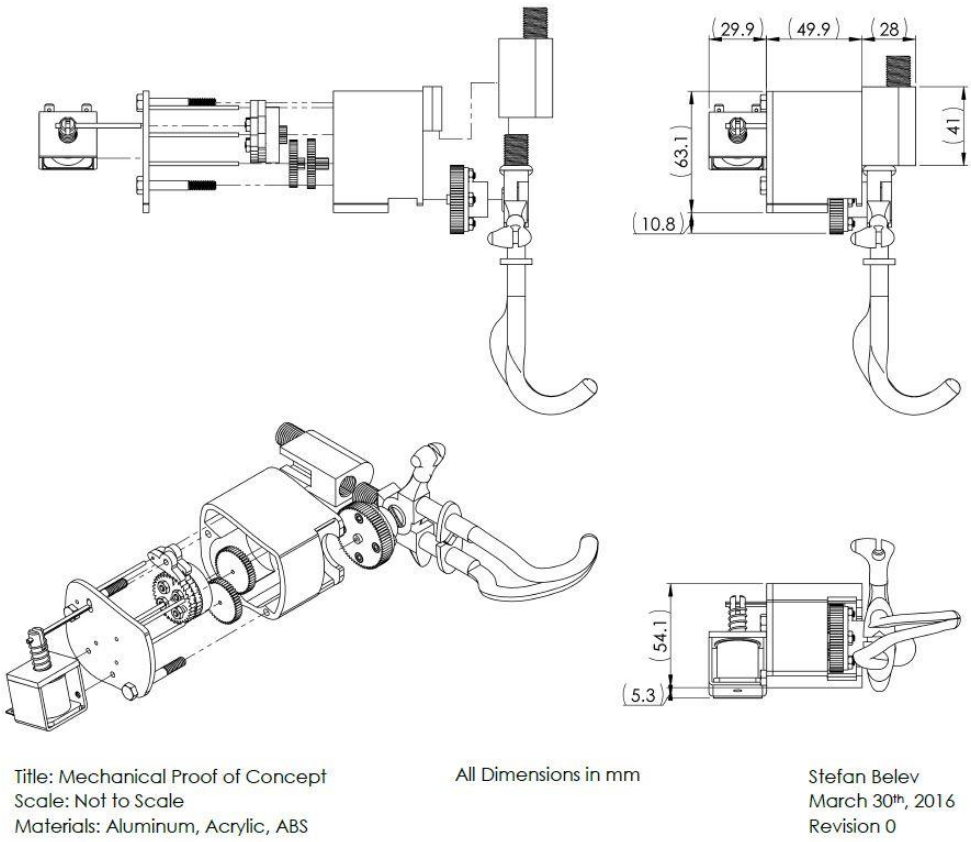

Figure 6. Mechanical Subsystem CAD Drawing

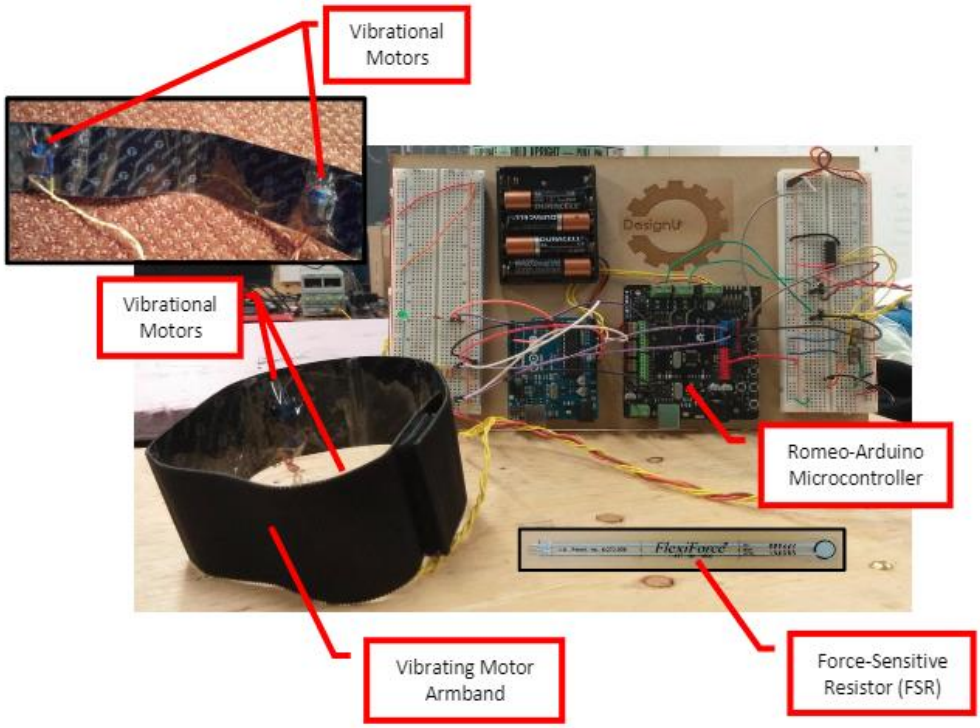

Figure 7. Electrical Subsystem Testbed

IEEE Engineering in Medicine and Biology Society (**EMBS**) International Student Conference (**ISC**) 2016
Design Competition

Redesigning a Recycling Process to Provide Secure Supported Employment for Those with Disability

Names Removed

Abstract— To enhance system flow-through and improve counting correctness, a computerized totalizing process was designed for a supported employment beverage container recycling center. Modular 3-hole, 1-trough intake and 6-hole sorting tables were designed and built, keeping in mind the capabilities of the workers with disability. For ease of later maintenance, commercial dual counter/displays and commercial sensors were used for the totalizer system. Each counter is interrogated via an RS485 link to a Red Lion G310 controller/display to provide customer and daily totals, and receipts for customers. The increased efficiency enables the disabled workers to remain employed given recent Federal law changes.

I. Problem Statement

The Federal Workforce Innovation and Act of 2014 changed how existing sheltered workshops operate where people with disabilities earn less than minimum wage. Individuals with disability <24 y.o. cannot be employed for a wage less than the federal minimum without first receiving pre-employment transition services and trying vocational rehabilitation services. The new act could interfere with the supported employment concept where workers are currently paid based on their productivity, unless a way can be found to increase productivity to the point where the minimum wage is justifiable.

The St. Lawrence County (NY) NYSARC program provides gainful employment for those with mental and physical disabilities. Their recycling centers handle 7M beverage containers annually, 40% of which are now plastic water bottles. The 1982 NY State Returnable Container Act set a handling fee at $0.035 per item, so the 7M volume translates to a gross income of almost $0.25M/yr. But NYSARC has calculated a yearly loss of ≥$15K due to overpayment of $0.05 per container at intake and under-collecting of the $0.085 fee from vendors. These count discrepancies arise from their current redemption process that uses outdated technology for counting and sorting (Figure 1), resulting in revenue shrinkage. Consequently, NYSARC looked for ways to streamline and generally optimize their collection process — in turn helping to ensure gainful employment for willing employees with disability.

II. Proposed Solution

Thus our XXXX University Biomedical Engineering Design team strove to improve the redemption center technology to limit these losses. Our **goal** was to turn bottle redemption into a statewide business capable of supporting jobs for individuals with disabilities under the new requirements of the Workforce Act. Our **mission** was to improve the efficiency of, and maximize the dollar return from, the returnable recycling business operated by St. Lawrence County NYSARC, while taking into account the capabilities of those with disability who are their employees. Our **aim** was to make intake and sorting faster, more accurate, and easier for workers by using better mechanical and electronic features. We developed in conjunction with NYSARC staff a list of desired elements: 1) the need for the operation to be such that workers and staff could become proficient at doing it with a short amount of training, 2) the need to read and reset every counter manually or remotely, 3) the need to keep track of not only a single customer's total, but also a daily input total of each commodity, 4) the need to eliminate a double count of any single item, and 5) the ability to print receipts and to analyze input data. Enhancing the flow through the Center really meant that the number of separate times that any one returnable was handled by the workers after the customer brought it in needed to be significantly reduced. These requirements led to the design and construction of 1) a new 3-hole, 1-trough intake table, 2) a 6-hole water-sorting table, and 3) a control and RS485-based data collection system via a Red Lion G310 controller programmed using Crimson 3.0 software.

We welcomed the expansion of our social skills that was brought about by our exchanges with the supervisors and those great individuals with disability at the Massena recycling center as we developed our solutions.

III. Impact

A significant positive effect arises from developing more employment opportunities for people with disabilities. People with physical and mental challenges have fewer opportunities than others in the workforce. This lack restricts many from participating in society and also makes it more difficult for them to self-support themselves. Gainful employment them with important roles and functions in their lives such as work ethic, responsibility, social skills, and a sense of appreciation. The assistive technology that we have provided has been created not just to benefit them and provide them with more opportunities, but also to improve efficiency and production for all redemption centers. Our technology is user-friendly and easy to learn, which is essential for ease of training of those with disability.

NYSARC runs an outstanding business at the redemption center in Massena that we work with, providing many individuals with job opportunities. These individuals are very qualified to perform the tasks especially using the intake table we have created. By providing them with employment opportunities, it gives them a chance to prove their worth. It also gives them the opportunity to be involved in the community, socialize with the customers, and fully participate in society.

While the creation of our tables is mostly focused on providing opportunities for individuals with disabilities, there are also community benefits. Many communities offer redemption center services. The device that we have created could bring a more efficient and potentially faster service for customers. It allows the customers to view the dollar value of their returns, adding to trustworthiness. This encourages customers to return their recyclables, thus promoting environmental friendliness and sustainability.

IV. Project Development

A proof-of-concept totalizer design used four 7-segment displays as well as toilet rings for housing optical sensors. A hobby computer and a keypad were used to enter a bottle count and to provide a payback total (Figure 2). We quickly realized that only commercial electronic components should be used, specifically for ruggedness and maintainability. A major key to the redesign was the use of totalizer dual-display/counters (Red Lion PAXI and CUB5B) that had RS485 communication cards installed in them, such that each could be read or reset by a computer or a commercial controller (Red Lion G310, running Crimson 3.0 software) that simultaneously has a remote display to gave staff a view of current (Counter A) and daily (Counter B) counts from each meter, plus the ability to do flow and cost analyses.

One solution that we designed to greatly enhance flow was to replace the current instrumented single intake totalizer (hole, sensor, counter, display) with a 3-totalizer table where the worker at intake separates out water bottles, plastic bottles and cans. On that table, we added a glass bottle slide-through trough with its own totalizer, as single glass bottles were hand counted before, without any totalizer. We also added a PAXI display that faces the customers to give a running total (in $0.05 increments) of what they are to receive for their returnables, and the ability to print a receipt for them. We put all of these totalizers in an ergonomically appropriate and modular table that we built. The table is easily disassembled (Figure 3), shipped and reassembled on site. The holes have Banner MINI-BEAM SM31E/R opposing beam sensors mounted in toilet rings that transmit across each hole for better counting. The glass bottle trough uses a Banner WORLD-BEAM® QS30ELVC retro-reflective bounce sensor. Delay circuitry (Banner MA4-2 non-retriggerable one-shot) prevents double counts by not allowing the sensor pairs to count when a label started and ended as two containers. All sensors had Euro-style cable disconnects. All wiring was professionally done by us in a galvanized steel raceway (Figures 4, 5).

To ease the sorting process, we additionally designed and built a 6-hole table (Figure 5) for use in sorting the plastic water containers. The Red Lion Cub5B dual counter/displays used have RS485 network capability installed and also have relay cards in them, such that the Banner LEDs can be switched from green to red when a bag reaches the full count required by the vendor. The completed 6-hole intake table awaits final bench testing before being delivered to the center. For demonstration purposes at other recycling centers, we lastly constructed a portable demo unit with one totalizer for a hole and another for a trough, both with RS485 network capabilities (Figure 6).

TESTING: The intake table is now in daily use. We went to the redemption center to compare intake times between the table that had one hole and the table that had three holes. All bags were pre-counted and the number of each type of container in the bag was recorded. The time it took for an employee to count the recyclables at each table was recorded as well as the number that each counter read after all containers were deposited. Timing tests showed that the new table required less that 5% more time to input than the original one-hole table. But, the sort process seemed to be simple and robust enough for staff and workers to operate, and that initial 3-hole sort greatly simplified downstream sorting. Another test was completed that confirmed bottle count accuracy where we put a known amount of bottles through each hole twice, once as a fast run and secondly as a slow run. Next, two bottles were run through a hole in a quick succession, to see how far apart the bottles had to be to be counted as two separate bottles, given the settings on the hole's debounce circuitry. We found it acceptable that two bottles counted as one only when they entered the hole when they were an inch or less apart from each other.

COMMAND AND DATA COLLECTION: The tables alone only gave partial help in improving process flow. To enhance its value, all counter/displays are equipped with electronic communications capabilities, such that both the customer and day counts can be externally read from any meter, or set or reset. A prototype custom LabVIew® program was written. An RS485 signaling line was daisy-chained between counters, each with a unique 2-digit identifier, so that any counter could be read, loaded, reset, or its set-points changed. However, the custom LabVIew® program was not appropriate for an industrial setting.

We acquired a G310 controller from the Red Lion Company for educational purposes. This industrial controller runs Red Lion's Crimson 3.0 software. We programmed it to interface with our tables and a demo unit. One G310 screen shows the customer and day count for each of the intake table's three holes and its glass bottle trough (Figure 7). Provision is made to manually add or subtract an amount to or from a tally. This is especially useful when glass bottles are returned by the case. Reset buttons on the display (and pushbuttons on the intake table) can separately clear either the customer or day counters. Another G310 screen represents the water-sorting table. There each totalizer needs to have its individual bag-full set-point sent to its counter, as the number of items needed to fill a bag might differ by hole. A set point relay in the CUB5B counter/display will switch a Banner EZ-LIGHT® S18L LED from green to red when the bag is full. An addition-al G310 screen works with the demo table. The RS 485 network can easily be expanded to handle 40 counters.

The G310 is programmed to continually read each meter. When any is reset, it stores the counter value previous to the reset in an Excel-readable file. Recorded on a line are the date, time, elapsed time between the first and last recyclable, the worker, customer and day counts of all meters, and the dollar amount paid to a customer. A small PC offloads data from the G310 for record keeping and later analysis of input, customer payout, throughput and productivity. When any counter is reset, a Brother QL-720NW Label Printer will print out a customer receipt for the intake table, a full-bag total label for the sorting table, or a daily tally for any meter. The date and time is noted on the screen and on the receipt or label. Before we can install this system in the recycling center, we need to find funding to purchase a separate G310 for use at the center, as the current G310 is University property and has other educational uses at the university.

V. Conclusions

Throughout the development of this project, countless skills were required to make the development possible. The first step was designing the carpentry needed to make the tables modular, which required drawing and brainstorming the best methods. Ergonomics and safety were considered in the final designs to develop tables and a system that would be a best fit for the capabilities of the workers with disability. Designs were adjusted to limit potential injuries that could accrue from repetitive work. We kept safety in mind throughout the project to ensure that there was nothing that could harm the worker, such as sharp metal edges, exposed screws, etc. Since the tables were made primarily of lumber, a significant amount of hands-on power tool experience was required. Every tool functioned differently, so learning the safe operation of each separately was essential. A table consisted of 4 or 6 sensors, so we needed to gain knowledge of electrical science, since two of us from Chemical Engineering had no previous background in it. We used the Red Lion PAXI and CUB5B counters, so acquiring knowledge of their functions and of how to program and operate the counters was important. Working with a Professional Electrical Engineer helped the entire team learn safe wiring practices and read schematics. The team's computer engineer had to first apply LabVIew® programming to this project and to deal with the vagaries of RS485 wiring and its protocols. Then he had to learn and apply Crimson programming, first by emulation on a PC, and then by its actions in the G310 display/controller. He also was the one to fine-tune the debouncing circuits and to internally program the PAXI and CUB5B counter/displays.

We achieved our overall goal to design and build efficient modular intake and sorting tables, both with rugged and reliable industrial-grade totalizing systems that appear to be easy to use by those with disability in a supported employment environment. We also were able to link the totalizers to a system that could provide control, staff information, and data collection and analysis. The technology employed should increase the recycling center's operating profitability and allow for continued secure employment of those with disability, both within this center and across New York State. This hypothesis will be studied by a future design group. Hopefully there will be a significant positive effect from our work in developing these assistive technologies to provide more employment opportunities for people with disabilities. It thus benefits the individuals themselves, society, and the government, as well as us, from what we learned and have achieved.

VI. Acknowledgments

We thank Tracy Tuttle, business development manager of Saint Lawrence County NYSARC, for her coaching support throughout the period of this ongoing project. Special thanks also goes out to the wonderful workers and staff of the Massena NY redemption center**.** We also thank NYSID CREATE and the Walker Foundation for their funding and Red Lion, Inc, for their in-kind donations to this project.

APPENDIX

Figure 1: The current counting and sorting systems used at NYSARC's Massena recycling center. The single-hole intake process and the totalizers are shown in the top row, and the bottom row shows the sorting table and an example totalizer. The totalizers were made by Red Lion Industries. The system is simple, with a totalizer paired up with a single detector. All counters must be hand-read and then reset as needed.

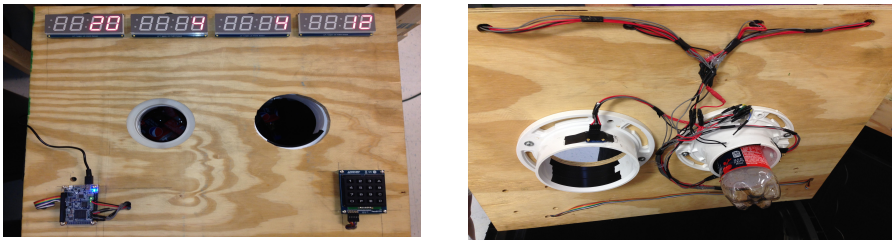

Figure 2:The completed prototype counting system. The two center counters (HT16K33) displayed the hole counts; the rightmost one, the keypad bottle count; and the left one, the total count. The Digilent PmodKYPD keypad and the DE0-nano Altera FPGA are also shown in the top view. The bottom view illustrates the placement of the VCNL 4000 proximity sensors.

Figure 3: All the tables have a modular design to allow them to be easily reproduced for implementation in other redemption centers. A theme throughout design and construction has been to strive for an IKEA type product, easy to transport, assemble, or disassemble. The intake table is composed of eight pieces that can be quickly (~5 min) disassembled into a 32"W x 74"L x 8"H (81.3 X 188 X 20.3 cm) package, and reassembled in about 10 min. Broken down, it can be easily transported by any large SUV or a truck. The sorting table also disassembles, but into a slightly longer package (96"L = 244 cm). Both tables include a drainage system.

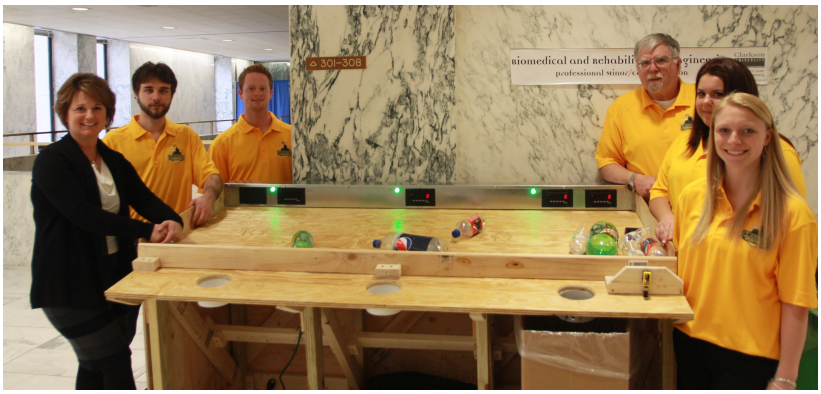

Figure 4: The completed Intake Table. The students were given the opportunity to demonstrate their table at the CREATE Conference at the NY State Legislative Office Building. NYSARC representative Tracy Tuttle was at that showcase, as were individuals form NYSID, the sponsor of the table and of the exhibition. Note the galvanized steel raceway at the back that houses the counter/ displays and the indicator lights. The glass bottle counting trough is at the right front of the table.

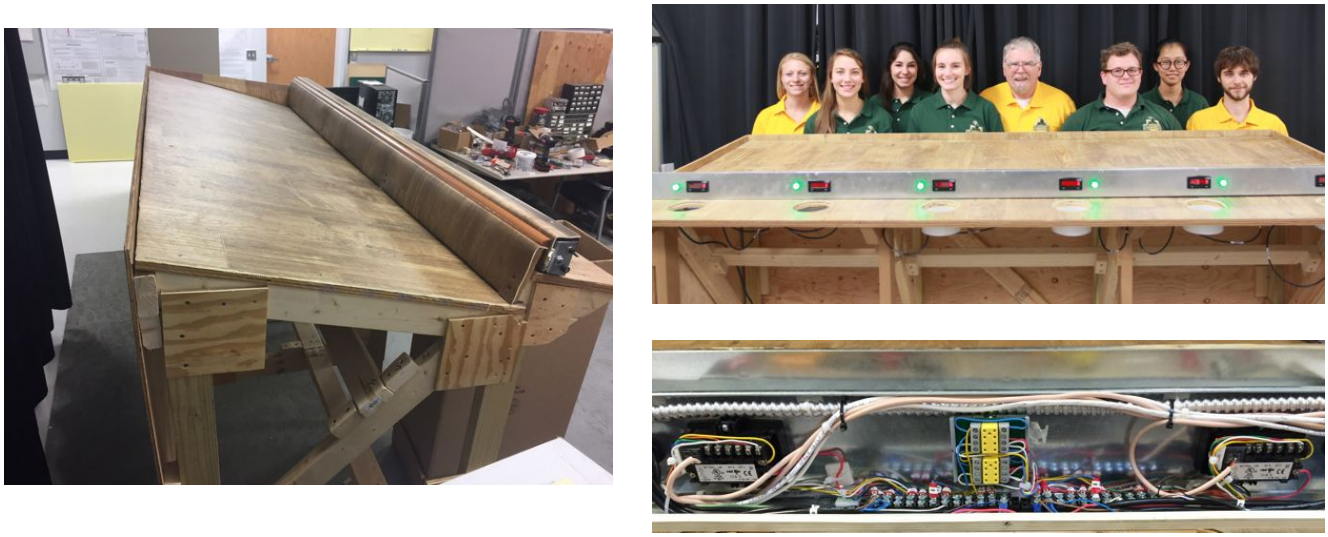

Figure 5: Side view of the finished sorting table in the lab with one side removed to highlight the leg construction. The front view shows the totalizer holes and the raceway that contains the counters and indicator lights. The Fall'15 student design team is behind the table. Two CUB5B counters can be seen in the raceway. All wiring was done via terminal blocks. The yellow sockets are for the Banner non-retriggerable one-shots. The pink and white cables carry the RS485 signals.

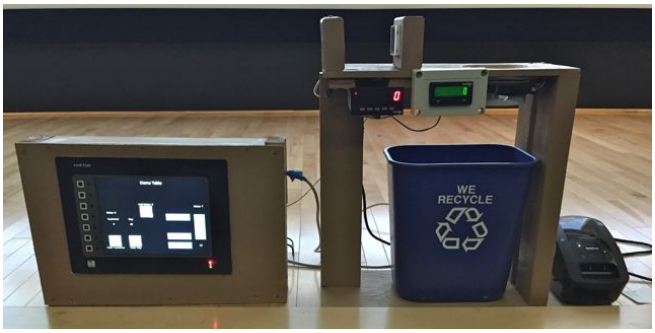

Figure 6: The demo fixture. A PAXI counter/ display services the retroreflective trough sensor, while a CUB5B counter services the emitter/ receiver sensor pair on the hole. Both counters have RS485 and set-point modules installed. The G310 display is also shown. One of its screens was programmed to interact with this demo table. The label printer is on the lower right side.

Figure 7: Prototype intake and sorting table display screens for our Red Lion G310 controller. It communicates with the counters via RS485. It can read, set or reset any of the counters and their set points. On the intake screen, staff will see the current count per customer and per day, can add or subtract to a customer count, and can reset the customer counter when that customer is finished. The G310 will then cause a receipt to be printed. On the sorting table screen, staff sets the bag-full limit for each hole, sees the current count under each hole and gets a visual flashing signal when a bag-full count is reached. At the point, the worker will see the indicator light on the raceway near the hole change from green to red. When that counter is reset, a full count label will be printed so that it can be attached to the just-filled bag. All data is stored for off-line retrieval.

Smart Medical Assessment and Review Technology Assistance (SMARTassist)

Abstract—Miscommunication is a multi-billion dollar problem in operating rooms across the US[1]. We propose SMARTassist: a simple solution that maximizes workflow efficiency to reduce communication gaps and role redundancies. SMARTassist is designed to prevent miscommunication before it occurs, and could improve the quality of surgical care. Thus far, the back- and front-end of SMARTassist prototype has been designed, as well as the wearable devices associated with this solution. Preliminary product testing has been conducted through consultations with surgeons. Future work will include evaluation of SMARTassist's performance in the operating room (OR) by measuring operating time, team stress reductions, and resource waste prevention.

I. Problem Statement

Miscommunication events occur in virtually every surgery performed, resulting in longer operational times, resource waste, and injuries to patients[2]. An average of 8.4 miscommunication events occur per surgery, 3 of which lead to visible consequences[2]. Miscommunication events can be classified as problems with "occasion", "content", "purpose", and "audience"[2], each of which is presented in more detail in Table 1. Considering that an estimated 51.4M operations occur yearly in the US[3], this problem poses a substantial drain to the healthcare system. To date, several solutions have been proposed. For example, Ascom[4] and Vocera[5] have developed headset systems to fit into the clinical setting. Albeit helpful, these solutions resolve only "audience" events, which account for 20.9% of all miscommunication instances that occur in the operating room (OR)[2]. Other solutions addressing different categories, such as Visi Mobile[6] or AwarePoint[7], cater towards non-OR nursing staff to optimize nurse-patient interactions. Unfortunately, these solutions each address one subcategory of miscommunication events, and are moreover insufficient in the context of a surgical team[8]. We therefore aimed to develop a system that encompasses the design elements of existing products, and that also satisfies additional criteria deemed critical to enhance surgical team synchronization, and hence reduce miscommunication. These criteria include the development of a solution that enhances surgical efficiency by improving communication among surgical staff, has a positive benefit-to-cost ratio, is easy to incorporate within ORs, is user-friendly, and does not interfere with pre-existing medical equipment and staff. Table 2 summarizes why each criterion was selected for consideration in our engineering developments.

II. Proposed Solution

There is no commonly applied method to address miscommunication between surgical staff, however whiteboards are routinely used to enhance team efficiency[9]. We propose to improve OR efficiency and communication with SMARTassist (Systematic Medical Assessment and Review Technology Assistance). SMARTassist consists of interactive software, OR monitors (Fig 2c), and two types of wirelessly paired headset communication systems (Fig. 2d). The monitor display is founded on the principles of the Toyota Lean Manufacturing Model, which describes a system that eliminates resource waste (including physical, time, and work resources) to maximize production outflow[10]. Previous attempts have been made to introduce the Lean Model into ORs via teaching approaches, but with unsuccessful adherence[11]. SMARTassist achieves this by methodically organizing and displaying information geared towards organizing the surgical staff in a way that eliminates gaps in coordination and role or task redundancy (see Fig. 1a as monitor display example). Ubertooth[12] forms the basis of the SMARTassist software and hardware: it can transmit with a bluetooth headset to apply the information into the SMARTassist program. The staff can edit the details that appear on the screen using the input software KiSSFLOW[13] (Fig. 2a), which will integrate into the Ubertooth platform via Zapier[14] integration software. Lastly, KiSSFLOW outputs an electronic form with the collected data, which can be added into the patient's chart. An example of this process is presented in Fig. 2b with noteworthy details of each software outlined in Table 3. The integration platform is presented in Fig. 2d. SMARTassist serves as a communication channel between surgical team members, but also takes an active role in organizing the staff. No competitor has yet achieved this goal. This has the potential to improve team efficiency, which may reduce operation times, resource waste, and staff stress levels. Additionally, this product helps hospitals become WHO[15]- and HIPAA[16] -compliant, as these standards are inputted into the SMARTassist program. This adds a quality-assurance function to this solution, ultimately improving the quality of surgical care received. Moreover, existing OR monitors can be integrated into SMARTassist, where a side-by-side display may augment surgeries. Most importantly, this product aims to reduce procedural errors and thus decrease resource waste and injury to the patient, while also minimizing team stress. It is important to note that the software constitutes in downloadable components, which can operate independently of an Internet connection, however hospitals can connect SMARTassist to their secure intranet network, allowing for facilitated

information sharing between staff. Lastly, this solution is affordable and user-friendly, encouraging acceptance into the hospital setting. For more information, Table 4 describes how SMARTassist achieves each of the five advantages presented here.

III. Impact

SMARTassist is designed to minimize resource waste in the OR, resulting in significant expense reductions for the patient and the hospital. It also aims to improve the quality of surgical care: reducing the number of communication errors in the OR will improve the quality of care received by the patient while decreasing operational times. It is difficult to approximate the cost of resultant visible consequences, however an estimated $24B is lost due to time waste alone in the OR[17]. Additionally, an average of 98,000 patients die yearly as a result of surgical team miscommunication[1]. Moreover, the workload of surgical staff has been consistently increasing over the past 5 years[3,18], producing accumulating strain on surgical teamwork dynamics. There is therefore a demand for a product that optimizes workflow to prevent miscommunication events before they occur. The implementation of SMARTassist is predicted to impact several stakeholders: the surgeon, surgical staff, patient, hospital, and government (stakeholder analysis in Table 5). While this forms the core group of directly involved professionals, SMARTassist can be applied to other team-based hospital units, such as the Emergency Department, ICU, or the Neonatal Unit, with some modifications. A fully functional program would therefore improve the overarching quality of healthcare by the systematic allocation of resource that prevents misuse leading to waste and unnecessary institutional spending.

IV. Project Development

This project was developed as part of BME498, a Biomedical Engineering Capstone Design course under the supervision of Dr. Sabine Weyand. The project development began with needs finding which comprised of research, interviews, and surgical observations to identify problems pertaining to the OR. A total of 52 issues were identified, then filtered to the top three problems, from which the need to address miscommunication errors was selected based on preference and feasibility (process outlined in Fig. 3). Next, this need was validated through further interviews, then proceeded into solution ideation. A concept map of potential solutions was initially developed (Fig. 4a). From here, the resultant solutions were merged into one product: the SMARTassist Communication System (Fig. 4b). The monitor display screens (Fig. 1a) and headset devices were concurrently prototyped to present a complete model to surgeons (Fig. 1b). Once these were finalized, back-end technology assembly planning proceeded, starting from the Ubertooth foundation, then accessorizing with KiSSFLOW and Zapier. Lastly, the updated prototype was presented to surgeons as means of product testing. SMARTassist was positively received, where surgeons expressed interest in applying our solution in their OR. To this end, a works-like and looks-like prototype of SMARTassist and headset system has been developed. Future advancements include the incorporation a Bluetooth-operated camera attachable to the surgeon's accessories (such as glasses, loupes, or light headband) to stream live images of the procedure on the SMARTassist display. This will allow for more staff to keep on track with the procedural steps, as well as add a teaching function to our solution. The immediate future directions center around robust product testing, where the performance of SMARTassist in the OR is measured in operating time and team stress reduction, and resource waste prevention. This data can be used to improve our product and provide an upgrade to our consumers.

V. Conclusions

With SMARTassist, hospitals will be able to efficiently spread resource use across more surgeries, while simultaneously improving the quality of surgical care provided. We have proposed a simple solution to the long-standing problem of OR miscommunications. SMARTassist organizes the surgical team workflow to systematically reduce gaps in staff roles and role redundancies. To this end, a works-like and looks-like model of SMARTassist has been developed and successfully undergone preliminary product testing, revealing initial positive evaluations by surgical staff. In a more holistic view, minor technical adjustments and further testing must first be resolved before SMARTassist can be fully tested in the clinical setting. Nevertheless, this rapid fine-tuning process does not pose a substantial impediment towards bringing SMARTassist into surgical rooms. Moreover, this solution has the potential to expand beyond the operating room, and could therefore impact healthcare at the institutional level.

Ultimately, SMARTassist is a pioneering solution to an aggressive upcoming problem echoing throughout the entire healthcare system: an increase in the workload of surgical staff leading to a more chaotic OR environment[18]. A decline in the quality of surgical health care is projected provided that hospitals remain unadapted to these accumulating stresses[3,18]. Instead, we propose a solution that improves surgical staff workflow efficiency to industry manufacturing standards that would allow healthcare centers to adjust to the forecasted workload and financial burdens.

REFERENCE

1. Wachs JP, Frenkel B, Dori D. Operation room tool handling and miscommunication scenarios: An object-process methodology conceptual model. *Artificial intelligence in medicine*. 2014;62(3):153-163. http://www.ncbi.nlm.nih.gov/pubmed/25466935. doi: 10.1016/j.artmed.2014.10.006.
2. Lingard L, Espin S, Whyte S, et al. Communication failures in the operating room: An observational classification of recurrent types and effects. *Quality & safety in health care*. 2004;13(5):330-334. http://www.ncbi.nlm.nih.gov/pubmed/15465935. doi: 10.1136/qhc.13.5.330.
3. Center for Disease Control and Prevention, (CDC). National hospital discharge survey: 2010 table, procedures by selected patient characteristics - number by procedure category and age. *National Center for Health Statistics*. 2010.
4. Ascom. Ascom wireless solutions. http://www.ascom.com/en/index/.
5. Vocera. Vocera healthcare communications. http://www.vocera.com/industry-solution/healthcare-communication.
6. Vandrico Inc. Visi mobile Wearable Device. http://vandrico.com/wearables/device/visi-mobile.
7. AwarePoint. AwarePoint Healthcare. http://www.awarepoint.com/industries?prodId=0.
8. Looi T. Interview with Dr. Thomas Looi. Nov 2015, Jan-Mar (monthly) 2016.
9. Burns D. Interview with Dr Burns . Jan-Mar (monthly) 2016.
10. Krafcik JF. Triumph of the lean production system. 2003:193-210. http://www.econis.eu/PPNSET?PPN=371850584.
11. Collar RM, Shuman AG, Feiner S, et al. Lean management in academic surgery. *Journal of the American College of Surgeons*. 2012;214(6):928. http://www.sciencedirect.com/science/article/pii/S1072751512001974. doi: 10.1016/j.jamcollsurg.2012.03.002.
12. Ossmann M. Ubertooth one. http://hakshop.myshopify.com/products/ubertooth-one (2016)
13. KiSSFLOW. Business process management tool and workflow software. 2016. https://kissflow.com/.
14. Zapier. The best apps, better together. https://zapier.com/. Updated 2016.
15. Alnaib M, Al Samaraee A, Bhattacharya V. The WHO surgical safety checklist. *Journal of perioperative practice*. 2012;22(9):289. http://www.ncbi.nlm.nih.gov/pubmed/23101171.
16. Laflamme FM, Pietraszek WE, Rajadhyax NV. Reforming hospitals with IT investment. McKinsey & Company Web site. http://www.mckinsey.com/industries/healthcare-systems-and-services/our-insights/reforming-hospitals-with-it-investment. Updated 2010.
17. Weinbroum AA, Ekstein P, Ezri T. Efficiency of the operating room suite. *The American Journal of Surgery*. 2003;185(3):244-250. http://www.sciencedirect.com/science/article/pii/S0002961002013624. doi: 10.1016/S0002-9610(02)01362-4.
18. American Hospital Association. Fast facts on US hospitals. 2016. http://www.aha.org/research/rc/stat-studies/fast-facts.shtml
19. CMOSIS. Naneye GS family module. http://www.cmosis.com/products/product_detail/naneyegs_module. Updated 2016.

APPENDIX

TABLES

Table 1. Miscommunication events subcategories and their respective definitions[2].

Miscommunication subtype	% of all miscommunication events	Description
Occasion	45.7%	The information was requested too late to be of maximal use
Content	35.7%	The information exchanged was missing or inaccurate
Purpose	24.0%	The issue remained unresolved
Audience	20.9%	The key staff member was absent

Table 2. Design criteria for our ideal solution and the reason for incorporating them into the engineering process.

Must-haves	Description	Nice-to-haves	Description
Improve surgical efficiency by enhancing communication among surgical staff	The key outcome that our product is going to solve	Positive benefit-to-cost ratio	Induce interest in potential customers
Neutral benefit to cost ratio	Maintain sufficient benefits for customers to be interested	Small product size	Support easy incorporation to the operating rooms
Easily incorporated within the operating room	Less work is needed to physically install the products into the operating rooms	Operation of the device does not require physically contacting it - free of hands	Avoid wide-spread cross contaminations
Easy to use (simple and straight-forward) by the surgical staff	Rapid incorporation of the product with the workflow of surgical teams	Multifunctional device → also include other different functions	Increase benefits and interest to the customers
Do not interfere with surgical staff/equipments within OR	Cause no malfunctions to the surrounding vital medical equipments		
Minimize the 4 types of miscommunication events	Reduce incidence of occasion, audience, purpose and content		

Table 3. Description of the functions and advantages of each SMARTassist components.

Component	Function	Advantages
Ubertooth	Transmit and receive bluetooth signals to apply information into the SMARTassist program	• open source software and hardware with a large support community • uses Python language • can perform highly complex tasks and algorithms • can integrate context-awareness • can integrate natural-language processing
KiSSFLOW	Input software that could flexibly transform the displayed information on the SMARTassit program	• uses flowchart model to define workflow (easier than programming) • can edit permissions where only certain individuals are allowed to answer specific prompts that appear on the screen • can add a timestamp of when a prompt should appear on the screen • user friendly platform that uses drag-and-drop commands • can add mathematical functions to commands
Zapier	Integrate the KiSSFLOW software with Ubertooth platform	• simple integration that does not require coding on behalf of the user

Table 4. Summary of the five advantages of SMARTassist system.

Advantage	Counteracts	How this is achieved	Outcome
Communication channel	Audience	Using the headset devices to improve direct communication between staff, and the SMARTassist prompts to encourage	Improves team efficiency, and therefore reduce time waste, resource waste and staff stress level
Electronic record generation	Content and occasion	End-screen with option to save the collected information into a file stored as electronic data	Advance hospitals' ability to become WHO- and HIPAA-compliant
Quality assurance	Content	Improves compliance with WHO, HIPAA, and hospital regulations each time a personnel confirms to SMARTassist that an action has been performed	Improved quality of surgical care provided by the surgical team
Reduces procedural errors	Occasion and purpose	Displaying predetermined prompts of events that are commonly forgotten or left incomplete, or when the action of one staff member must follow the action of another teammate	Reduces resource waste, injury to the patient, unnecessary team stress
Affordable and user-friendly	Audience and occasion	Aesthetic graphics and easy-to-follow instructions	Increases acceptability of SMARTassist into the OR by surgical staff

Table 5. The analysis of all stakeholders that will be affected with our product.

Stakeholder	Category	Impact of our need	Details
Surgeon	Direct involvement	Highly positive	Improved synchronization of the team could relieve unnecessary stress experienced by the surgeon to ensure that all members of the surgical team are caught up in the procedure; improve communication between surgeon (team leader) and the rest of the staff; decreased operational time
Surgical Staff	Direct involvement	Highly positive	Improved and easier management and different staff roles; improved communication between staff, and to the surgeon
Patient	Direct involvement	Positive	Decreased surgical time with potential reduced recovery period
Hospital	Direct involvement	Highly positive	Longstanding decreased in cost per surgery would far outweigh the initial purchase and implementation of the system; patient flow would also be enhanced
Government	Secondary involvement	Highly positive	Decreased cost per surgery; improvement in the overall quality of healthcare would have a positive impact on the country's economy.

FIGURES

Figure 1a. Example of a sequence of SMARTassist screens.

Figure 1b. Example of the headset incorporated with the SMARTassist display system. **Left:** headset recommended for use by nursing and anesthesia staff. **Right:** headset recommended for use by surgeons, surgical residents and fellows.

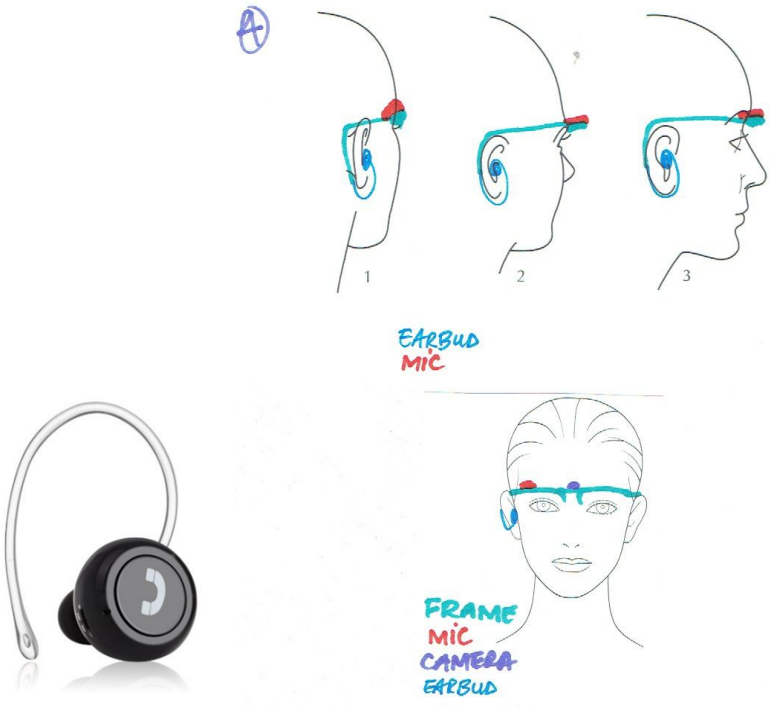

Figure 2a. Editing software for SMARTassist (KiSSFLOW). **Top**: form-defining input to edit checklists. **Bottom**: Workflow-defining input to edit the prompts that appear on the monitor display.

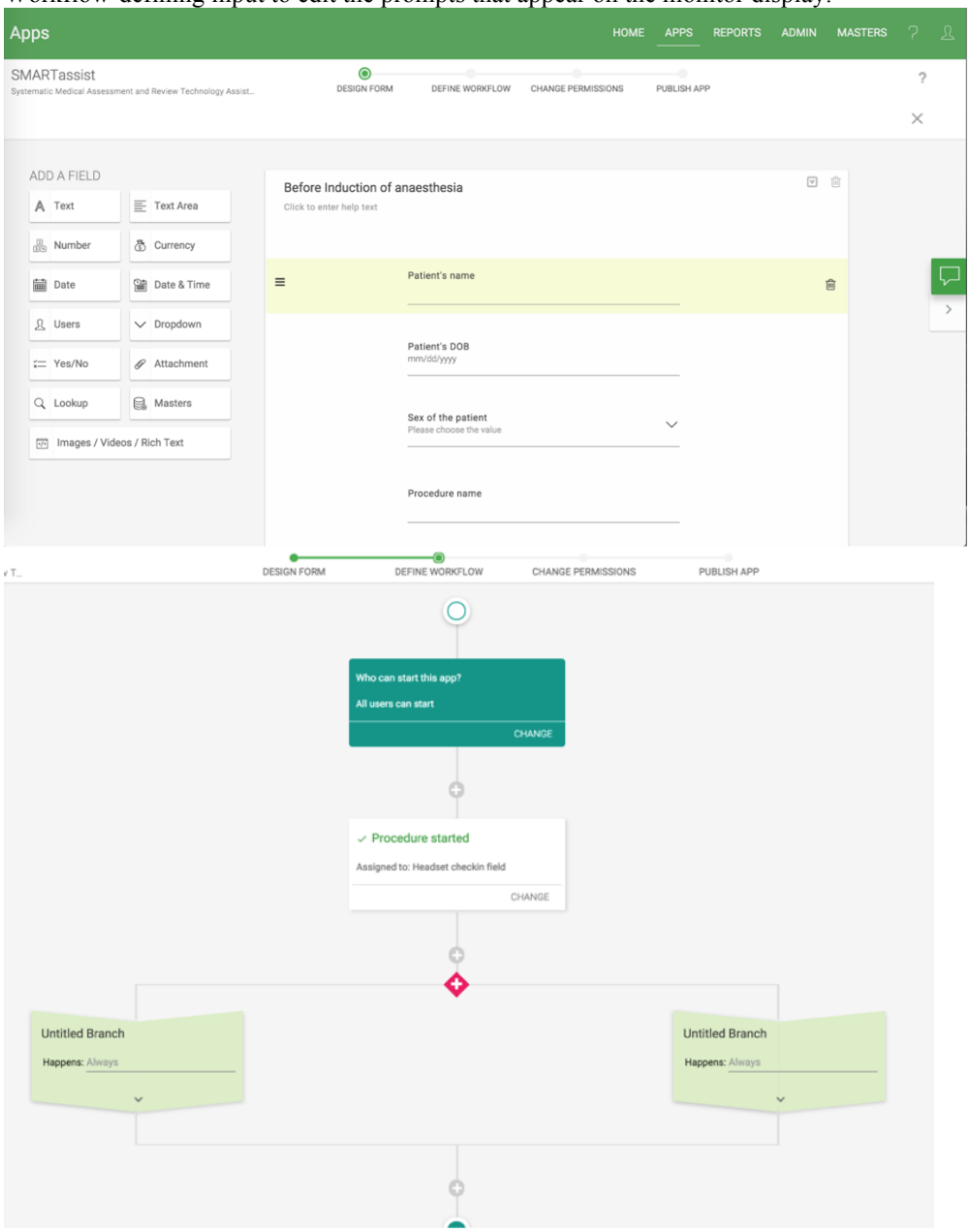

Figure 2b. Example of fields of an electronic patient chart as outputted by SMARTassist.

Before Induction of anaesthesia

Patient's name
N/A

Patient's DOB
N/A

Sex of the patient
N/A

Procedure name
N/A

Mandated requirements
N/A
Example: DNR

Optional requirements
N/A
Example: glasses must be kept with patient

Please list the name of all staff and non-staff present during the procedure
N/A

Headset checkin

Headset checkin
N/A

Pre-op checklist

Before the incision
N/A

Anticipated critical events - Surgeon
N/A

Anticipated critical events - Anesthesia
N/A

Anticipated critical events - Nursing Team
N/A

Surgical props

Have antibiotics been administered
No
Propofol (25mg); Warfrin (100mg)

Has the trigeminal nerve been located?
No

Figure 2c. Set up of the SMARTassist monitors in the OR.

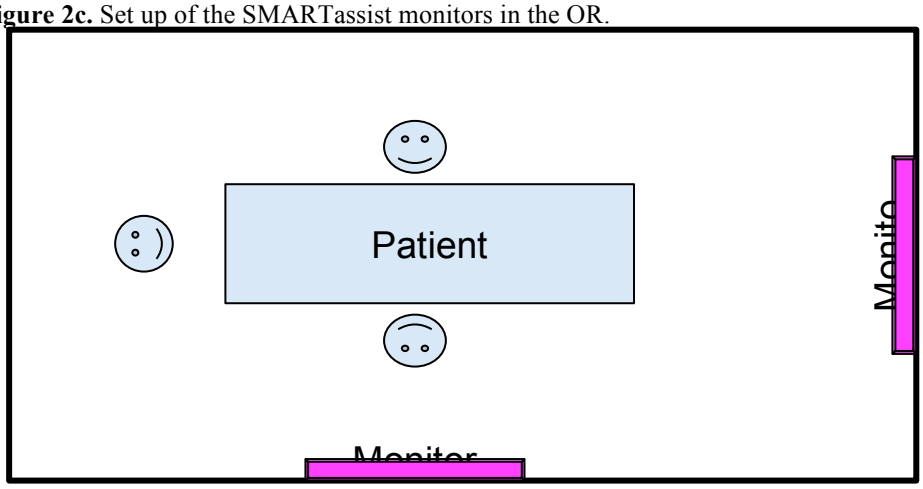

Figure 2d. Software interactions among Ubertooth, Zapier and KiSSFLOW within the SMARTassist system.

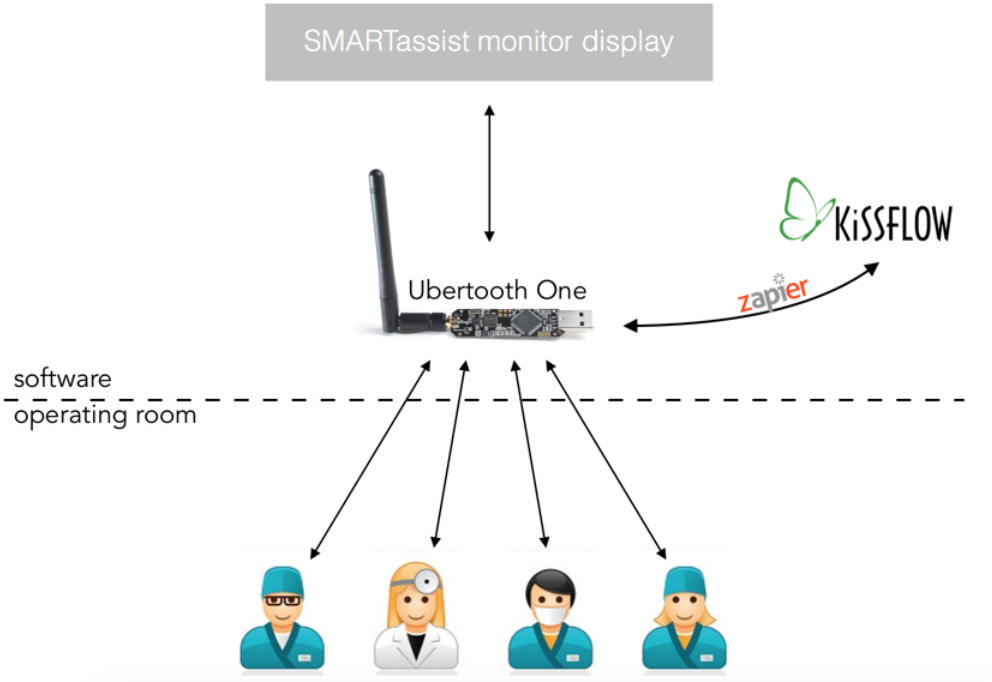

Figure 3. Need finding and need screening process, where 52 needs were identified initially and then filtered to the top three needs. The final need selected was to address miscommunication based on preference and feasibility.

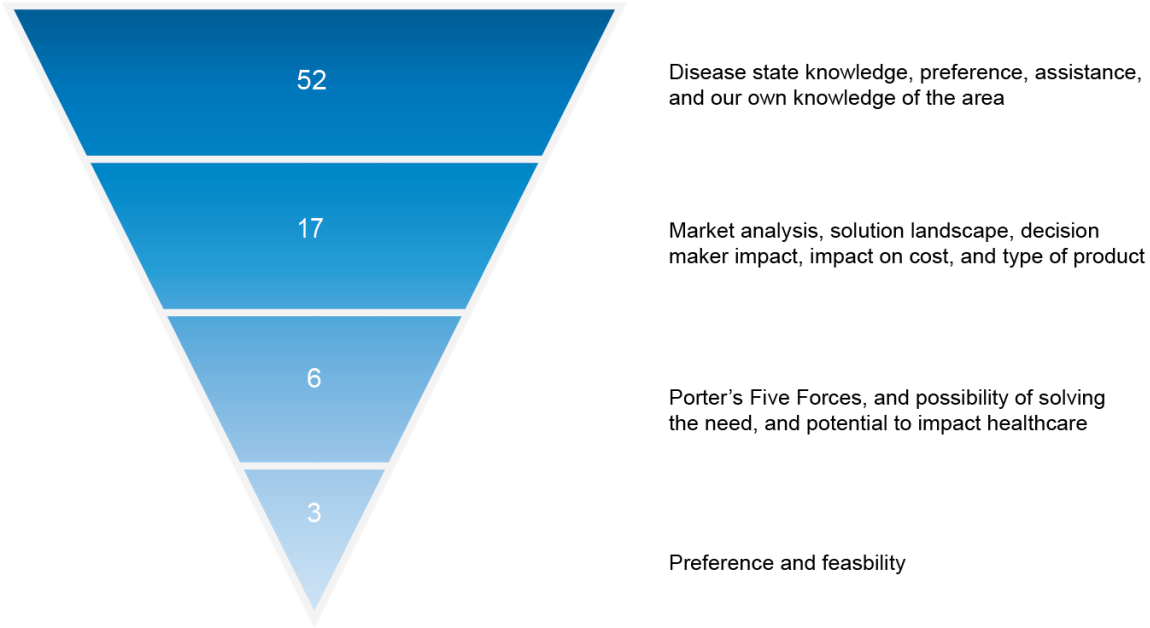

Figure 4a. A concept map development of the potential solutions for our selected need.

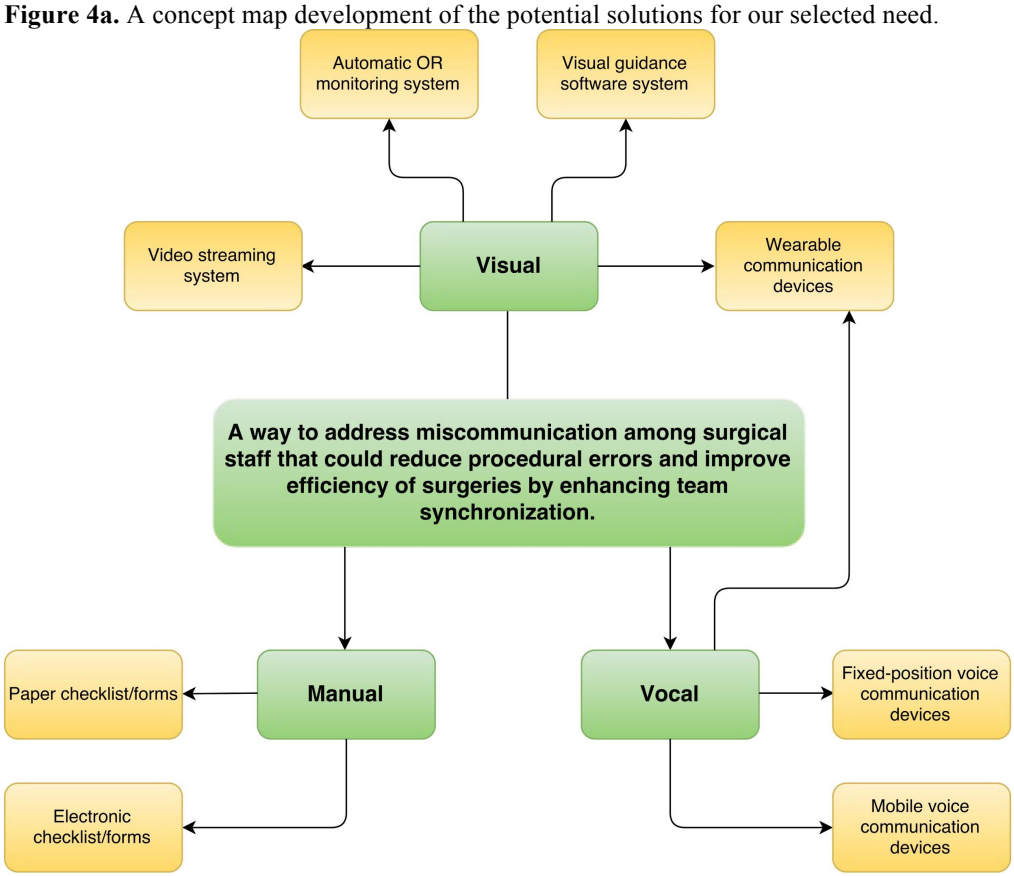

Figure 4b. Illustration of merged resultant solutions into the SMARTassist Communication System.

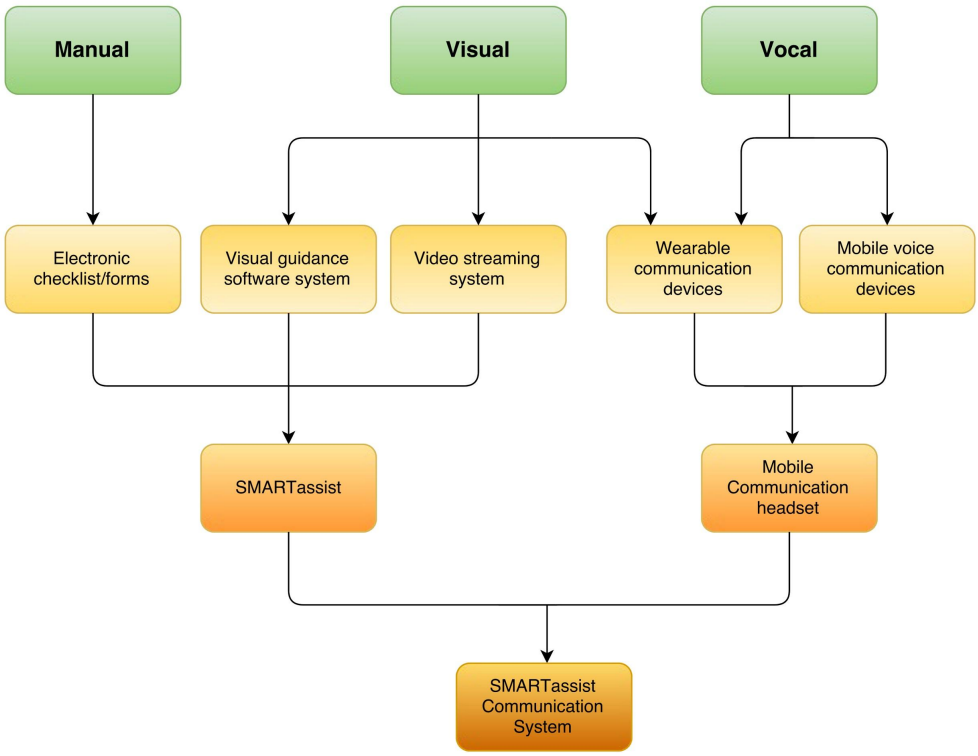

Tissue Simulation in Crash Test Dummies

Capstone Carleton University Crash Test Dummy Project

Abstract— Tissue simulation is a new area of focus in the Crash Test Dummy project. It allows for components in the dummy to behave similar to a human, which has an impact on injury analysis and collision incident investigation.

The previous design of foam limb coverings was replaced with a new design of a 3D printed Filaflex muscle mimicking both shape and stiffness of real muscle tissue. A redesign of the dummy's neck was done to allow the neck to have the ability to change stiffness throughout the crash, to better simulate a cyclist. This design incorporates FilaFlex and ferromagnetic fluids.

I. Problem Statement

The goal of the Carleton University Crash Test Dummy Project is to create a crash test dummy that can be launched on a bike and used in a cyclist-vehicle collision. Currently there are no features of the dummy that have similar properties to human tissue. This is a problem because, as a result of this inaccuracy, the dummy does not react to the crash as a human would. Without an accurate impact and crash, the effectiveness of the dummy, and the data collected is extremely limited. The current coverings of the crash test dummy were created to protect the dummy from damage. However, in order to properly understand the effect of a cyclist collision, the dummy should be designed to have an accurate range of motion, and absorb impact energy similarly to how a human would during a crash.

Current crash test dummies for commercialized use are primarily for vehicle collisions. With little data in the field it was important to improve the accuracy of the current project designs. Looking at vehicle collision dummies it was found that the main material selections were consistent across different models. In terms of muscle coverage, foam and vinyl are used to simulate muscle and skin for most current models [1]. For neck designs, models vary depending on the desired collision type. This is because the neck reacts differently depending on if an impact is from the front, rear, or side. However, the main components are of aluminum and of rubber. In both cases, there has been some progress in attempting to achieve stiffness through the application of springs and actuators to simulate muscle stiffness for the neck and limbs [2]. However, these designs do not properly display a biofidelic design, and were very specific for vehicle collisions.

When creating limb coverings, the designs had to provide full covering of exposed parts. This was necessary to limit unwanted scrapes to the ground that could confuse the investigation. However, it did not allow any injury analysis of the dummy to be completed, as it did not absorb impact energy in any way measurable to how human tissue would. In terms of the intervertebral neck design, the neck had to have the ability to change in stiffness. During the launch phase of the crash, which is when the dummy is on the bicycle accelerating down a track, the neck must limit motion. As well, the design had to be able to withstand various crash configurations. This design had to achieve this with the dummy in order to have an accurate launch, and limit noise in sensing data that would occur if head oscillations were present. Previous designs were unable to achieve these requirements. Overall, this design will provide a solution to creating a more anatomically accurate crash test dummy, which will allow a more effective use of crash test dummy testing to be made.

II. Proposed Solution

This year, simulated muscle tissue was added to the crash test dummy, as well as a design for intervertebral disks that could be used in the neck of the dummy.

The current design of the dummy involves foam covering steel limbs, this protects the steel limbs from scraping the ground but does not absorb impact energy like real muscle. Therefore, a 3D printed Filaflex muscle was designed to mimic the shape and stiffness of real muscle. This was done to not only continue protecting the bone but also allow for the dummy to behave more accurately during crashes thus also allowing for more effective measurements.

For the intervertebral disk, current designs involved a neck brace breaking on impact in order to change the range of motion of the neck. Although this method was successful, it did not provide anatomical accuracy, and required a new piece for every test. In order to achieve the stiffness transition, the proposed intervertebral disk design uses ferrofluids to allow the neck to change in stiffness. When a magnetic field is applied, the magnetic moments of the ferrofluid line up along the field in order to create a more solid material change [3]. As ferrofluids have the ability to quickly change properties with a magnetic field, they were selected. In order to achieve this, the rugged encasement of the intervertebral disk will be simulated through a FiliaFlex 3D printed capsule. This will provide the necessary stiffness to allow motion. Encased in this capsule is the ferrofluid, which during the launch phase will be induced with a magnetic field in order to achieve the additional stiffness in order to achieve mechanical stability in the neck.

III. Impact

This project has a special importance in Ottawa. As of a 2011 study, there are over 300 cyclist collisions per year in Ottawa alone [4]. The implementation of tissue simulation in a crash test dummy will allow better scene analysis, and

hopefully more accurate injury analysis that can help to lead to fewer cyclist collision deaths. As this project is affiliated with the Ottawa police, one of the main impacts this design will have is on the improvement of crash simulations.

Tissue simulation in the crash test dummy allows the dummy to react to the events of a crash in a more similar way to how a human would. A more accurate design would allow the Ottawa police to collect more valuable data from the crash test. The use of simulated tissue also opens many areas of improved injury analysis. During impact, the energy absorption in tissue is an important factor on the injuries a person will sustain. Through tissue simulation, similar properties are obtained, which means the injury analysis completed in the dummy will be more realistic to what a person would sustain during impact. Focussing specifically on the spine, the movement of the cervical spine, or neck dictates the positioning of and movement of the head. With this accuracy, sensing information obtained from the head allows an analysis of whether a crash would lead to a fatal cranial injury. Even more so, this information could impact bicycle helmet research. As the dummy can be used for different crash configurations, the effectiveness of various helmet designs can be tested and rated for various uses.

Overall, this design project does not only aids police in the recreation of a cyclist-vehicle collision in order to improve incident investigations, it also provides more opportunities for injury analysis, which can develop new safety standards. As there are no current cyclist dummy simulations currently available, this design project helps to solve the current lack of information on cyclist injuries and deaths that are occurring everyday. Through this design, the goal for improved safety on our roads is being reached.

IV. Project Development

Simulated Muscle

As a base for the 3D printed muscle, a carbon fibre rod with aluminum end clamps was made this year to replace the large steel limbs, see Figure 1, Appendix A. This new compact and lightweight design has now opened the door for adding simulated muscle to replace the foam that currently covers most of the dummy. The first thing to take into account was to find out the approximate infill and wall thickness required to simulate the stiffness of muscle tissue using flexible 3D printable materials.To do that compression testing was done to aquire the force displacemnt curves and from that of both a pork muscle sample and various samples of 3D printable materials. From these graphs the first linear slope of each sample was taken as the stiffness of the sample. When correlated together the graph in Figure 2, Appendix A, was obtained showing various materials and the effect the infill and wall thickness has on their stiffness. From this graph any of the materials could be used to replicate the stiffness of tissue which was found to be 7.49 N/mm but filaflex was chosen based on its workability as it's the easiest to print and has the best quality of the three after being printed.

From here, a model of the forearm was needed to be made which was anthropomorphically correct. To do this the visible human project was used to get CT cross sections of a male forearm and from these cross sections a model was made in Creo which was designed to anchor to the clamp of the wrist of the dummy, see Figure 3, Appendix A. This design was applied to the forearms of the crash test dummy for testing this year. As shown in this figure, the finalized model was able to properly fit its design requirements. During testing, it was found that the design had minimal damage between crash tests, which was desirable for the design in order to limit testing time for trials. As the dummy was not in the stage of completing full injury analysis, the results of the applied muscles were unable to be tested further.

Intervertebral Neck Design

The preliminary disc design consisted of a solid magnetic material that was a mixture of latex and iron filings. Many prototypes were made, however the one that was tested consisted of 55% latex and 45% iron filings, and can be see in Figure 4 in Appendix B. Using MTS Compression testing, the material was tested under increments of set displacements, while the resulting forces were recorded. The testing apparatus is shown in Figure 5 and Figure 6 in Appendix B. A block of aluminum was used as a base for the material to be tested on. The block had a slot for an electromagnet that was inserted flush into the aluminum. This allowed a magnetic field to be applied to the material without changing the base.

An initial test was done to precondition the material, before meaningful results were recorded. Two compression tests were then performed, once with a magnetic field and once without. The displacements and forces were recorded for these two tests. From this data, the forces and displacements were plotted (Figure 7, Appendix B). The stiffnesses of the material were found using the slope of the linear regions of the plot. It was found that the stiffness of the material did increase when introduced to a magnetic field, however the overall increase was less than 3%. From these findings, it was concluded that the design should be changed to incorporate ferrofluids, as ferrofluids have the ability to act as a solid immediately with a magnetic field, and would have a more effective change when a field is applied. Testing is currently being done to validate the use of ferrofluids.

The final design of the neck is shown in Figure 8, Appendix B. The intervertebral discs would be 3D printed using Filaflex. This would serve as a capsule for the ferrofluid. An advantage to 3D printing the discs is the ability to create a stiffness similar to human intervertebral discs, using the same method used to produce simulated muscle. The vertebrae would be made of aluminum discs that contain slots for electromagnets. This would allow for electromagnets at each level of the neck. The crash test dummy has a battery that is capable of powering the magnets, as well as a switch that controls when the battery is in use. With these features, and this design, the stiffness of the neck can be controlled with the ability to change the properties of the ferrofluid. This prototype has currently not been tested and applied to the crash test dummy.

V. Conclusions

The new design components allow a higher level of accuracy in the cyclist crash test dummy. Tissue simulation through a muscle sleeve, have improved the dummy skin coverings. In addition, it has helped to improve crash impact analysis as it allows the dummy to behave in a more accurate manner. Current proof of concept designs in the intervertebral disk designs have shown that the use of a ferrofluid can be used to induce a magnetic field in order to stiffen components of the neck and create a more realistic launch and crash simulation.

If a crash test dummy is not able to accurately represent a human during an impact, it has little effectiveness in rating safety devices. In order to improve safety, tissue simulation in crash test dummies should be continued and expanded. Through accurate simulations greater understanding of a collision will be known, which can lead to improvements in police investigations, first responders injury analysis, and helmet manufacturing. The innovation of creating a tissue simulation on a crash test dummy is a new avenue that has not been explored in previous years of cyclist-vehicle crash simulations.

References

[1] “Hybrid II 50th Male Dummy”, Humanetics Innovative Solutions, [online], http://www.humaneticsatd.com/crash-test-dummies/frontal-impact/hybrid-ii-50th (Accessed: 25 April 2016).
[2]”BioRID-II”, Humanetics Innovative Solutions, [online], http://www.humaneticsatd.com/crash-test-dummies/rear-impact/biorid-ii (Accessed: 25 April 2016).
[3] “Ferrofluid: Magnetic Liquid Technology”, FerroTec, [online]. https://www.ferrotec.com/technology/ferrofluid/ (Accessed: 30 March 2016).
[4] “2011 Ottawa Road Safety Report”, City of Ottawa, 2011, [online], http://ottawa.ca/en/2011-ottawa-road-safety-report (Accessed: 05 March 2016).

APPENDIX

Appendix A : Simulated Muscle Design Figures

Figure 1. Prototype carbon fibre and aluminum clamp design for this year's dummy forearms

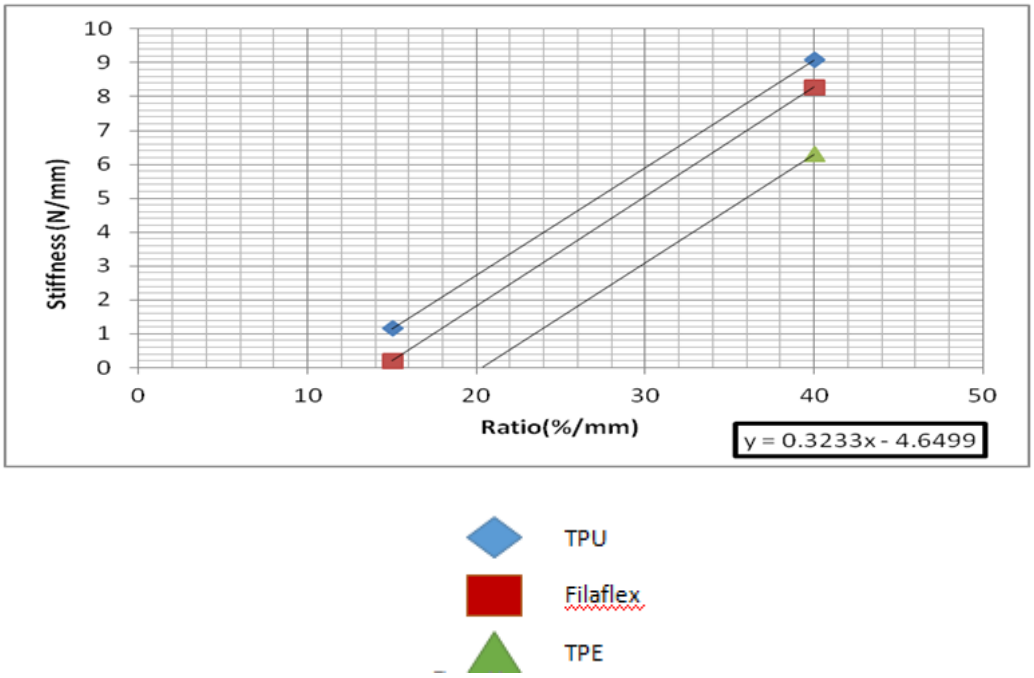

Figure 2. Stiffness vs Ratio of infill/wall thickness of 3 flexible 3D printable materials

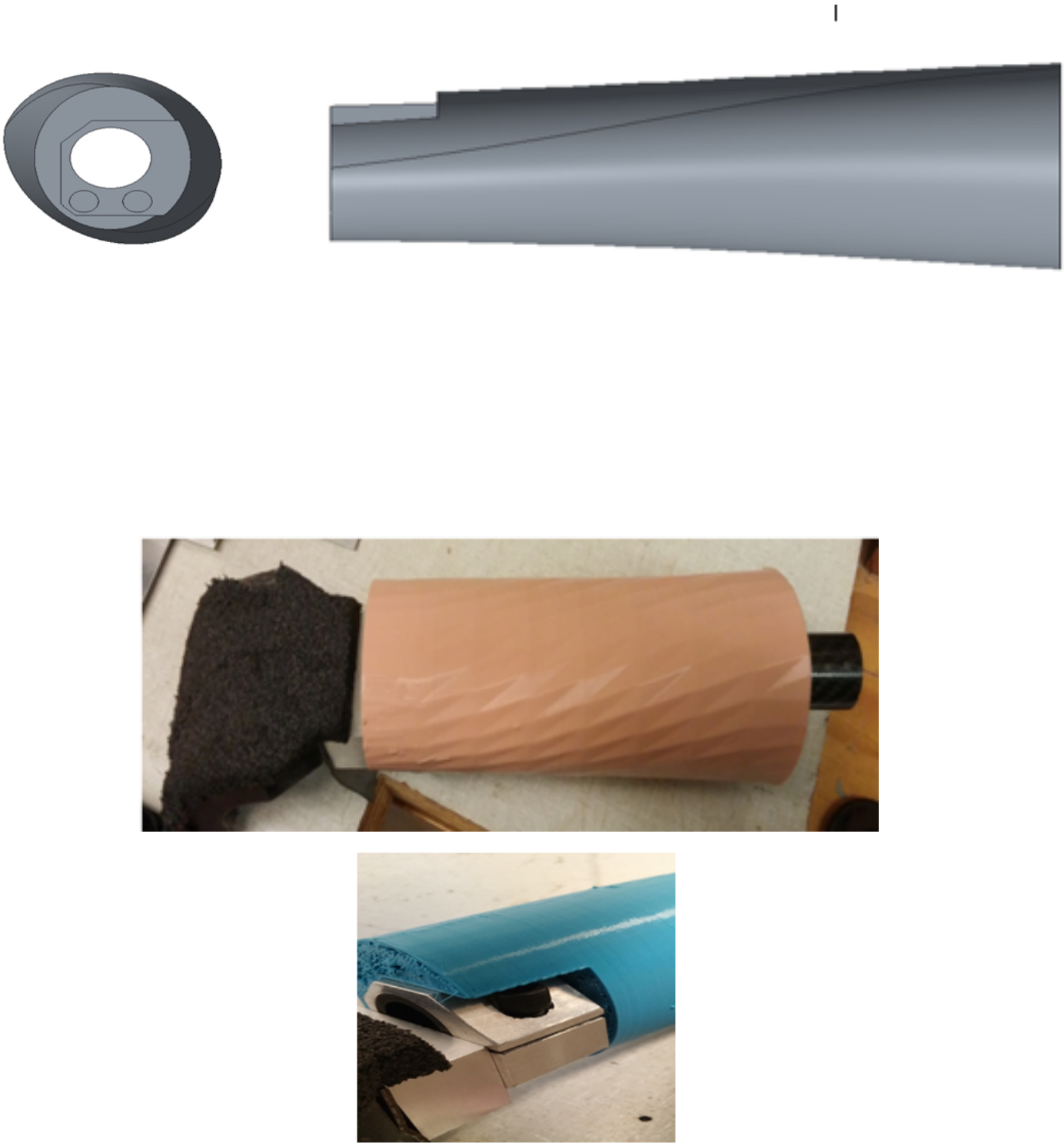

Figure 3. Above is the creo model based on real human cross sections and below is the final project printed in filaflex mounted on the dummy

Appendix B: Intervertebral Disk Design Figures

Figure 4. Magnetic latex disk for the preliminary design of the crash test dummy's neck

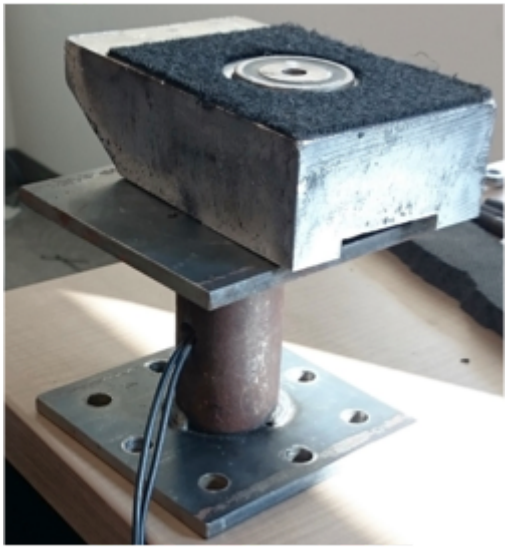

Figure 5. Aluminum block with a slot for an

Figure 6. Compression testing apparatus electromagnet to be inserted flush on the MTS, with actuator head of MTS shown.

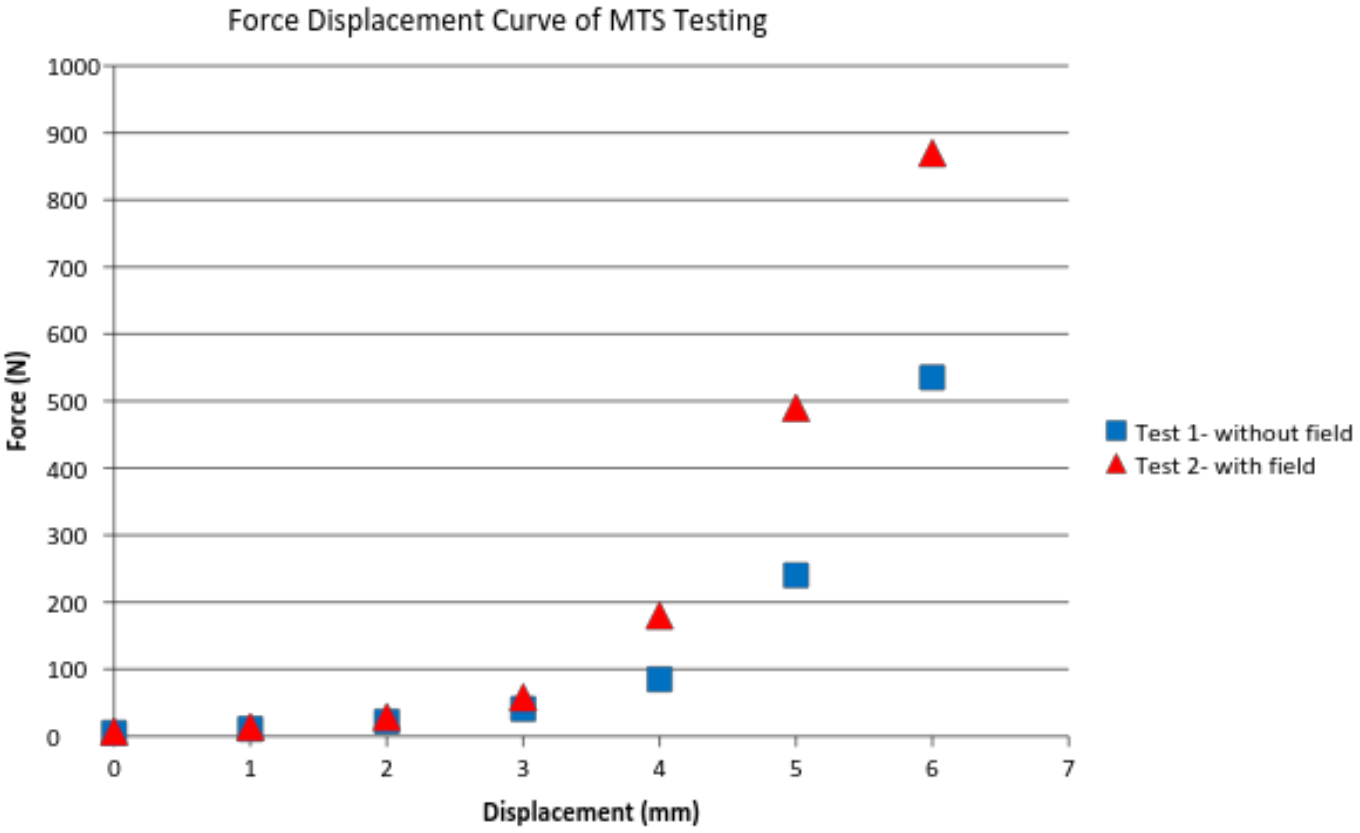

Figure 7. Force displacement curve for the magnetic latex disk, tested with and without a magnetic field

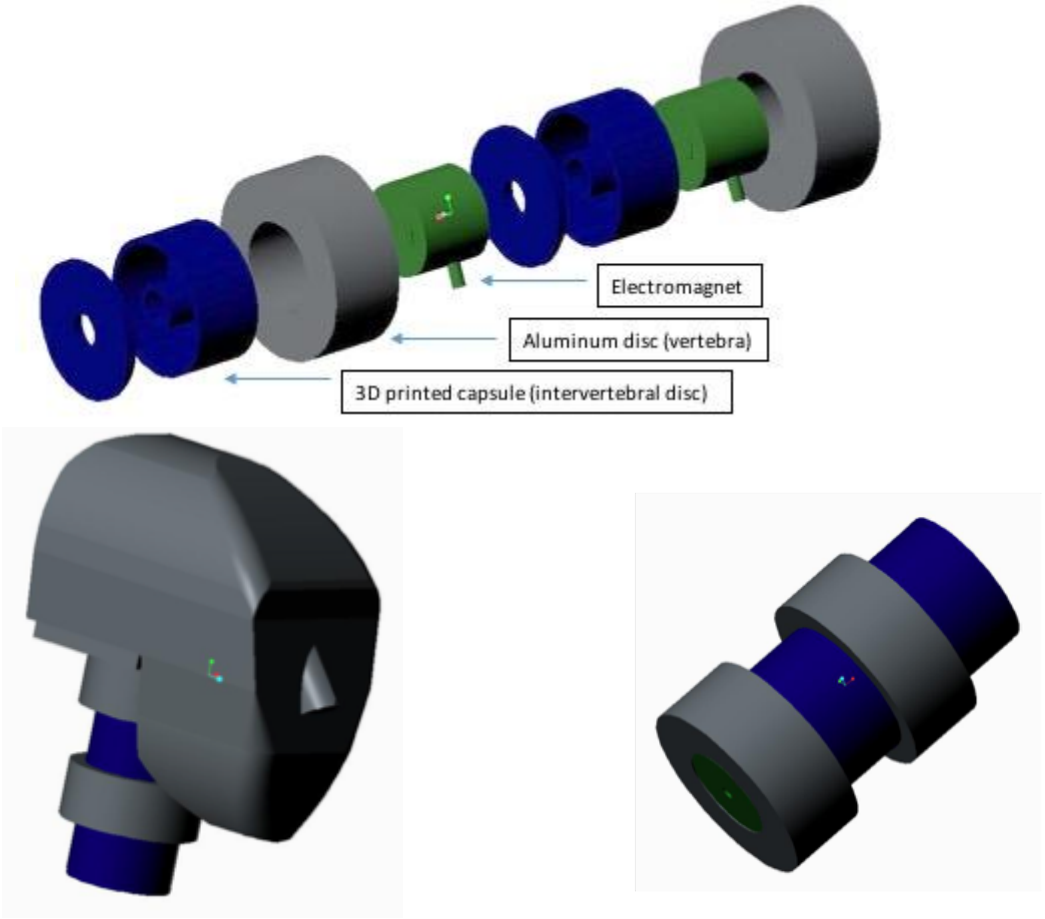

Figure 8. Overall design for the crash test dummy neck, including 3D printed intervertebral disks (blue), electromagnets (green) and aluminum vertebrae (grey)

IEEE EMBS ISC 2016

Expanding the Boundaries of Biomedical Engineering and Healthcare

Medical Glossary for Aboriginal Interpreters

Ottawa, Canada

Abstract

This report describes the results in the design, development and implementation of a Medical Glossary for Aboriginals Interpreters application. The application's objective is to provide First Nations Canadians, and dwellers of Canada who work in the medical sector, a conversational tool, and to facilitate their communication in the case of any language barriers concerning medical terminologies. The solution to this problem was implemented taking into consideration the various environments in which users can navigate through the App. The results were successful. The application has a correct functioning on the web and on Android and iOS environments as well.

I. Problem Statement

First Nations people living off-reserve exceed those who live on-reserve by 20 percent. Their presence in urban centers will continue to grow [1]. The problem arises when rural or urban medical professionals without knowledge of Cree need to communicate with First Nation peoples who do not have strong English/French language skills. In this case, the aboriginal patient would benefit from an interaction with someone who has some knowledge of Cree terminology and both parties interacting would benefit from having a tool to facilitate communication across the two languages.

II. Proposed Solution

The proposed solution to these problems is to create a web application that will allow the user to navigate through a medical database, and search for terms, conversational phrases, audio sources, images, and finally the translation of all these searchable contents within the medical context. It is also taken into account that we are living in the mobile era hence the need to deliver this solution across mobile platforms that are currently on the market, i.e. Android and iOS. A full description of the stages of the design, implementation and development of the medical glossary for aboriginal interpreters application is presented in detail in the following sections. The App has been successfully deployed on the web, and across Android and iOS platforms.

III. Impact

According to 2011 census, aboriginal peoples in Canada totaled 1400685 people, or 4.3 percent of the national population, spread over 600 recognized First Nations governments or brands with distinctive cultures, languages, art, and music [2]. This project is motivated by the idea that in Canada there is a vast First Nations ethnic group that could make use of language tools to better communicate within the medical domain. Other majorities would also benefit from having the possibility of improved coping with language barriers, as well as expanding their knowledge about aboriginal languages. Effective communication is an asset from which society has always benefited. The development of this project will provide an alternative tool of communication to aboriginal groups in North America whose first language is Cree; as well as to people who need to communicate with these minorities, when they have poor or no knowledge of Cree.

An example of this language barrier problem is seen in the communication between doctors or nurses and their patients. Doctors usually use specific and scientific terms that patient are not necessarily familiar with. The communication and necessary explanation of these terms is further complicated when is done from one language to another. Languages barriers can lead to misunderstandings and frustration, both of which can have harmful effects in the realm of medical care. Misunderstandings could lead to patients following medical advice partially or incorrectly, which can lead to medical complications. Furthermore, the cultural differences in opinions about health that might arise would be navigated in a more instructive manner, if medical professionals and patients could clearly better communicate their perspectives, identify the source of difference in opinion, and problem-solve around it. For these reasons it would be helpful to have a source of information that patients and the physicians or nurses can use in order to find the necessary terminology and to understand each other effectively. It is believed that this facilitated communication would be specifically helpful for Cree speaking aboriginals and their medical professionals as well. Given that Cree is one of the most spoken aboriginal

language by First Nations in Canada[3]; the solution was narrowed to the design, development and implementation of an application that targets the Cree, English and French Languages.

IV. Project Development

The realization of the Medical glossary for Aboriginal Interpreters consists of a web and mobile application. The user can navigate through the application independently of the platforms (i.e. Operating Systems(OS)) used to run the App on and without noticing any change on the User Interface(UI) view or behavior. Basically the same look and feel is transported from the web environment to the various mobiles platforms in which the system is deployed. The idea behind a multi-platform application is to extend its accessibility, and usability. A relational database was designed favoring the structure of the application. Medical terms and translations have an unique identification key as well as a parent/child relationship that is conveniently applied during the development of the App.

IV.I. Solution Approach

An Agile development process is a suitable methodology for this project. It provides the guidelines to peruse iterative access to the project's life-cycle throughout the implementation and development process [4]. Multiple iterations were performed until the completion of the alpha version of the App. A combination of Feature-Driven Development(FDD) and Extreme Development(XP) agile methodologies best describe the development process. Design, and implementation were part of these iterations, and are explained in detail in section IV.II. The opportunity of getting feedback at early stages and, having continuous revisions was thought to reduce the development cost. Agile methodology, in particular FDD and XP, re-evaluates the direction of the project after each iteration [4].

IV.I I. Design and Implementation

The App was built with apache Cordova software and ionic framework. This decision was made after meeting with the client's technical contact, and collaboratively eliciting the requirements. It was concluded that using these softwares was one of the best approaches to cope with non-functional requirements. These requirements are: Having a product that could be deployed in Android, iOS devices and on the web. The Mobile App should have the same look and behavior regardless of which native platform is used. Following the functional requirements: The App will display medical terms in English or French and provide the correct translation to Cree North or Cree South at Users' request. It will provide media (video and images) corresponding to the terminology queried.

Fig. 1 is a use case diagram representation of the overview of design of the user interface. The application provides the user with tab Glossary, tab Diagrams, tab More, and tab Bookmarks. In tab Glossary the user will have the option of selecting or search for medical terms under the corresponding category in English or French, and see the translations in Cree. In tab Diagrams, diagrams can be selected for display, and the audio of the terms displayed on the figures are also provided at users request(on-click). In Tab More the user can set the languages preferences (English or French), can search for conversational phrases, which also display their translations in Cree, and play voice translations, finally the user can view the acknowledgments. Tab bookmarks is not fully implemented in the released version of the application, however it is still part of the UI.

The implementation of the App follows the guidelines of the Model-View-Controller(MVC) architecture pattern. The MVC implementation ensures a high level of modularity within the application components [5]. This is in fact very useful when working in an agile environment. It makes it easier to understand and design a particular unit without affecting others. It establishes a dynamic flow on each iteration during the development process of the application. In Fig. 2 the MVC components of the system are presented. Medical Glossary Controller manipulates the model(Medical Glossary Model) and updates the scope of the view of the system. The model corresponds to a relational database that was provided by the client's technical contact and its design was developed favoring the easy access to the categories, terms, and terms translations, as shown in Fig. 3. It is a Relational database diagram, where Category object is described by name, unique identifier number(uuid), the location in which the object is found(locale), this location is related to the language of the object, the number of terms this object is parent of (term_count), and the actual list of term objects(term[]), lastly the parental description of the object(parent). Term object is described by its unique term id number(termUUID), Its corresponding translation or translations (termTranslation), its category dependency(termCategory) and the language in which it is presented(termPublicNote). Translation Object is described by its term dependency(term), its actual translation(definiton), and its description of location relating to the language of the translation(locale).

The application was implemented as a web page. It executes in a web view by default and make reference to HTML, AngularJS, CSS, and the database file resources. It was deployed on an Android phone using Apache Cordova. Apache Cordova is a software that implements the iOS and Android native version of the App. It is a JavaScript Application Programming Interface(API), which serves as a wrapper for native code and is consistent across devices [6]. It uses a web view that can run the HTML app on each different platform. Ionic framework provides the style and behavior like UI native applications using HTML5 CSS and JavaScript [7]. In the same manner Cordova allows to use standard web technologies to develop the App and has pre-developed plug-ins that allows to execute targeting different platforms (eg.

Android, iOS, Windows) [8]. This structure is shown in Fig. 4. This is how having a multi platform application of the Medical Glossary for Aboriginal Interpreters was achieved. Figures 5 and 6 capture the app running on the web browser. In Fig. 7 a minimized view of the web App is shown. Note that the look and feel of the web version is practically the same as in the mobile versions shown in Figures 8, and 9. Fig. 8 captures the state of an entry translation in the android environment, as well as the preference settings in the iOS virtual platform. And Fig. 9 represents the state of conversational phrases in Android virtual environment, and tab More in iOS.

IV.III. VERIFICATION AND VALIDATION

As previously mentioned AngularJS supports dependency injection(i.e., passing components dependencies to a function). Essentially testing individual parts of the system becomes relatively easy. Components that have their resources injected can be mocked on a test by test basis without having to affect the rest of the system that is not being under test. This high level modularity is also achievable because the MVC implementation of the application favors high cohesion and low coupling [9]. Any request from the system can be simulated by mocking the dependencies and passing them into the components under test. The Document Object Model(DOM) is abstracted so the model can be tested without having to do any extra manipulation on it [10]. It is important to mention that the correctness on the behavior of each individual component of the App is verified on the web environment. This means that testing is done in only one environment. Apache Cordova is used to wrap-up the HTML code and build the application package for Android or iOS(e.g. apk, ipa). Once the packages are built for the native platforms the application is ready to run on them. So even though Medical Glossary for Aboriginal Interpreters is a multi-platform application. Testing only needed to be done in the web environment. By default angular applications run on Google Chrome however there are tools that can be used to test Angular applications against a number of browsers in which the web application is wanted to work on. For example Karma is JavaScript command tool that allows to run the test cases of the web application against different browsers [10]. In that case the App would not only function on Android, iOS, or Google Chrome but also in other web browsers. It is necessary to add that due to time constrains the application was not tested on other browsers. During each iterations in the development process the functional and non-functional requirements were addressed and validated with the client's technical contact as they were introduced to the system, modified and verified accordingly.

V. CONCLUSIONS

Developing a single application for multiple platforms can be time consuming even for experienced developers. The softwares used to develop mobile Apps are updated at a fast pace compared to the softwares used to develop web Apps. It might take the same amount of time for someone to implement an App for a specific platform e.g. iOS, as for a new update to come through. For instance the beginning of HTML goes back to the 1990s and up to today only 5 versions have been released [11]. It is true that native application had its advantages over web applications running on natives environments in the past. However this has changed over time. With the developers' investments in HTML5 and the use of AngularJS to manipulate the DOM of an application, web Apps run as fast as in native environments. They can efficiently update the browser's DOM improving performance [12]. Therefore the solution to this problem can be found in the implementation of hybrid Apps, Web based Apps that with a platform independent wrapper can be deployed on different mobile environments without affecting the look and feel of the application over cross-platforms. Medical Glossary for Aboriginal Interpreters application was successfully implemented and deployed over multiple platforms. It is an example of a web-based application that is functioning across multiple platforms. Users will be familiar with the application's layout independently of the environment, e.g.(web, Android, iOs), and will feel comfortable navigating through the App's components.

REFERENCES

[1] "Urban first nations health research discussion paper, "2016. [Online]. Available: http://www.naho.ca/documents/fnc/english/UrbanFirstNationsHealthResearchDiscussionPaper.pdf/
[2] "Projections of the aboriginal population and households in Canada," 2016. [Online]. Available:http://www.statcan.gc.ca/pub/91-552-x/91-552-x2015001-eng.pdf
[3] "Aboriginal languages in Canada," 2016. [Online]. Available: https://www12.statcan.gc.ca/census-recensement/2011/as-sa/98-314-x/98-314-x2011003 3-eng.cfm
[4] "Agile methodology," 2016. [Online]. Available: http://agilemethodology.org
[5] "A description of the model-view-controller user interface paradigm in the smalltalk-80 system," 2016. [Online].Available:https://web.archive.org/web/20100921030808/http://www.itu.dk/courses/VOP/E2005/VOP2005E/8 mvc krasner and pope.pdf
[6] A. Cordova, "Developing mobile applications with Cordova," 2016. [Online]. Available:http://www.toptal.com/mobile/developing-mobile-applications-with-apache-cordova
[7] "Welcome to ionic," 2016. [Online]. Available: http://ionicframework.com/docs/guide/preface.html
[8] A. Cordova, \Apache Cordova," 2012. [Online]. Available: https://cordova.apache.org/docs/en/latest/guide/overview/
[9] "Cohesion vs coupling separate concerns," 2016. [Online]. Available: http://www.agile-code.com/blog/cohesion-vs-coupling-separate-concerns/
[10] "Unit testing," 2016. [Online]. Available: https://docs.angularjs.org/guide/unit-testing
[11] "The history of html," 2016. [Online]. Available: http://www.ironspider.ca/webdesign101/htmlhistory.htm
[12] "React may have just ended the native vs. web debate," 2016. [Online]. Available:http://readwrite.com/2015/09/25/react-native-mobile-apps-web-apps-marc-shilling

APPENDIX

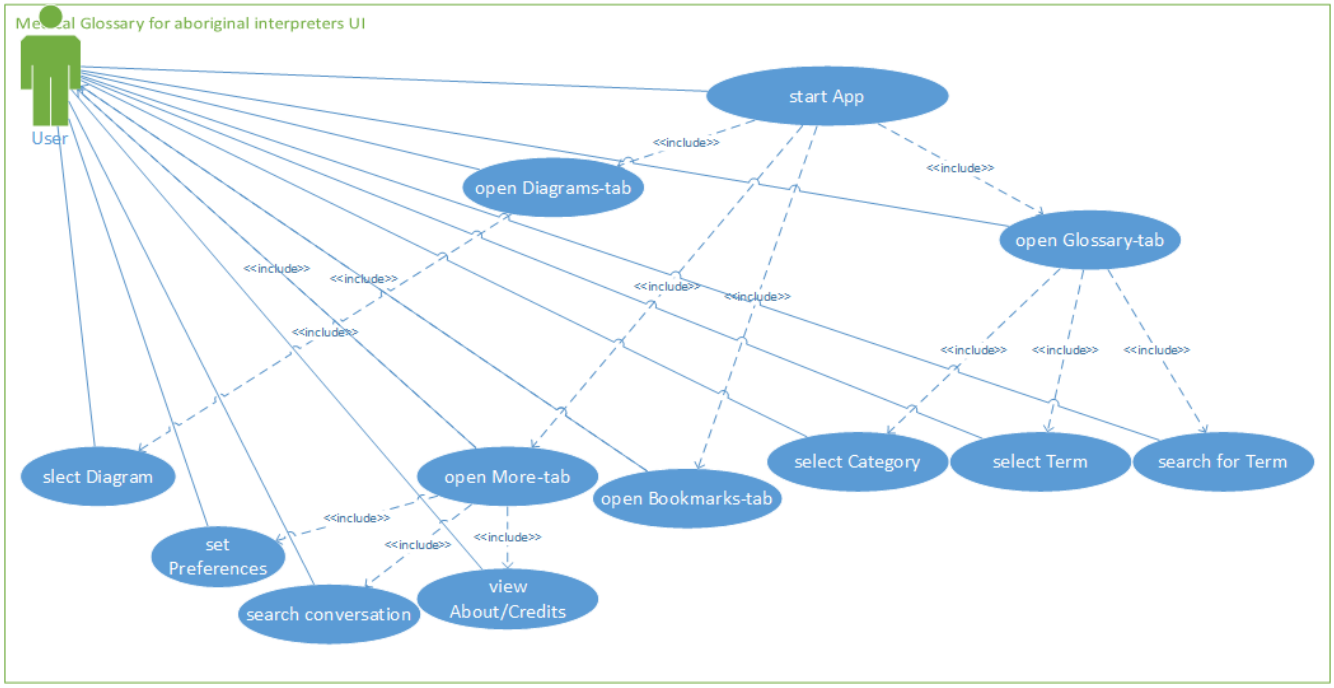

Figure 1: Use Case Diagram model

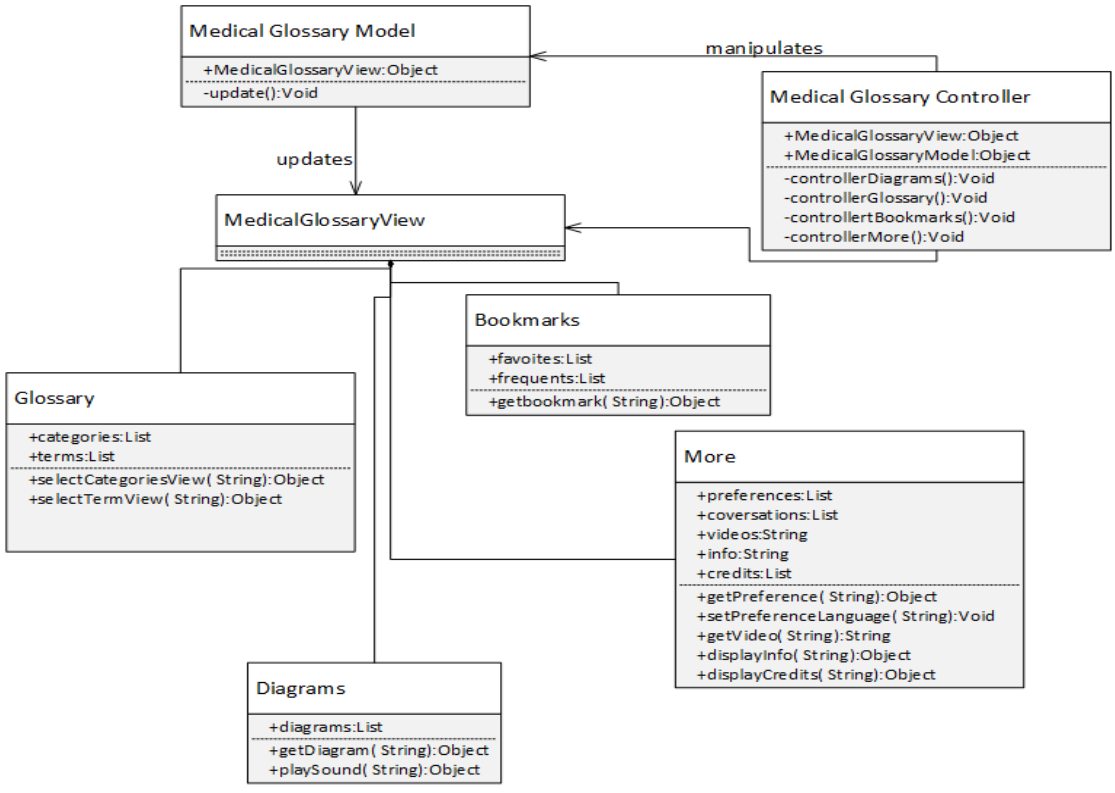

Figure 2: MVC Medical Glossary for aboriginal interpreters

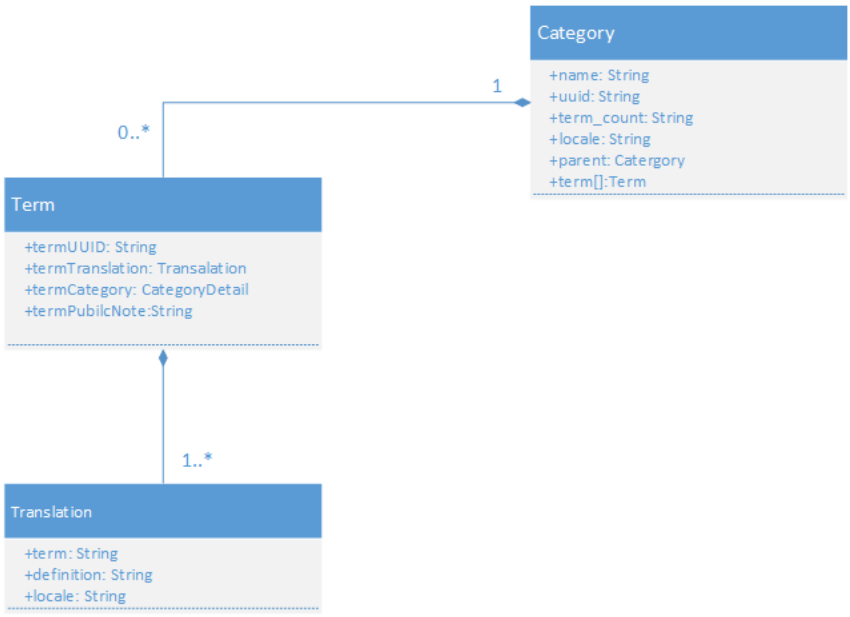

Figure 3: Relational database diagram

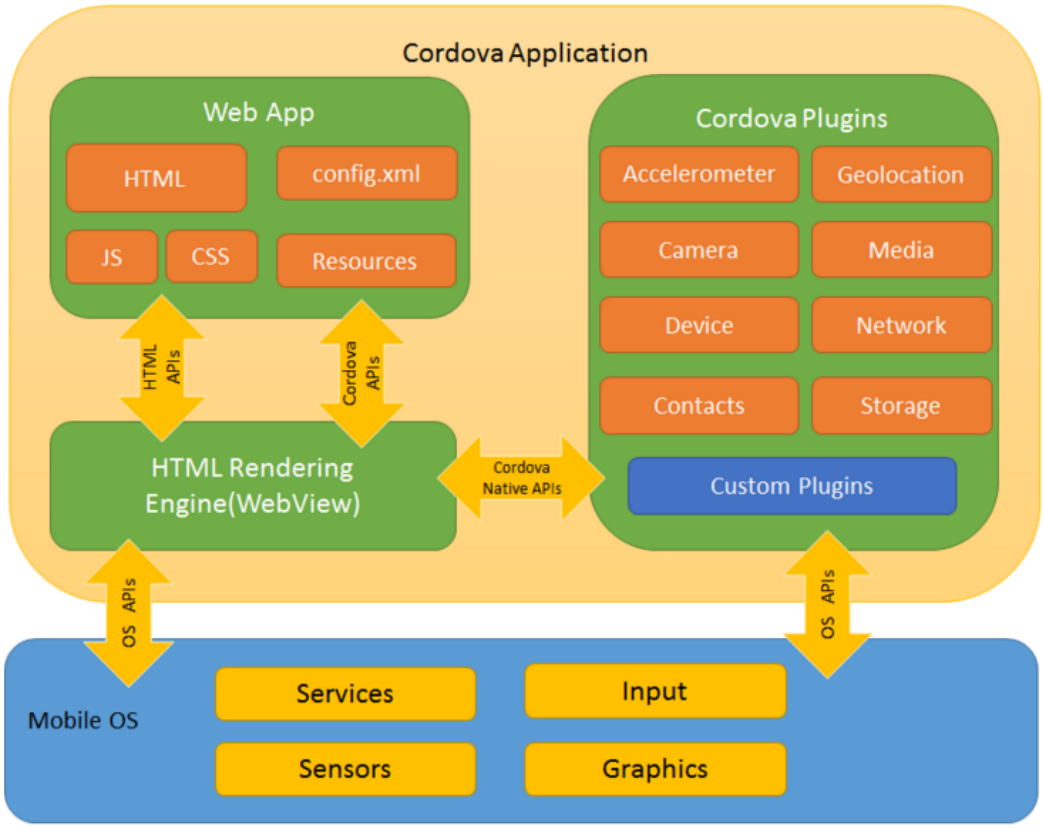

Figure 4: Cordova Application [8]

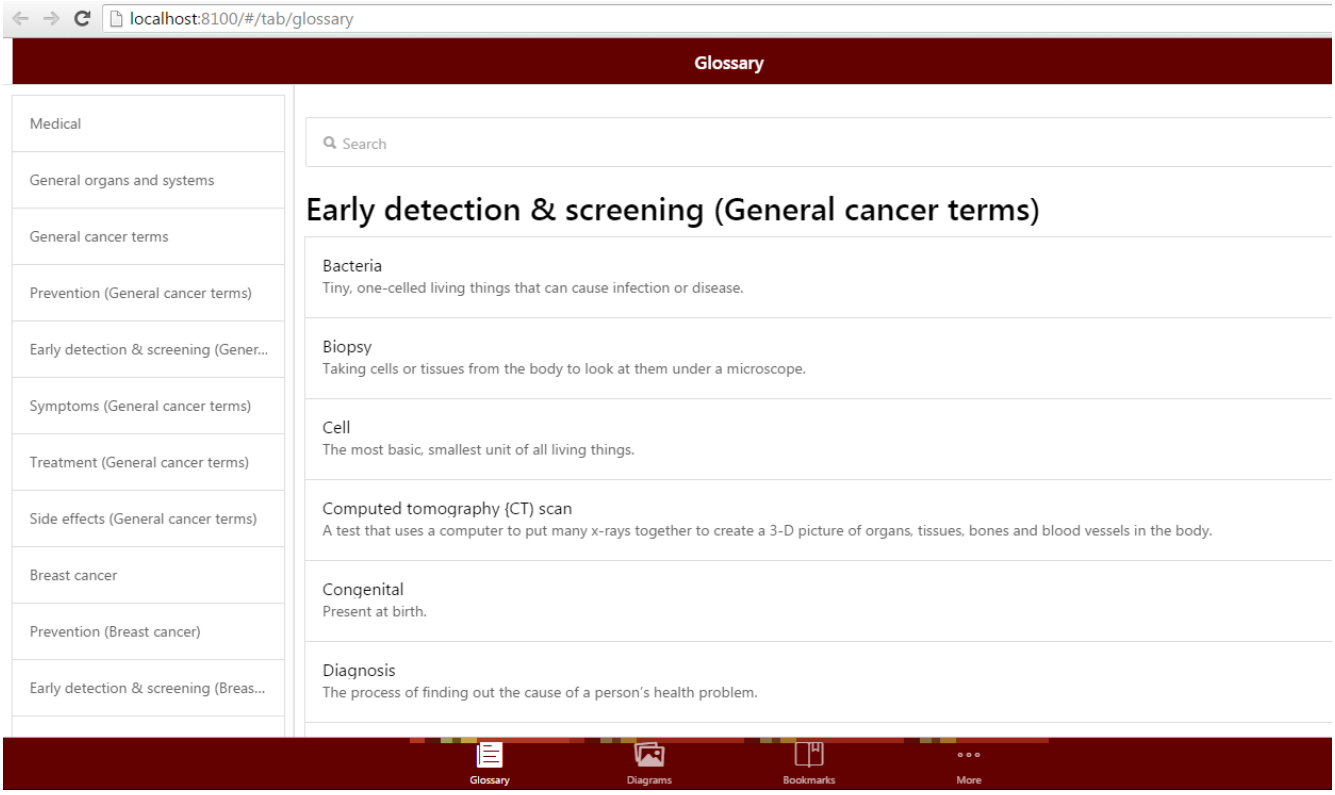

Figure 5: Web view Glossary-tab

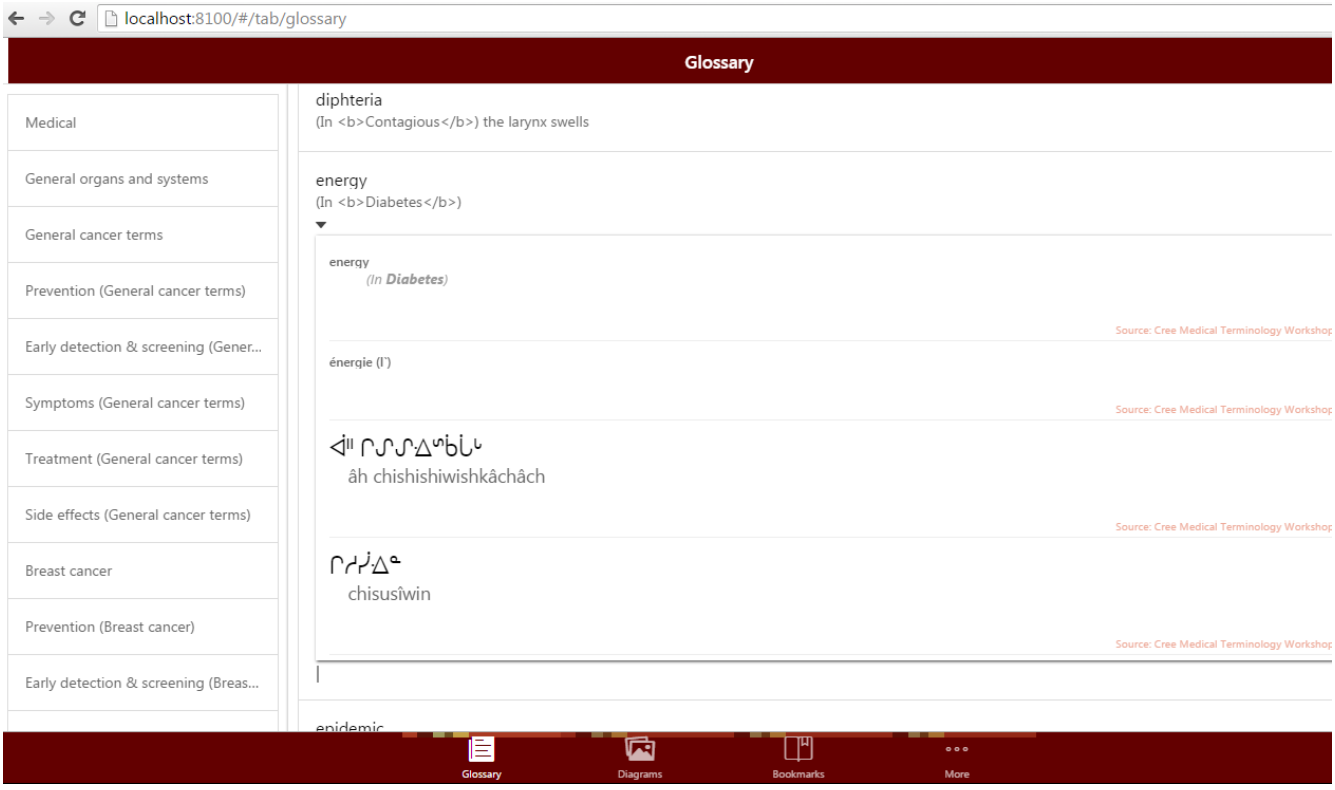

Figure 6: Web view Glossary-tab Cree entry translation

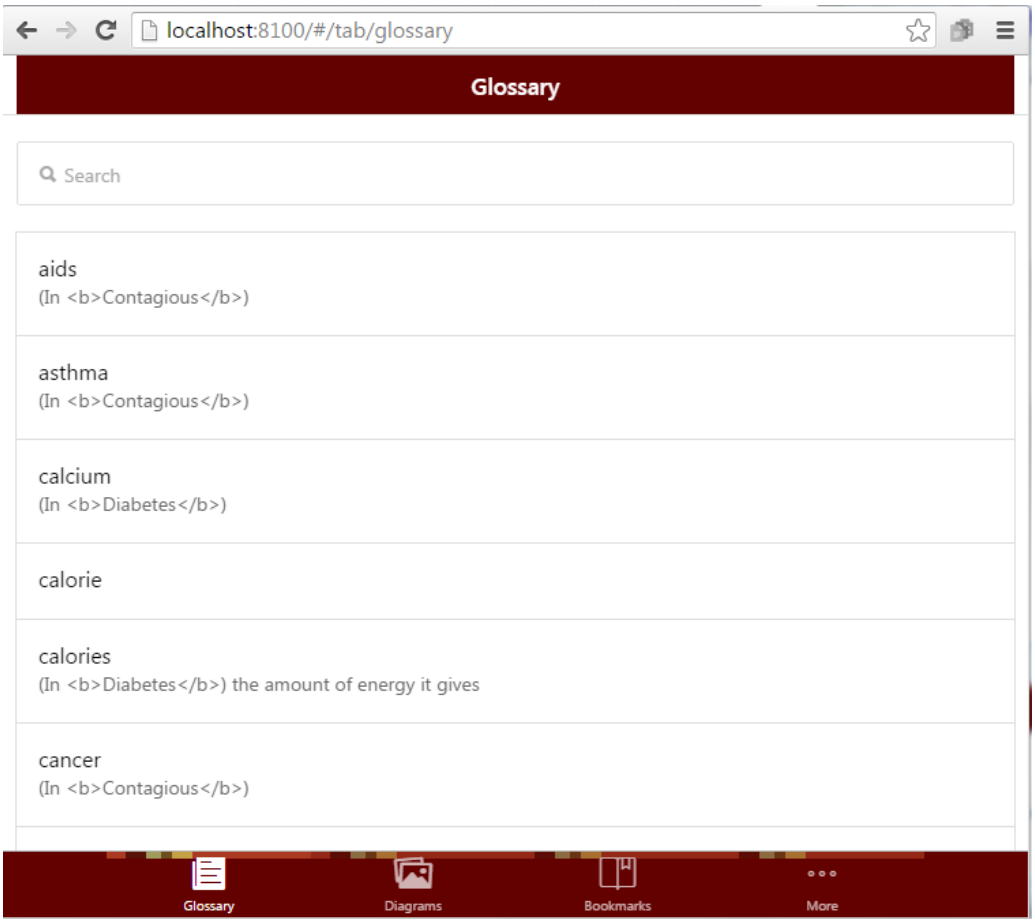

Figure 7: Web view Glossary-tab minimized

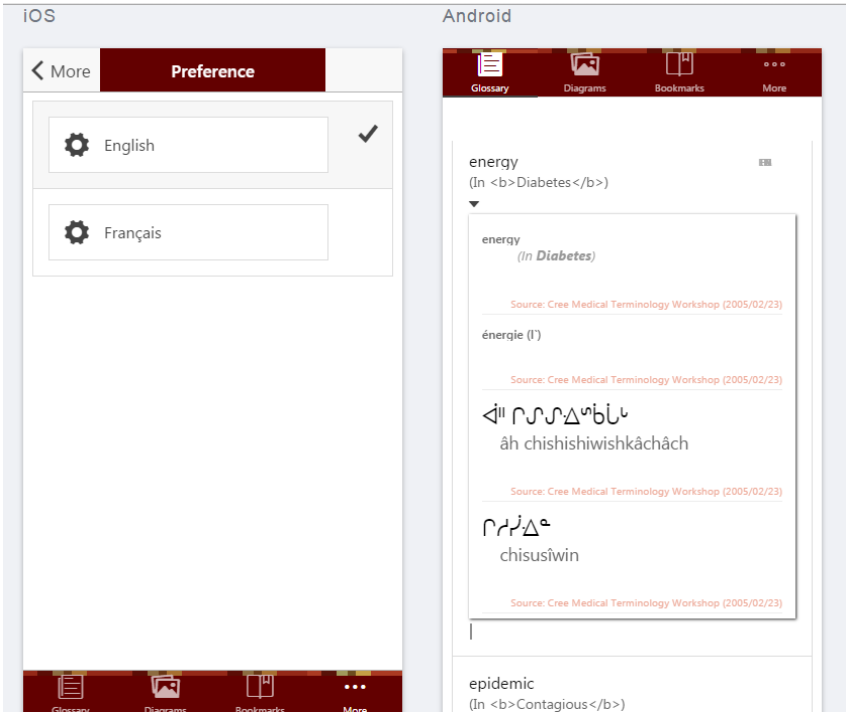

Figure 8: iOS & Android virtual platform view Glossary-tab Cree entry translation

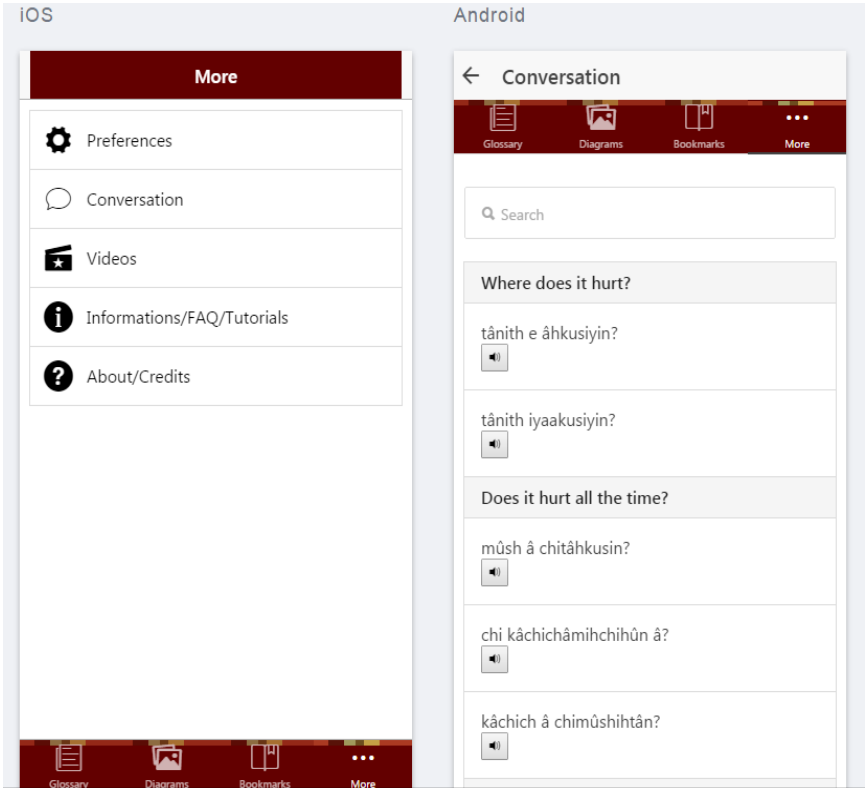

Figure 9: iOS & Android virtual platform view More-tab Cree conversation

Development of DNA Aptamers Against Human Red Blood Cells

A Novel Drug Delivery System

Abstract

Current drug delivery systems are limited by low residence time in bloodstream and inability for targeted drug delivery. This project has optimized and employed a cell-SELEX protocol to isolate DNA aptamers binding to human red blood cells (RBC) under physiological conditions. Preliminary results indicated the aptamer pools isolated had a propensity to bind to RBC at 37°C over room temperature. The impact of these aptamers are significant, as aptamer-drug conjugates can be developed and coupled to the surface of RBC for a novel drug delivery system which can result in longer drug circulatory half-lives and targeted delivery via bi-specific aptamers.

I. Problem Statement

Biomedical engineering has contributed to understanding and developing effective drug delivery systems, yet challenges remain as even novel strategies in drug delivery systems still result in undesired off-target effects from drugs[1]. Administering drugs locally can result in targeted delivery, but some therapeutic agents can only be administered systemically[1]. Efficacy of drug delivery systems are often limited by immune responses and premature elimination and degradation of drugs from body[2]. Such limitations can be addressed by selecting an appropriate drug delivery system.

Liposomes are small, spherical phospholipid bilayers which can entrap drugs[3]. They are non-toxic, non-immunogenic, biocompatible, and biodegradable[3], making them an attractive vehicle for drug delivery. The variable composition of liposomes can be modified to attach antibody moieties, and these specialized liposomes are termed immunoliposomes[3]. Immunoliposomes can be used as a drug carrier for targeted delivery, since the antibody can direct the vehicle to a particular area by binding to a target receptor with high specificity and affinity. One major limitation of liposomes is their low circulation half-life *in vivo*[3], which would eliminate the drug prematurely. Although adding polyethylene glycol-phosphatidyl ethanolamine (PEG-PE) to liposome surface can increase their circulatory half-life[3], recent evidence has indicated PEGylation *in vivo* can induce production of anti-PEG antibodies and result in undesired immunogenic effects[4].

Using red blood cells (RBC) as drug carriers is a safer alternative, particularly when autologous RBC are used for their non-immunogenicity and biocompatibility[5]. RBC also have an extensive circulatory system and a long circulatory half-life of 120 days[6]. It has been reported that free floating drugs stay in bloodstream for a few hours to a day, coupling drugs to synthetic carriers prolongs drugs' presence to several days, and using RBC as carriers can prolong drugs' presence in bloodstream to several weeks[7]. Drugs can be loaded onto RBC by direct encapsulation with hypotonic dialysis and then resealing[5] (Figure 1), yet this method disrupts RBC membrane integrity and reduces RBC half-lives in circulation[6]. This problem can be circumvented by coupling drugs to surface of RBC instead of encapsulation[8]. Recently, a study has engineered RBC with sortase modifiable proteins on the plasma membrane, which can carry drugs by a sortase-mediated site specific covalent attachment to these modified proteins[6]. However, this method requires genetically engineered RBC and issues of biocompatibility may arise. Another disadvantage is this technology does not resolve the issue of targeted delivery of drugs. The authors of the study proposed that targeting modules, like antibodies, can be coupled to RBC surface[6]. These antibodies can then bind to their target cell to direct RBC carrying the sortase attached drugs to the targeted area[6]. Yet, protein antibodies for *in vivo* applications is hindered by several factors, such as their high production cost, immunogenicity, thermal instability, and laborious method for chemical modifications[9]. As such, this project proposes to design a novel drug delivery system which uses RBC as drug carriers and couples them to a targeting ligand without compromising the integrity, biocompatibility, or non-immunogenicity of the drug delivery system. It aims to develop a delivery system which will allow prolonged circulation of drugs while simultaneously allowing targeted delivery.

II. Proposed Solution

One solution to the problem outlined previously is to develop aptamers as targeting ligands, which can be conjugated to drugs and coupled to RBC for a novel aptamer facilitated drug delivery by RBC system. Aptamers are short, synthetic single stranded DNA (ssDNA) or RNA oligonucleotides which can form unique three dimensional structures to bind target molecules with high specificity and affinity[10] (Figure 2). Aptamers are rendered as "chemical antibodies" with binding affinities similar to antibodies, and rival antibodies as affinity ligands for therapeutics, since aptamers can be chemically synthesized and are cheaper to produce[10]. Aptamers can also have a higher specificity than antibodies, since their smaller size allow them to distinguish between different functional groups in similar structured molecules[11]. Most importantly, aptamers are non-immunogenic, which make them ideal candidates for *in vivo* applications, such as drug delivery.

This solution would solve many aspects of challenges associated with drug delivery outlined previously. Several aptamer-drug conjugates have been developed by covalent/noncovalent interactions (Figure 3). For example, an RNA aptamer against epithelial cell adhesion molecule has been conjugated to the Dox drug to inhibit cancer cell proliferation

and treat retinoblastoma[9]. However, aptamer-drug carriers have low circulation half-lives due to low molecular weights of aptamers[12]. Like liposomes, aptamers can also be PEGylated[13], but this introduces immunogenic responses from anti-PEG antibodies[4]. An alternative solution is coupling aptamer-drug conjugates to RBC surface in order to increase circulatory half-life of drugs. Using such a drug delivery system with RBC as carriers has numerous advantages. RBC typically do not undergo extravasation from circulation into tissues, this system can deliver therapeutic agents to intravascular targets[8] with high specificity, and optimal localization can be further achieved with bi-specific aptamers. Both aptamers and autologous RBC are non-immunogenic and the issue of biocompatibility would also be resolved. Additionally, the natural elimination of RBC would offer a natural mechanism to eliminate this drug delivery system from the body[8].

This project focuses on developing aptamers binding to RBC under *in vivo* conditions. These aptamers may be conjugated to drugs and coupled to RBC surface to serve as a vehicle for anchoring and delivering drugs to specific intravascular targets. Aptamers binding specific targets are developed through an *in vitro* procedure known as Systematic Evolution of Ligands by Exponential Enrichment (SELEX)[14]. This procedure (Figure 4) first incubates aptamers with target, then isolates bound aptamers and enriches the pool through PCR amplification before incubating the pool with the target again. This cycle is repeated for several rounds until the aptamer pool converges to sequences binding to target with high affinity and specificity[14]. A modified version of SELEX, called cell-SELEX[15], was used to develop these aptamers against RBC. SELEX is typically performed against a purified target molecule, but cell-SELEX isolates aptamers against whole live cells for target recognition on extracellular surfaces. Cell-SELEX conserves membrane proteins of cell surface to allow aptamers to adopt natural folding structures in order to bind to native states of molecules, similar to *in vivo* conditions[15].

Recently, aptamers binding malaria infected RBC at room temperature (RT) have been identified[16]. The authors aimed to use these aptamers for malaria diagnostics and as a tool to identify appropriate surface antigens for developing malaria blood stage vaccines[16]. The Berezovski BioAMI research group at University of Ottawa recently developed aptamers binding normal RBC at RT to improve cell purification/isolation from whole blood. However, no aptamers binding normal RBC under *in vivo* physiological conditions, such as 37°C, have been developed. Nucleic acid folding is sensitive to several factors, including temperature[17]. Hence, it is important to conduct incubation step of cell-SELEX under physiological temperature for aptamers that need to bind to target *in vivo*. Not all aptamers binding at RT can bind at 37°C, since lowering temperature during aptamer binding allows formation of complex motifs like junctions, loops, and bulges that are otherwise unstable at higher temperatures[17]. Thus, this project modified and optimized the existing cell-SELEX protocol for aptamers against normal RBC to identify aptamers binding at 37°C for use in *in vivo* applications, such as drug delivery.

III. Impact

Aptamer facilitated drug delivery by RBC can eliminate problems associated with existing drug delivery systems. Coupling RBC to DNA aptamers conjugated to a drug can increase drug blood residence time, which would be ideal for diseases such as chronic obstructive pulmonary disease requiring anti-inflammatory glucocorticoid drugs to be released in low and effective doses over a long period of time[2]. The proposed system would not require constant intravenous drug administration. This system would not be limited to diseases requiring drug carriers with long circulatory half-lives. Future research can develop bi-specific aptamers against specific intravascular targets. Bi-specific aptamers targeting two different cells have recently been developed by using a dsDNA linker to conjugate two different DNA aptamers[9]. The Dox drug was intercalated into the DNA linker, and the bi-specific aptamer recognized two different cancer cell targets with same affinity and specificity[9]. This knowledge can be harnessed to optimize aptamer facilitated drug delivery by RBC system by developing a bi-specific aptamer in which one aptamer binds to RBC and anchors the drug (as was this project's aim), while another aptamer targets an intravascular target for binding in order to localize the drug delivery system to that target. Targeted delivery is necessary for patients requiring complex therapeutic agents like enzymes, which need to be localized to precise targets for enzyme's active site to interact with ligand's binding pocket[8]. Hence, this drug delivery system can be used to treat numerous diseases requiring drugs with intravascular targets. A variety of drugs can be conjugated to aptamers, ranging from nucleic acids to peptides, nanoparticles, and chemotherapeutic agents[18]. DNA aptamer pools binding RBC at 37°C can spawn further studies to narrow the aptamer pool to converge to more specific sequences. For example, this project used blood type O RBC. Antigens from different blood types present on RBC surface can interact differently with specific aptamers. Thus, aptamers binding RBC at 37°C can undergo cell-SELEX for more rounds to isolate aptamers binding specifically to particular blood types. These aptamers can be a step towards personalized medicine and lead to better drug delivery systems which are tailored to an individual's autologous RBC for more effective patient treatment.

IV. Project Development

The first objective of this project was to optimize the existing cell-SELEX procedure to isolate aptamers binding RBC at 37°C. Since aptamers contain GC rich regions, they may form stable loops which makes it difficult for the polymerase to access these regions during amplificaiton[19]. Thus, two different polymerases were tested to see which polymerase amplified aptamers optimally. One polymerase was phire II polymerase and one was a GC rich polymerase designed for better access to GC rich regions during amplification. The results indicated phire II polymerase was optimal for amplification of aptamers (Figure 5). Further modification to the cell-SELEX procedure indicated eliminating the gel purification step after selection was optimal for isolating aptamers (Figure 6). The aptamer concentration is usually low after selection and purification by gel did not allow any aptamers to be detected immediately after the selection step. Eliminating purification and going straight to amplification and digestion allowed the detection of the aptamers via gel electrophoresis at a later step, when purification was necessary prior to a second round of the cell-SELEX procedure. Overamplification with many cycles of PCR (such as 30) leads to amplification of background contaminants. Thus, reducing the number of PCR cycles to 15 was deemed optimal (Figure 7), as it eliminated background amplification and resulted in much higher yields of amplicons.

Next, the modified and optimized cell-SELEX procedure (Figure 8) was performed on a pool of DNA aptamers with known binding to RBC at room temperature (RT). After three rounds of cell-SELEX where incubation and selection was conducted at 37°C, aptamers binding RBC at physiological temperature were successfully isolated (Figure 9) after undergoing repeated rounds of selection, amplification, digestion, and purification by gel electrophoresis.

The binding affinities of the three aptamer pools against RBC were checked at both RT and 37°C with flow cytometry. The flow cytometry results (Figure 10) indicated after round one, aptamer pools had a higher propensity to bind at 37°C than at RT, which demonstrated the original pool's affinity for binding at RT was changed and later rounds were successfully enriched for binding at 37°C. Binding affinities were low, since the aptamer pools from round 2 (R2) and 3 (R3) had binding affinities at 37°C which were only 0.01 relative fluorescent units higher than binding affinities at RT. Additionally, the binding affinities of R2 and R3 overlapped with aptamer library negative control of randomized sequences. These low binding affinities were likely due to low aptamer concentrations used for flow cytometry. Due to time constraints, only three rounds of cell-SELEX were performed, while other aptamer studies typically perform 8 – 15 rounds before seeing a significant shift in binding affinity. Therefore, the cell-SELEX protocol needs to be further optimized to yield higher concentrations of aptamers and further rounds of cell-SELEX need to be performed to enrich the aptamer pool further for binding at 37°C with higher affinities.

V. Conclusions

The cell-SELEX procedure for isolating aptamers against RBC binding at 37°C was modified to include 15 cycles and phire II polymerase during PCR amplification. These modifications and elimination of gel purification step after selection all helped to successfully isolate aptamers binding RBC at 37°C. Screening aptamer pools after three rounds of cell-SELEX with flow cytometry indicated the protocol worked, as the last two rounds were enriched to bind preferentially at 37°C. The binding affinities were low and likely because low concentrations of aptamers were used. Thus, the protocol can be optimized further to increase aptamer concentrations and more rounds of cell-SELEX can isolate higher affinity aptamers. In conclusion, results indicated DNA aptamers can bind to RBC under physiological conditions and therefore has the potential to be used in a novel aptamer facilitated drug delivery system for improved and efficient delivery of therapeutic agents to intravascular targets.

References

1. NA. (2013). Drug Delivery Systems. National Institute of Biomedical Imaging and bioengineering. National Institute of Health.
2. Biagiotti S, Paoletti MF, Fraternale A, Rossi Luigi, Magnani M. (2011). Drug delivery by red blood cells. *IUBMB Life*, 63(8), 621 – 631
3. Sharma G, Anabousi S, Ehrhardt C, and Ravikumar MNV. (2006). Liposomes as targeted drug delivery systems in the treatment of breast cancer. *Journal of Drug Targeting*, 14(5), 301 – 310.
4. Saifer MG, Williams LD, Sobczyk MA, Michaels SJ, Sherman MR (2014).Selectivity of binding of PEGs and PEG-like oligomers to anti-PEG antibodies induced by methoxyPEG-proteins. *Mol Immunol*, 57, 236–246.
5. Magnani M, Rossi L, Fraternale A, Bianchi M, Antonelli A, Crinelli R, Chiarantani L. (2002). Erythorcyte-mediated delivery of drugs, peptides and modified oligonucleotides. *Gene Therapy*, 9, 749 – 751.
6. Shi J, Kundrat L, Pishesha N, Bilate A, Theile C, Maruyama T, Dougan SK, Ploegh HL, Lodish HF. (2014). Engineered red blood cells as carriers for systemic delivery of a wide array of functional probes. *PNAS*, 111(28), 10131 – 10136.
7. Borman S. (2014). Hitching a ride on red blood cells. *American Chemical Society*, 92(27), 5.
8. Muzykantov VR. (2010). Drug delivery by red blood cells: vascular carriers designed by mother nature. *Expert Opin Drug Deliv*, 7(4), 403 – 407.
9. Sun H, Zhu X, Lu PY, Rosato RR, Tan W, Zu Y. (2014). Oligonucleotide aptamers: new tools for targeted cancer therapy. *Mol Ther Nucleic Acids*, 3, 182.
10. Ni X, Castanares M, Mukherjee A, Lupold SE. (2011). Nucleic acid aptamers: clinical applications and promising new horizons. *Curr Med Chem*, 18(27), 4206 – 4214.
11. Jayasena SD. (1999). Aptamers: An emerging class of molecules that rival antibodies in diagnostics. *Clinical Chemistry*, 45(9), 1628 – 1650.
12. Osborne SE, Matsumara I, Ellington AD. (1997). Aptamers as therapeutic and diagnostic reagents: problems and prospects. *Curr Opin Chem Biol*, 1(1), 5 – 9
13. Healy JM, Lewis SD, Kurz M, Boomer RM, Thompson KM, Wilson C, McCauley TG. (2004). Pharmacokinetics and biodistribution of novel aptamer compositions. *Pharm. Res*. 21(12), 2234–2246
14. Tuerk C, Gold L. (1990). Systematic Evolution of Ligands by Exponential Enrichment: RNA ligands to bacteriophage T4 DNA polymerase. *Science*, 249(4968), 505 – 510.
15. Sefah K, Shangguan D, Xiong X, O'Donoghue MB, Tan W. (2010). Development of DNA aptamers using Cell-SELEX. *Nature Protocols*, 5(6), 1169 – 1185.
16. Birch CM, Hou HW, Han J, Niles CJ. (2015). Identification of malaria-parasite infected red blood cell surface aptamers by inertial microfluidic SELEX (I-SELEX). *Nature Sci Rep*, 5, 11347.
17. Tinoco, I, Bustamante, C. (1999) How RNA folds. *J.Mol.Biol*. 293, 271-281
18. Zhu G, Niu G, Chen Xiaoyuan. (2015). Aptmaer-Drug Conjugates. *Bioconjugate Chem*, 26, 2186 – 2197.
19. Ellington AD, Szostak JW. (1990). *In vitro* selection of RNA molecules that bind specific ligands. *Nature*, 346(6287), 818 – 822.

APPENDIX

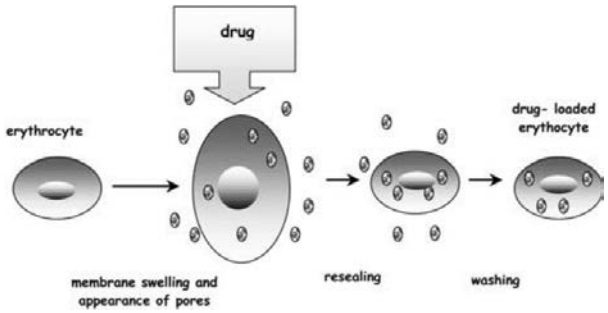

Figure 1. Direct encapsulation of therapeutic agents inside RBC[10]. The RBC pores are opened by dialysis with a saline solution to allow drugs to pass through. Membrane pores are resealed by restoring the osmolarity, and the cells are subsequently washed to eliminate any drugs that were not encapsulated inside.

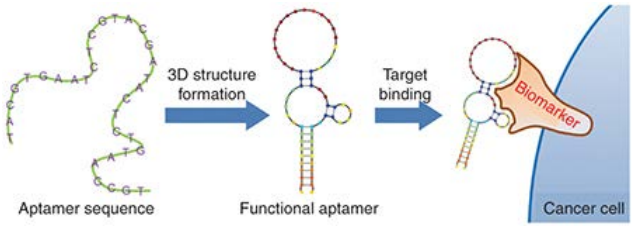

Figure 2. Schematic representation of an aptamer binding to its target[25]. Aptamers use structural recognition to bind to and interact with their target by folding into specific three dimensional structures. They bind with high specificity and affinity, like a key fitting into a lock[7].

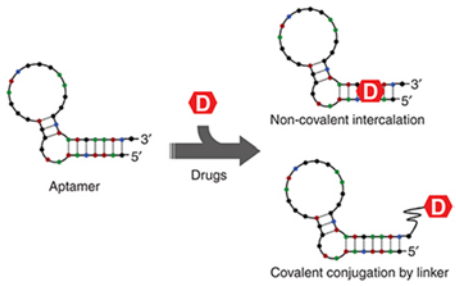

Figure 3. Schematic representation of aptamer drug-conjugates[25]. Covalent conjugation of therapeutic agents to aptamers by linker moieties are more stable than noncovalent intercalation of the therapeutic agent into the nucleic acid structures of aptamers.

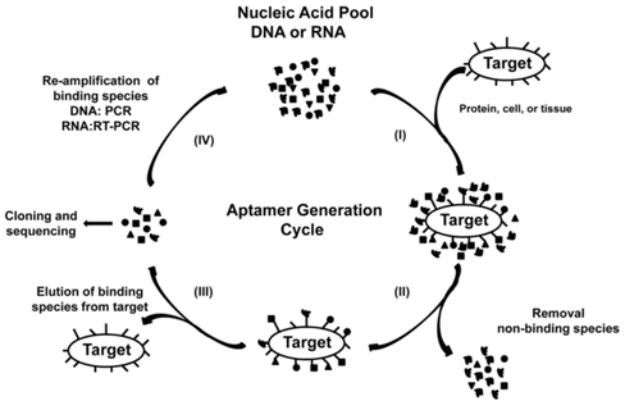

Figure 4. General *in vitro* SELEX procedure to develop aptamers that bind to a target with high affinity and specificty[15]. An aptamer library of randomized single stranded (ss) DNA or RNA sequences are incubated with a target, and the bound aptamers are subsequently separated from the unbound aptamers and amplified, after which point the enriched aptamer pool is subjected to another round of the procedure. The procedure is repeated for several rounds until the pool is enriched and converges to particular sequences. Individual clones are then tested for binding affinity and specificity to target.

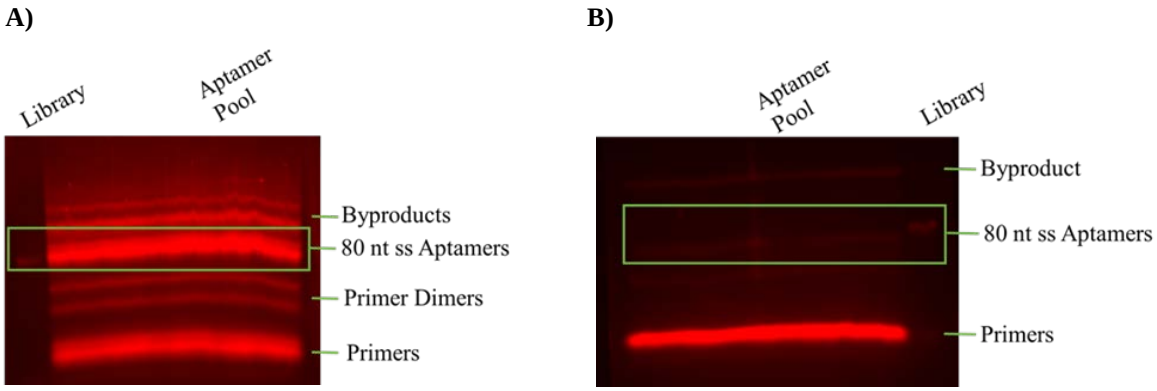

Figure 5. Optimization results for best polymerase. Agarose gel electrophoresis results for aptamer pools after PCR amplification and then digestion with exonuclease. The 4% agarose gel electrophoresis was carried out at 150 V for 45 minutes with 0.5X TBE buffer. The aptamer pool was run against the 100 nM aptamer library of randomized sequences with length of 80 nucleotides. The library was used to identify the target ssDNA aptamer band that aligned with it (indicated by green box). Alphaview software was used to determine band intensities, which are indicative of the aptamer yields. **A)** The ssDNA aptamer band when amplified with phire II polymerase was 886% more intense than the aptamer library. **B)** The ssDNA aptamer band when amplified with GC rich polymerase was only 4% more intense than the aptamer library. The aptamer yield was higher when phire II polymerase was used for amplification.

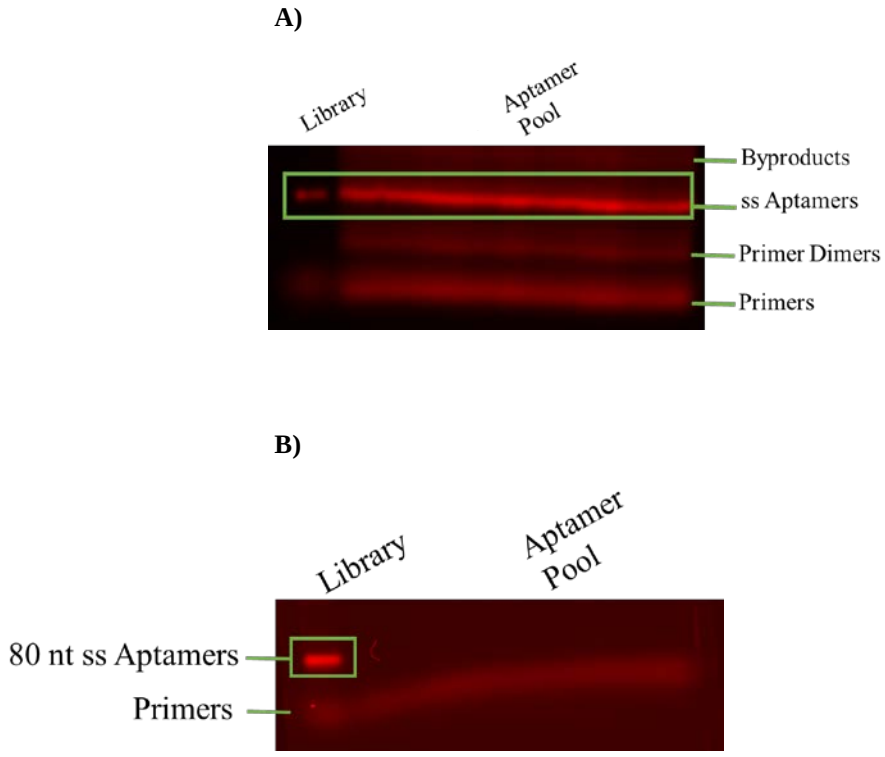

Figure 6. Eliminating post selection gel purification was optimal for cell-SELEX. The 4% agarose gel electrophoresis was carried out at 150 V for 45 minutes in 0.5X TBE buffer. The aptamer pool was run against 100 nM aptamer library (80 nucleotides) to identify the ssDNA aptamer band (indicated by the green box). The band intensities were analyzed with Alphaview software and are indicative of the aptamer yields. **A)** Post selection gel electrophoresis of recovered aptamer pool after selection against RBC at 37°C. The aptamer pool prior to being subjected to selection was amplified with GC rich polymerase, digested with exonuclease, and then purified by gel extraction. No R1 ssDNA aptamer band detected. **B)** Post digest gel electrophoresis of recovered aptamer pool after selection against RBC at 37°C, amplification with phire II polymerase, and exonuclease digestion. The ssDNA aptamer band present was 114% more intense than the 100 nM library. No post selection gel purification step was performed after selection.

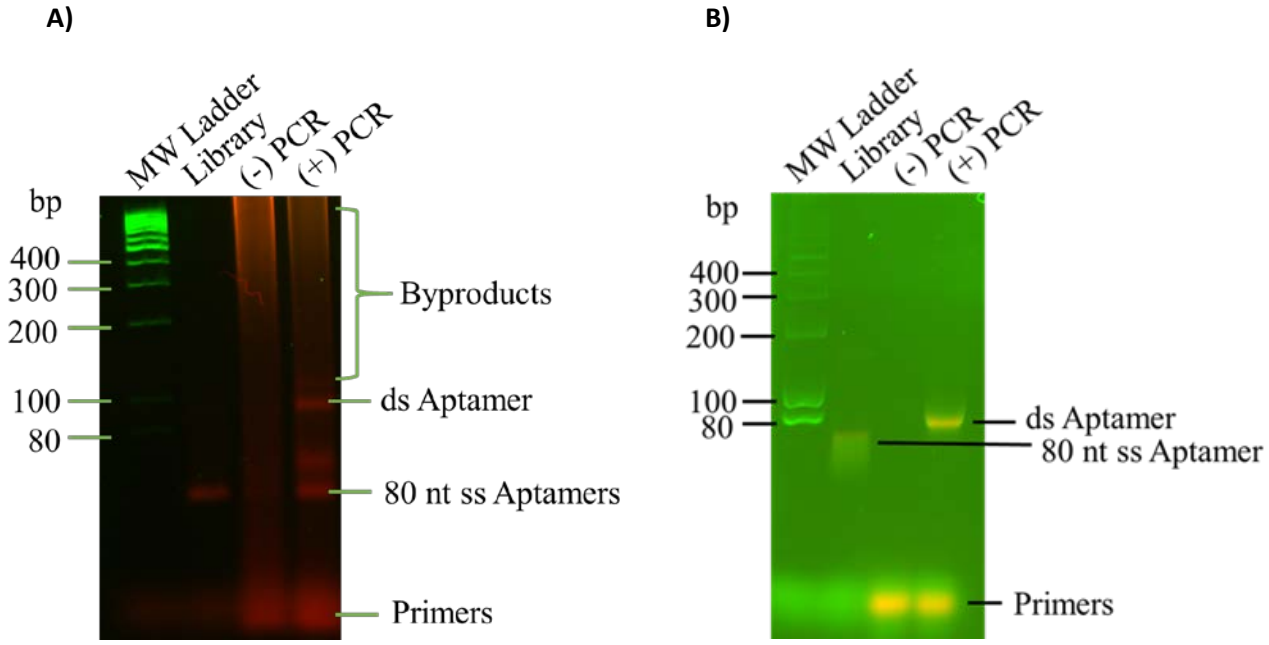

Figure 7. Optimization results for number of PCR cycles. All samples were symmetrically amplified with phire II polymerase and loaded onto 4% agarose gel electrophoresis, which was carried out at 150V for 45 minutes in 0.5X TBE buffer. Low range molecular weight DNA ladder was loaded to determine the molecular weights for some of the bands in the gel. 100 nM aptamer library with length 80 nucleotides was also loaded and used to identify the ssDNA aptamer bands. The negative PCR control was an amplification of the PCR reaction mixture with no DNA template. The positive PCR control amplified 100 pM library as the DNA template. The band intensities were analyzed with Alphaview software and are indicative of the aptamer yields for each round. **A)** Amplification with 30 cycles of PCR. There was background amplification present in the negative PCR lane, and the positive lane also contained nonspecific byproducts. There was ssDNA present in the positive lane even after symmetric amplification, which was approximately 57% more intense than the aptamer library, while the dsDNA aptamer band was 40% more intense. **B)** Amplification with 15 cycles of PCR. No background amplification in negative lane or byproducts in positive PCR lane. The positive PCR lane contained only a dsDNA aptamer band which was 230% more intense than the aptamer library. Therefore, background amplification was eliminated and a higher aptamer yield was achieved by reducing PCR cycles from 30 to 15.

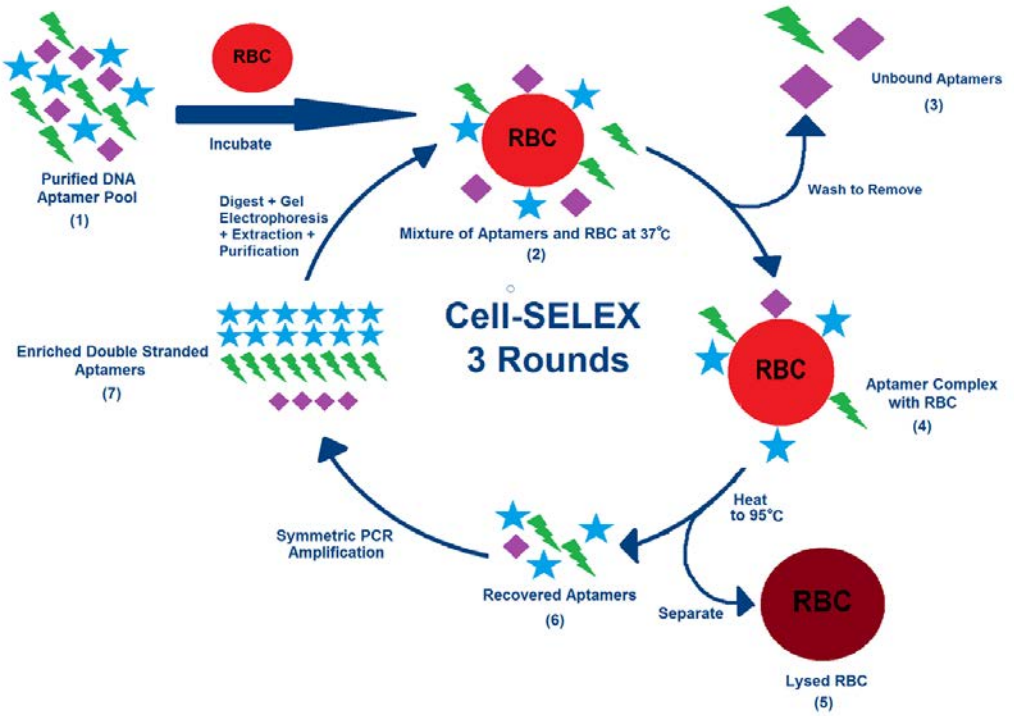

Figure 8. Schematic diagram of modified and optimized cell-SELEX procedure used to develop aptamers binding to RBC at room temperature and 37°C. A pool of DNA aptamers with known binding to RBC at room temperature was used to begin the cell-SELEX procedure and was purified before incubation with the RBC at 37°C for one hour. Phosphate buffer saline (PBS) buffer was used during incubation, as it mimics the salinity and pH levels of physiological conditions, since salinity and pH are also important factors for aptamer binding. The aptamers that did not bind were removed by washing them away, so that only bound aptamers remained. The cells were then heated to 95°C to lyse the cells, and centrifugation allowed the supernatant containing the bound aptamers to be removed. This aptamer pool was enriched by symmetric PCR for 15 cycles with phire II polymerase. Since aptamers need to be single stranded, this double stranded aptamer pool was subjected to exonuclease digestion to result in only single stranded aptamers. The aptamers were isolated by gel electrophoresis and purified by nucleospin column clean up to elute the DNA aptamers. This pool was then subjected to incubation again and the cycle was repeated. A total of 3 rounds of cell-SELEX were performed.

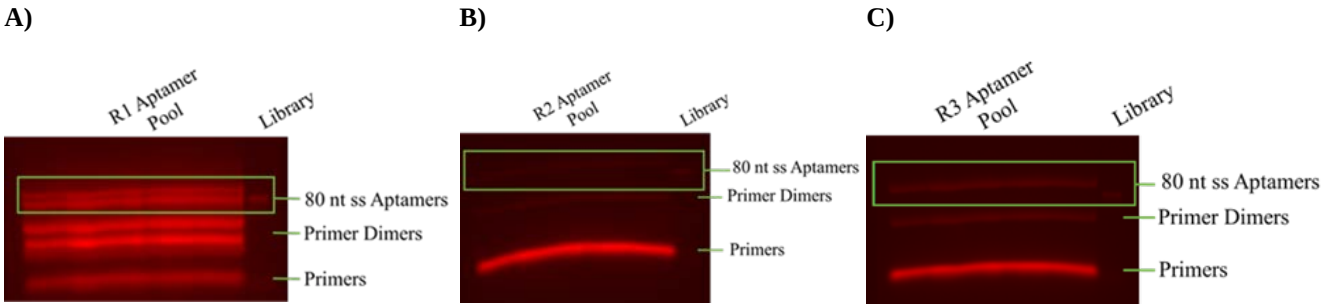

Figure 9. Post digest gel electrophoresis for rounds 1 to 3 of cell-SELEX. After incubation with RBC at 37°C for one hour, isolation and enrichment of the bound aptamers by 15 cycles of PCR amplification using phire II polymerase, and digestion with lambda exonuclease for 5 hours, the aptamer pools were run through 4% agarose gel electrophoresis for 45 min at 150 V in 0.5X TBE buffer. The 100 nM library was loaded against each aptamer pool to determine which band corresponded to the 80 nucleotide ssDNA aptamers (indicated by the green box). The band intensities were analyzed with Alphaview software and are indicative of the aptamer yields for each round. **A)** Post digest gel for round 1 (R1) aptamer pool. Two different populations of ssDNA aptamers that were 157% more intense than the 100 nM library were observed. **B)** Post digest gel for round 2 (R2) aptamer pool. A single population of ssDNA aptamer band with an intensity 27% less than the 100 nM library was observed. **C)** Post digest gel for round 3 (R3) aptamer pool. A single population of ssDNA aptamer band with an intensity 84% higher than the 100 nM library was observed. The ssDNA aptamers from each gel were extracted and purified before analysis with flow cytometry.

A)

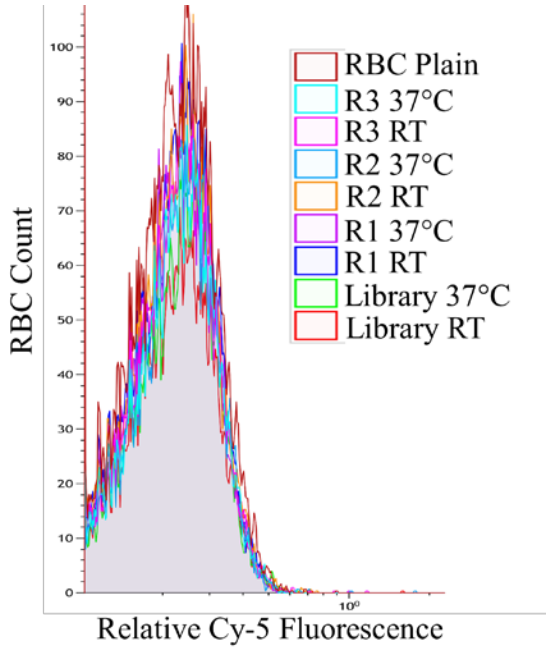

B)

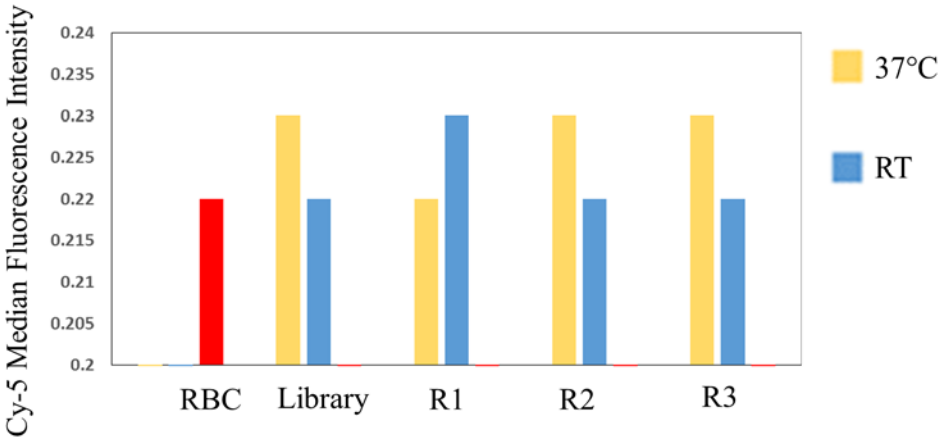

Figure 10. Flow cytometry results for binding affinities of the aptamer pools from rounds 1 to 3 and negative controls. The aptamer pool from each round and the aptamer library were diluted to 2.06 nM and split into two sets, where one set was incubated with RBC at room temperature (RT) and another set incubated at 37°C for one hour. Plain RBC with no Cy-5 labelling were used as a negative control to account for autofluorescence. The aptamer library was also used as a negative control to represent randomized aptamer sequences. Each aptamer was labelled with a Cy-5 fluorophore, so binding of the aptamers to the RBC can be verified by checking the Cy-5 emission. Better binding affinity is indicated by a shift of the emission to the right and is related to a higher fluorescence emission **A)** Cy-5 emission distribution for the aptamer pools and negative controls. Most of the samples had overlapping Cy-5 emission distributions. **B)** Cy-5 median fluorescence values for each sample represented by a bar graph. Round 1 (R1) had a higher binding affinity at RT by 0.01 relative fluorescence units. Round 2 (R2) and round 3 (R3) had a higher propensity to bind at 37°C by 0.01 relative fluorescence units compared to at RT. The binding affinities for R2 and R3 at both temperatures overlapped with the binding affinities from the library samples.

Battery-Powered Real-Time PCR Machine

Abstract— The quantitative Polymerase Chain Reaction (qPCR) is a key medical tool for diagnosing and monitoring viral infections. Due to the high cost and immobility of large scale qPCR machines, it is not viable for remote and resource limited areas. In this work, a solution is proposed that uses widely available technology found in mobile phones and tablet computers, integrated with an affordable battery powered thermal cycler, to effectively run real-time PCR reactions. The demonstrated prototype performs 2-step and 3-step PCR reactions, and fluorescence is measured in real time using a tablet-integrated camera.

I. Problem Statement

The polymerase chain reaction (PCR) is used widely in biology and medicine for the many-fold, region-specific replication of DNA, including applications in DNA cloning, gene expression, and clinical molecular diagnostics [1]. Quantitative PCR (qPCR) is especially valuable for diagnosis and monitoring of individual treatment response for chronic viral infections, such as HIV. Quantitation is achieved through the use of a fluorescent intercalating dye, where the concentration of double-stranded DNA can be assessed at each cycle. This fluorescence measurement typically requires sensitive detectors and expensive, calibrated optics as part of the instrument. While qPCR has become a near-ubiquitous diagnostic tool in large hospitals, as described above, these basic technical requirements typically yield bulky, complex, fragile, and expensive instruments that are infeasible for portable, remote, or resource-limited applications. A move toward low-cost optical detection and low-power thermal cycling is required to address these significant limitations of traditional qPCR instruments.

II. Proposed Solution

Previously published work has demonstrated portable qPCR instruments in both bench-top and hand-held formats, often leveraging microfluidic sample handling [2-3]. These systems typically employ discrete optical systems and require an external power source. Recent work has also demonstrated the ability to perform fluorescence quantification of PCR samples using the integrated optics of a mobile phone [4]. Such advances are critical demonstrations of the potential for truly portable, low-cost qPCR instrumentation.

The goal of this project is to leverage advanced technology available at low-cost in tablet computers and modern smart phones to provide imaging, control, and computation for a low-cost, self-contained qPCR system. By utilizing the processing power of a tablet this design reduces the other hardware requirements allowing for a lower cost system.

The core of a PCR instrument is a thermal cycler; it needs to be able to heat, cool, and hold samples at specific temperatures, typically in a range from 40-100ºC. At a high temperature (~95ºC), double-stranded DNA is melted, or denatured, into single-stranded DNA. At a lower temperature (40-50ºC), short DNA strands of known sequence can bind to the single-stranded DNA in a process termed annealing. This creates sites at which DNA polymerase, in the presence of free nucleotides, will copy the single-stranded DNA if held at the right temperature (70ºC). In a typical PCR reaction, these three steps are repeated for a total of 20-40 cycles, during which time a few copies of DNA can be amplified exponentially to produce more than a billion identical copies. Additionally, to monitor PCR in real time, there must also be a way to view the samples to collect data, and the samples must be optically isolated from each other in order to accurately measure fluorescence. As such, the primary components of a qPCR system include the thermal cycler, sample holder, optical measurement system, and system controller. These core functions are illustrated in the system block diagram shown in Figure 1, as well as the CAD rendering Figure 2.

III. Impact

A small, battery-powered, tablet-based qPCR machine solves two primary issues with conventional qPCR: the high cost and limited portability, driven primarily by fluorescent imaging optics. While a larger machine can handle more samples, a scaled-down system decrease power, cost, and weight, allowing remote and resource limited areas access to qPCR –

applications that may not require a large number of samples. Additionally, a custom Android app utilizes the processing power of a tablet computer to perform complex data analysis, such that a separate laptop or desktop computer is not required. The app also simplifies user interfacing, reducing the technical knowledge required to collect data and perform analysis. The current prototype outputs raw data in the form of a graph and a text file. Future developments could also provide the user with pre-calculated results, such as the initial amount of DNA in a given sample. While power is still required to charge the instrument, the option to run on battery power also makes the instrument useful in portable applications, or in areas with unreliable or intermittent power.

IV. Project Development

The instrument development can be broken down into the system blocks outlined in Figure 1. We summarize the development of each of these system components:

Thermoelectric Heating and Cooling

The core of the thermal cycler design revolves around a Peltier junction device, used as a thermoelectric heater and cooler. This device is compressed between a heat sink and a machined aluminum block designed to hold samples as well as a thermistor. The Peltier junction creates a temperature differential between its two sides, up to a 68ºC difference. The heatsink acts as a reference point for the temperature difference. The Peltier junction's temperature polarity switches depending on the direction that current flows through it; current in one direction causes heating, current in the opposite direction causes cooling. This is utilized by driving with an H-bridge circuit, similar to standard motor controller.

Embedded Control and Data Acquisition Electronics

Temperature control, thermal cycling, laser toggling, and internal data are managed by a Teensy 2.0 development board with an Atmel ATMega32 microcontroller. This device communicates to the tablet wirelessly via Bluetooth using a HC-05 RS232 Bluetooth module. Before starting a PCR run, the microcontroller receives the cycle number, phase duration, and temperature settings from the tablet. It then manages thermal cycling based on these settings while outputting up-to-date information about current temperature and cycle conditions.

Closed-loop Temperature Controller

A NTC thermistor is used to measure the instantaneous sample temperature. The thermistor is placed in a sample capillary tube in the aluminum block to give an accurate estimate of the temperature of the samples. The microcontroller uses an onboard analog to digital converter (ADC) to read voltage values across the thermistor. With a resolution of 8 bits, this ADC offers sufficient precision for a maximum margin of error of 1 ºC. The microcontroller then drives the thermoelectric cooler to either heat or cool until the thermistor reaches the desired temperature, where it holds for the specified time. This provides closed-loop temperature control. Every 150ms, the microcontroller reads the temperature value and sets the Peltier module to heat, cool, or idle via the H-bridge. This information, including cycle number, cycle phase (heating / cooling / holding), and current temperature is sent to the tablet via Bluetooth. Once per cycle, during the PCR extension phase, the laser is turned on to allow the tablet to image the samples.

Fluorescence Measurement Setup

The system is designed to perform real-time PCR on samples using standard intercalating dyes, such as SYBR Green and EvaGreen. For these dyes, viewing the contents of each sample requires illumination by light with a wavelength of just under 500 nm. LEDs and lasers were both considered for accomplishing this goal. In the end, lasers were used due to the higher concentration of light and the fact that LEDs would require additional filtering in this application. Even when an intercalating dye is emitting fluorescent light, the emission can be very difficult to detect in the presence of the large amount of blue excitation light produced by the laser. Thus, an optical high-pass filter is inserted on the enclosure between the phone camera and the sample holder.

Battery and Power Management

A lithium polymer (LiPo) battery is used to supply the high current and capacity demands required by the thermoelectric cooler. The battery capacity needed to run 30 cycles of PCR can be estimated by multiplying the average current draw (approximately 2A) by the time it takes to complete 30 cycles (3 hours.) Thus, a battery of at least 6Ah capacity is needed. To be safe, an 8Ah battery was used in the design. The demonstrated prototype uses a three cell battery capable of supplying 11.1V nominal.

Tablet Integration

The tablet communicates to the microcontroller through a custom Android application, which also takes pictures and analyzes images. In order to easily send and retrieve information from the microcontroller, the tablet is connected to the microcontroller via Bluetooth. Data and commands are exchanged by sending a system of flags between the tablet and a microcontroller. Most information is displayed to the user on the tablet screen as PCR is running. Initial settings are entered by the user on the tablet before PCR is started.

The samples are visible to the camera through small conical holes in the sample-holder. Once every cycle the microcontroller sends an indicator that the laser is being turned on. The app takes a picture of the samples through a filter

at the top of the enclosure. The app then uses an image processing algorithm that scans the three regions of the screen, which contain samples for green pixels. Depending on the amount of light above a preset threshold, each sample is assigned a fluorescence value for that cycle. Calculated values are graphed each cycle, making it easy for the user to identify positive and negative samples.

System Demonstration

The complete PCR system was tested to demonstrate closed-loop temperature control and thermal cycling, as well as the ability to perform real-time qPCR from both external power and battery power, though the data in figures 4 and 5 resulted from running the device from an external power supply. These experiments were conducted in parallel with a commercial thermal cycler to verify functionality. Individual experiments and results are described below.

Thermal Cycling

The core thermal cycler was characterized independently to show that heating, cooling, and holding function as design. For testing we used a three-phase run; each cycle reaches hold temperatures targeted at 40ºC, 70ºC, and 90ºC, with hold times of 30s, 30s and 90s, respectively. A typical measured temperature profile is shown in Figure 3. This was measured using a type K thermocouple installed in a glass capillary sample tube filled with mineral oil, and recorded with an external thermocouple reader.

A typical thirty-cycle run takes approximately three hours, with each cycle taking between five and six minutes. The hold temperatures typically show a variance of approximately 1ºC at 40ºC and 70ºC, with a variance of up to 2ºC at 90ºC. These precision values are comparable to a commercial PCR machine for the 40-70ºC range. However, it does take significantly longer to change temperatures when compared to a retail machine, especially in the cooling phase, as the Peltier is based on creating a temperature difference and as the heatsink heats up it becomes increasingly difficult to bring the samples down to 40ºC.

Real-Time PCR

While many PCR reactions employ three temperature steps for denaturation, annealing, and extension, in some cases a two-step process can be used in which the annealing and extension phases happen at the same temperature. For one two-step reaction template DNA from bacteriophage lambda was combined with primers and all PCR reagents, supplied as a bead-based mastermix (Edvotek). The commercially available primers target a 500bp region of the lambda genome and have a predicted annealing temperature of 71oC. This PCR reaction employed a denaturation step of 94oC and a combined annealing/extension step of 71oC, each for 30 seconds. A total of 20 two-step cycles were run. A total sample volume of 25µL per reaction was used, and the samples were run in real-time PCR capillary tubes (Roche). Positive and negative (no template control) samples were run in parallel, and real-time fluorescence data is shown in Figure 4.

A more typical three-step PCR reaction was run on DNA template using commercial primers design to anneal at 45ºC and targeting a 1000bp region. This PCR reaction employed a denaturation step of 94ºC, annealing at 45ºC, and extension at 72ºC, each for 45 seconds. A total of 30 three-step cycles were run. A total sample volume of 25µL per reaction was used, and the samples were run in real-time PCR capillary tubes (Roche). Positive and negative samples were run in parallel, and control reactions were also run at the same time on a commercial thermal cycler (Edvotek). Real-time fluorescence data is shown in Figure 5, and samples from the prototype thermal cycler and the commercial thermal cycler are shown in Figure 6 under UV illumination.

V. Conclusions

A prototype real-time PCR instrument was designed, built, and demonstrated that utilizes an Android tablet for system control and fluorescence imaging. The core thermal cycler was validated by direct temperature measurements, and real-time PCR was successfully demonstrated using both two-step and three-step reactions. This prototype serves as a proof-of-concept that the high performance imaging and computation capability of tablets and smartphones can be used to analyze, record, and display relative sample fluorescence. While qPCR has been traditionally limited to complex instruments, we have demonstrated that a low-cost, high-performance real-time PCR machine can be built by leveraging modern, consumer grade electronics.

References:

[1] T. Ishmael and Cristiana Stellato, “Principles and applications of polymerase chain reaction: basic science for the practicing physician,” Annals of Allergy, Asthma & Immunology, 101 (4), 2008, pp. 437-443

[2] P. Belgrader et al., “A Battery-Powered Notebook Thermal Cycler for Rapid Multiplex Real-Time PCR Analysis”, Analytical Chemistry 2001 73 (2), 286-289.

[3] C. Ahrberg et al., “Handheld real-time PCR device,” Lab Chip, 2016,16, 586-592.

[4] F. Walker, “Transformation of Personal Computers and Mobile Phones into Genetic Diagnostic Systems,” Anal. Chem., 2014, 86 (18), pp 9236–9241.

APPENDIX

Figures:

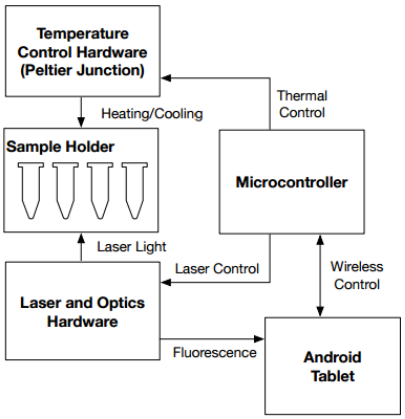

Figure 1: System block diagram of tablet-driven qPCR instrument. Shown are the core thermal cycler functionality, as well as fluorescence measurement using laser-based excitation and the tablet camera.

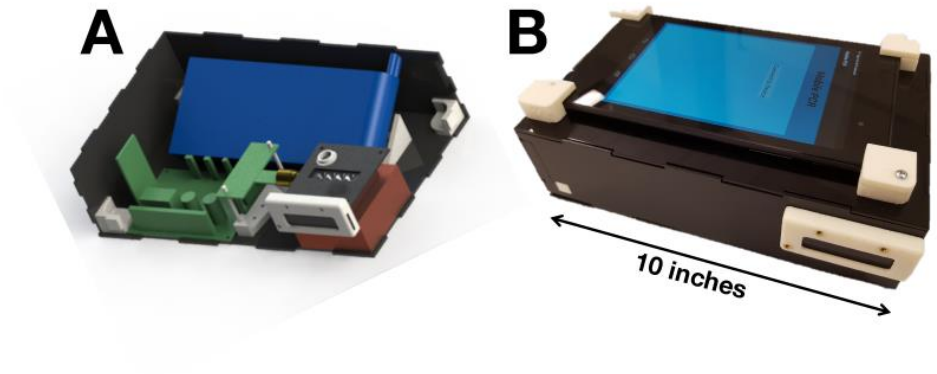

Figure 2: In (A), a 3D CAD rendering of thermal cycler's internal arrangement is shown. In (B), a photograph of the complete integrated system, including the tablet.

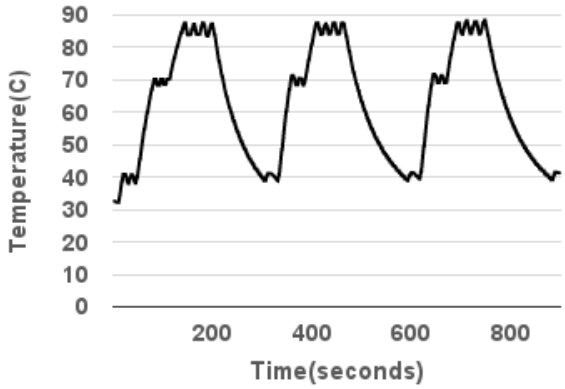

Figure 3: Plot of measured temperature data from inside the sample holder over several cycles, recorded using an external thermocouple reader.

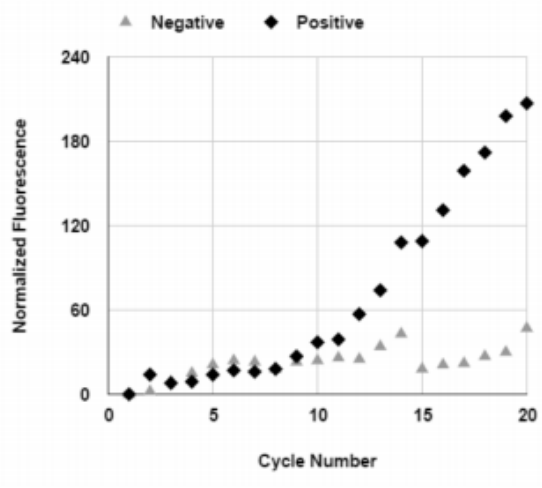

Figure 4: Real-time fluorescence data plotted for 20 cycles of 2-step PCR. A clear exponential region can be observed in the positive sample.

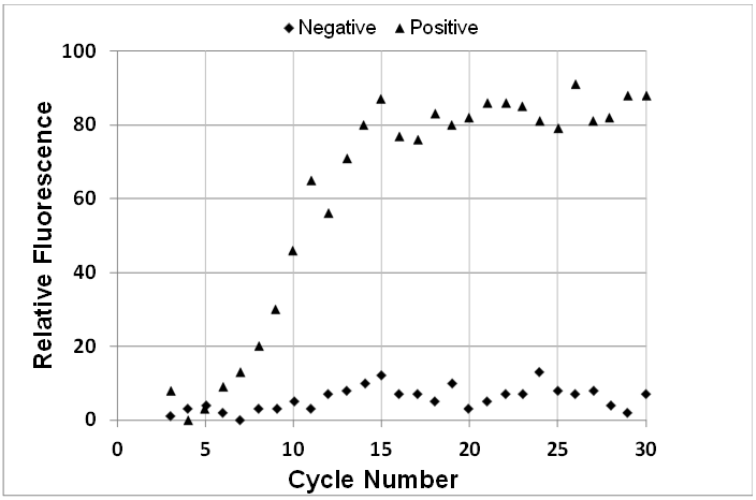

Figure 5: Real-time fluorescence data plotted for 30 cycles of 3-step PCR.

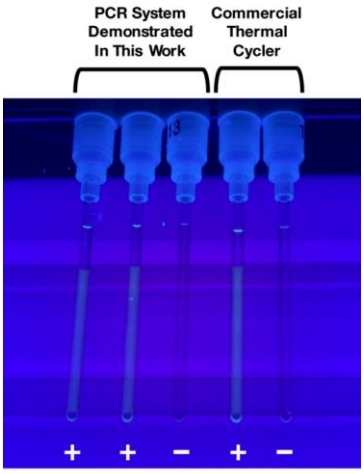

Figure 6: The photo above was captured after running 30 cycles in the mobile PCR system in parallel with an industrial PCR machine, backlit with a transilluminator.

IEEE Engineering in Medicine and Biology Society (**EMBS**) International Student Conference (**ISC**) 2016
Design Competition

Development of a Lifelike and Functional Passive Prosthetic Hand for Small Infants

[author information redacted for peer review process]

Abstract— For infants who have congenital upper limb absence, commercially available terminal devices focus on providing either functionality or cosmesis. A low-cost passive hand was developed to achieve both, using a 3D-printable thermoplastic elastomer reinforced with steel wires to allow independent positioning of the digits. The use of 3D printing allowed for rapid prototype iteration and ease of customization. The final prototype was validated through benchtop tests and a clinical pilot test. This design encourages early prosthesis use and enables infants to meet their developmental milestones by providing a lifelike and functional device that can be quickly and inexpensively customized.

I. PROBLEM STATEMENT

Children with congenital upper limb differences are born with one or both arms that terminate before the hand. A first prosthesis fitting is seen as valuable when the child begins to sit [1], which typically occurs at the age of 3-7 months [2]. At this stage, a passive prosthesis is used to support actions such as weight bearing and bilateral (two-handed) grasping, while stimulating hand-eye coordination [3]. In addition to promoting developmental milestones, an early first fitting helps to establish the habit of wearing the prosthesis at a young age, thereby helping to integrate the prosthesis with the child's motor development and body image. This promotes symmetrical muscular development and reduces the need for the intact limb to compensate, which in turn may reduce the risk of overuse injury later in life [3].

There are few solutions currently available for the first prosthesis fitting. One company, TRS Inc., offers a variety of products for children as young as 4-6 months (see Appendix, Figures 1a and 1b). These products have support for basic grasping and are soft, durable, and weight-bearing [4] but compromise cosmesis for functionality, especially at smaller sizes [5]. This trade-off is significant, as many parents place great emphasis on body image, symmetry, and appearance, and thus are much more willing to have their child use a prosthesis if it has a lifelike appearance. Another company, Otto Bock, offers a prosthetic hand for children as young as 6 months (see Appendix, Figure 1c). It mimics the natural hand both in texture and hand positioning more closely [6]. However, its relaxed, open hand position makes unilateral (one-handed) grasping more difficult [5]. These gaps in the existing market solutions leave space for a small-scale design that achieves a high level of cosmesis without sacrificing functional concerns of weight bearing as well as bilateral and unilateral grasping.

Based on the gaps identified above, the project addressed congenital transradial (below the elbow) amputations, including the wrist joint but excluding the forearm. The solution was to focus on creating a device of an appropriate size for a small 3- to 12-month-old infant that provides greater passive functionality than is currently available at that size; in particular, the device was needed to grasp objects and to support the child's weight. Objectives concerned improving the look and feel of the prosthesis while minimizing cost. These requirements were developed with the input of clinicians and researchers at *[redacted for peer review process]*.

II. PROPOSED SOLUTION

The final design consists of a 3D-printed unibody hand made of a flexible thermoplastic elastomer and reinforced with steel wire in each digit extending into the palm (see Appendix, Figure 2a). This design with separated fingers allows for each digit to be positioned individually and retain its shape, enabling a variety of palmar and bilateral grasping activities. A series of notches featured on the palmar side of the digits and palm (see Appendix, Figure 2b) control the bending arcs while distributing stresses in the printed material and metal wires. In addition, the high elasticity of the plastic allows spring-like bending under loading at the wrist, where a large notch has been placed on the dorsal side (see Appendix, Figure 2c), and gives the device a soft, fleshy texture while maintaining enough rigidity to support the infant's weight. The printed device is housed inside a cosmetic glove for improved appearance (see Appendix, Figure 3). The glove is a readily available, off-the-shelf component and is relatively low-cost and replaceable. Additionally, gloves can withstand tearing and abrasion, and can be washed with common household cleaning agents.

3D printing is a manufacturing method that lends itself well to this application. As the device is small and consists of unique geometry, it would be difficult to manufacture otherwise. Furthermore, due to the low incidence of the medical condition it seeks to remedy, the prosthesis would be manufactured in small quantities, and customization would be required for each instance. 3D printing, in combination with modelling software, allow for quick changes and replacement at this low volume and at a lower overall cost than sculpted or moulded products. The combination of modelling software and the additive manufacturing method also allow for precise control over the shape and location of the embedded wires and facilitate their insertion process. By contrast, conventional manufacturing methods require a greater initial capital, for example to create moulds and dies, making them unsuited to low-volume applications requiring customization.

III. IMPACT

The prosthesis design developed in this project will have a positive impact on the infants and their families. As the prosthesis is lifelike, parents will be more likely to adopt the use of a prosthesis early on, while the functionality of the design will allow the infants to develop their motor skills, such as bimanual grasping, and promote symmetrical development of their muscles and body. Additionally, the prosthesis will become part of the child's body image as they grow, encouraging them to continue using one later in life. As the design is simple and is manufactured using 3D printing, the device can be fabricated more quickly and cheaply than the currently available commercial solutions. This increased affordability makes the prosthesis more accessible to children and their families. The total material costs for the 3D-printed hand body are estimated to be less than $10, excluding labour costs. This low cost could allow for the prosthesis to be replaced frequently to match the child's size as it grows. However, the cosmetic glove is expensive, at approximately $200. Eliminating the need for a glove would significantly reduce the overall prosthesis cost.

Congenital upper limb absence affects approximately 1500 children (4 in 10,000) per year in the United States [7], which correlates to approximately 150 children per year affected in Canada. Since the occurrence of congenital upper limb absence is relatively infrequent, the private sector does not have a significant drive to improve their product offerings to tailor to this small market. It is therefore important that research, such as this project, is carried out to ensure that the needs of this population are met.

The development of the prosthesis in this project serves as a proof-of-concept for the use of 3D printing and flexible plastics in the prosthetics industry. 3D printing allows for the creation of unique geometry at small sizes and for ease of customizability for individuals, while maintaining low materials and manufacturing costs. Furthermore, flexible 3D-printable materials, which are relatively new on the market compared to traditional 3D-printed hard plastics, increase the potential for this manufacturing process to be applied to prosthetics: the higher elasticity and lower hardness of the flexible materials provide more lifelike texture and movement than conventional hard plastics.

IV. PROJECT DEVELOPMENT

1. Research and Conceptual Design Phase

Research began with detailed benchmarking of existing commercial solutions, including TRS and Otto Bock prosthetic infant hands. Next, silicone and other moulding materials were investigated as well as possible flexible materials that could retain their shape. Materials were evaluated based on the suitability of their material properties for this application, their manufacturing complexity, and related cost. Mechanisms for passive finger and wrist actuation were considered against their design and manufacturing complexity, and their ability to withstand the loading conditions a typical infant hand could expect during daily activities. Finally, applicable testing standards and safety regulations were researched to validate the final design's safety and durability.

The design process then started with the generation of potential solutions, which yielded a shortlist of conceptual designs and associated materials. Rough partial prototypes of the shortlisted solutions were generated to compare the design concepts through preliminary testing of mechanical properties and estimation of manufacturing complexity and cost. Based on these tests and analyses, the best design and corresponding materials were selected for prototyping.

2. Iterative Prototyping and Benchtop Testing Phase

Multiple improved prototype versions were generated with cycles of feedback from the clinicians and researchers at *[redacted for peer review process]*. This feedback included preliminary qualitative evaluations of the printed prototypes for stiffness, durability, and cosmesis. Performance was also evaluated in simulated grasping of toys and in weight-bearing activities.

Satisfactory prototypes were subjected to mechanical benchtop tests to ensure functionality and safety. The prototype design had to successfully pass the worst-case scenario defined for each test. The details and results for each test are detailed in Table 1 in the Appendix. The prototype was examined after each of the tests for failure in terms of permanent deformation of the plastic body, breaks in the inner metal wires observed as loss of bending functionality or punctures through the plastic material, and signs of stress in the epoxy at the wrist such as cracking, discoloration, and debonding. Numerical modeling was not performed as prototypes could be iterated quickly and inexpensively, allowing experimental data to be captured in realistic usage conditions as frequently as any design changes were made.

3. Clinical Pilot Trial Phase

Once the final prototype was tested and proven to be safe, it was provided to an infant and their family to test the design in its service environment. The planned test consisted of one controlled testing session at *[redacted for peer review process]* and one at-home evaluation period, now in progress, after which the family will provide feedback about their experience with the prototype in prolonged everyday usage. This clinical trial received research ethics approval by *[redacted for peer review process]*, and full informed consent was received from the family regarding their participation in the study and the publication of the results.

During the controlled testing session, the child was guided through a series of grasping and weight-bearing activities, which were all performed successfully. The parents indicated satisfaction with the functionality and cosmesis of the design, and noted that it bridged the gap between the Otto Bock and TRS offerings that their child had used previously. They also provided input regarding the design's ease of use and potential integration into their child's motor development. The qualitative data from this observed session was assessed to identify areas where the device may be improved. Further participant feedback about the performance of the prototype as well as information regarding its durability and ease of use will be incorporated into the design after the at-home trial is completed.

V. CONCLUSIONS

Through close collaboration with clinicians, this project generated a design that fills a clear gap in the pediatric prosthetics market by balancing prosthesis functionality and cosmesis at a small size and low cost. In addition, the initial observations from the ongoing clinical pilot trial with a patient indicate that the design meets the physical needs of children of the target age and size, and parental feedback suggests that the design satisfies their desire for cosmesis and represents an improvement over commercial solutions currently in use. The results of this project will be valuable to children with congenital upper limb absence in their development of motor skills and body symmetry from an early age. In addition to improving on existing prosthesis designs, this project presents an innovation in prosthesis manufacturing by implementing a novel, flexible-material 3D printing process to achieve a fully customizable, low-cost solution.

REFERENCES

[1] J. Shaperman, S. Landsberger and Y. Setoguchi, 'Early Upper Limb Prosthesis Fitting: When and What Do We Fit - Journal of Prosthetics and Orthotics', American Academy of Orthotists & Prosthetists, 2003. [Online]. Available: http://www.oandp.org/jpo/library/2003_01_011.asp. [Accessed 23 Sep 2015].

[2] D. Smith, 'inMotion: Congenital Limb Deficiencies and Acquired Amputations in Childhood, Part 2', Amputee-coalition.org, 2006. [Online]. Available: http://www.amputee-coalition.org/inmotion/mar_apr_06/congenital_part2.html. [Accessed 23 Sep 2015].

[3] M. Fairley, 'Early Prosthetic Fit: Yes or No?', Oandp.com, 2008. [Online]. Available: http://www.oandp.com/articles/2008-04_12.asp. [Accessed 23 Sep 2015].

[4] 'TRS Product Catalog', TRS Inc., Boulder, CO, 2015, pp. 4-5. [Online]. Available: http://www.trsprosthetics.com/catalog-view/?lang=en. [Accessed 23 Sep 2015].

[5] *[redacted for peer review process as reference was an interview]*

[6] "Within Reach", no. 110, pp. 24, Summer 2009. [Online] Available: http://issuu.com/petren/docs/reach/23. [Accessed 23 Sep 2015].

[7] Centers for Disease Control and Prevention, "Facts about Upper and Lower Limb Reduction Defects," 28 October 2014. [Online]. Available: http://www.cdc.gov/ncbddd/birthdefects/ul-limbreductiondefects.html. [Accessed 1 Apr 2016].

[8] Otto Bock, "Physolino Babyhand", 2016. [Online]. Available: https://professionals.ottobockus.com/zb2b4ob/us01/en/USD/Prosthetics/Upper-Limb-Prosthetics/Cosmetic-Devices/Physo-Passive-Hands/Physolino-Babyhand/p/8K5. [Accessed 24 Mar 2016].

APPENDIX

(a) (b) (c)

Figure 1. Existing Commercial Solutions.
(a) TRS Infant 2 Hand [4]. (b) TRS Greek Series [4]. (c) Otto Bock Physiolino Silicone baby hand [8].

(a) (b) (c)

Figure 2. Final prosthesis design.
(a) Cut-out view showing wire channels in each digit (note that wires are on different planes).
(b) Palmar side of printed prosthesis showing notches in the fingers, thumb, and palm.
(c) Dorsal side of the printed prosthesis showing the wrist notch.

Figure 3. Final prosthesis design housed in cosmetic glove.

Table 1. Benchtop Tests and Results.

Test Applicable Standard	Related Prosthesis Function	Testing Procedure	Testing Results
Repeated Bending ASTM D747-10	Mimicking a child's palmar grasp Long term use, repeated grasping cycles over time	Original: Four-bar mechanism performing cantilever bending of fingers at 0.5 Hz until failure Revised: Manual finger flexion over full bending range	Original: Wires withstood approximately 200 bend cycles without failure; however, bend arc too short to be representative of expected usage, and machine could not produce consistent bending over extended periods Revised: Wires typically failed after 40-50 cycles, but did not protrude through plastic; failure determined safe for use in clinical pilot trial
Compression N/A	Bearing weight while crawling, sitting, pushing/pulling to stand	40 lbf of axial compressive force applied at bent wrist for 30 seconds then relaxed for 30 seconds, 20 cycles	No noticeable damage or permanent deformation
Impact ASTM D3332	Withstanding rough use, e.g., banging toys on surfaces	Drop from 10 m height, 10 iterations	No noticeable damage or permanent deformation
Tension ASTM D412, Government of Canada Toys Regulations SOR/2011-17	Withstanding rough use, e.g., child or pet pulling on fingers Structural integrity	20 lbf axial tensile force applied to fingers for 10 minutes	No noticeable damage or permanent deformation

IEEE Engineering in Medicine and Biology Society (**EMBS**) International Student Conference (**ISC**) 2016 **Design Competition**

AlertBuddy

Wearable Emergency Alerting Device for the Hearing Impaired

Abstract— Emergency alarms save lives. However, hearing impaired individuals may not be able to depend on existing solutions. Auditory alarms have almost no impact on the hearing impaired. While there are other means of warning such as bright flashing lights and special vibration devices, their potency can be seriously reduced in circumstances. Existing solutions are also bulky and require special installation. AlertBuddy offers a solution in the form of compact wearable assistive device. By using a microphone, embedded hardware and a mobile application it can reliably detect and alert the user of emergency alarms.

I. Problem Statement

The motivation of this project began with the inconveniences and disadvantages experienced by individuals with hearing loss when it comes to responding to audio alarms. Although over the years, alarm systems technology, society's understanding of hearing impairment, and safety legislations have progressed, there are still gaps to be filled and improvements to be made. There are unsolved problems regarding the feasibility of auditory alarm and sirens. Just by considering the effectiveness of the traditional fire alarm for a hearing impaired individual fast asleep in the middle of the night, it's not difficult to see that a solution is needed to overcome such problem. Fortunately, there have been continuous efforts in increasing the accessibility of alarming systems, either directly through adding both visual and physical components to the alarm, or indirectly through introducing a third medium such as an assistance dog or additional visual or vibration devices.

AlertBuddy provides a compact wearable assistive device that can be configured using a smartphone. It is a practical and beneficial solution that uses advanced technology available.

II. Proposed Solution

This project implements a wearable system consisting of a wearable wrist device and a mobile application running on a smartphone. The wrist device includes two embedded microphones and performs digital audio signal processing on the captured data in real-time. Using Bluetooth Low Energy technology, the wrist device sends the processed audio data to the mobile phone application for additional data processing. The mobile application executes a classification algorithm that utilizes neural networks to detect and identify an alarm sound based on the data received. In the event of an emergency sound, the mobile application sends data back to the wrist device where it will alert the user by vibrating and visually displaying the detected sound on the LCD screen.

Current solutions to alert the hearing impaired person of an emergency event are not sufficient because they are unable to visually capture the individual's attention. During the event of a police siren, the individual may be facing the wrong direction. Fire alarms in buildings will have flashing lights, but if the individual is in a room such as a bathroom that does not have these lights, they will not be alerted. Other existing solutions involve a vibrating bed or pillow for when the user is sleeping, but these products are not portable and useful only in one case. However, our wearable solution solves all of the issues previously mentioned. It is a small and portable device where the user can always wear and be alerted of emergency sounds.

III. Impact

This wearable system will benefit the hearing impaired by alerting them when an emergency alarm is detected around them. In addition to alerting the user, the wearable system also identifies the sound and visually displays on the wrist device and the mobile application. The system is customizable to allow users to select sounds that they want to be notified or alerted.

The current implementation of the system detects four types of selected emergency sounds which include police siren, smoke detector beeps, fire alarm and tornado sirens. What is currently implemented is a general way of recording a sound from a wrist device and running a detection algorithm on a smartphone. This can be extended to further detect more types of sounds, either predefined or customizable by the user. Furthermore, adding direction finding feature to detect the direction of the alarm sound could be a major improvement to the current design. It would be also possible to package the system as an "alarm sensor" so that it can be implemented on existing smart watches and wearable devices.

IV. Project Development

The wearable system is divided into four major subsystems: siren detection algorithm, wrist device hardware, wrist device firmware and mobile application.

Siren Detection Algorithm

The main goal of the algorithm is to analyze sounds and detect emergency sirens. The algorithm design and implementation includes two parts: training and detection. The purpose of training is to generate a model that will be later used for the detection. The model represents an artificial neural network, which is a mathematical representation that is inspired by biological neurons in the brain. To train the neural network, audio samples were collected to extract useful features using Mel-frequency Cepstral Coefficients (MFCC). The detection and classification part of the algorithm were implemented using Artificial Neural Networks (ANN) for pattern and sequence recognition.

Sample collection

The audio samples collected were pre-recorded audio files as well as extracted audio from video recordings of real events. The samples were separated into two groups: ones that include either of the four types of sirens, and ones that do not (the ambient group). Each sample was trimmed to length of 1 second and resampled at 8 kHz. Some of the samples were used for training while the rest were kept for testing.

Feature Extraction

MFCCs were used for feature extraction. As part of the MFCC extraction, the audio data was broken into frames to calculate the magnitude spectrum using discrete Fast Fourier Transform, followed by filtering and windowing. This is shown in Appendix VI. [1]

Neural Network Training

For training, 12 MFCC features were provided as inputs and also the expected outputs. After computing the outputs based on the current values, a training algorithm was applied to tune the weights by minimizing the error between the current value and expected value. The scaled conjugate gradient back propagation training algorithm was used.

Classification

The output model from training phase was used for classification. Features extracted from a single frame of audio data were passed as an input to the model which outputs the normalized values corresponding to each detection class. To classify a sample of audio data, these output values were summed for the number of frames selected. Then the maximum sum was used as an identifier of the classification.

Result

The current implementation of the siren detection algorithm was able to achieve an accuracy of 95% in detecting four types of emergency alarms. A neural network training confusion plot with five classes, one class for each type of sound and ambient noise class is attached in Appendix I.

Wrist Device Hardware

The wrist device is the core component of the wearable system that will notify users of emergency sounds. It features two embedded microphones to collect incoming sounds surrounding the user. The wrist device also includes a Bluetooth Low Energy (BLE) module to provide communication with the mobile phone while consuming low power. The device also has a LiPo battery cell for a rechargeable power source with a targeted battery life of 12 hours. The wrist device features a 1.44" LCD screen to display the alarm detected. The wrist device hardware design block diagram and prototype piictures are attached in Appendix II and III.

Wrist Device Firmware

The wrist device firmware is the software running on the hardware that processes recorded sound data and controls peripherals. It implements a graphical user interface, BLE communication interface, microphone interface, haptic interface and navigation switch interface. The wrist device firmware design block diagram is attached in Appendix IV.

Mobile Application

This mobile application communicates with the wrist device by using Bluetooth Low Energy technology to receive stream of raw audio data and then processes the data to detect and identify emergency sounds. The detected emergency sound is displayed on the application's home screen and the sound information is sent back to the wrist device for visual display and vibration notifications. The application also implements push notification feature to receive notifications when the app is not open or the phone is in sleep mode.

The siren detection algorithm is developed in MATLAB and implemented on the mobile application with the use of Java Native Interface (JNI). JNI defines a way for managed code written in Java programming language to interact with the native code written in C. The app runs the detection algorithm as a background service.

The mobile application screenshots are attached in Appendix V.

V. Conclusions

A system consisting of a wearable wrist device prototype and a mobile application was developed to detect emergency alarm sounds. The current implementation can identify four types of sounds with 95% accuracy.

This system provides the hearing impaired user with a smart and compact solutions for being notified of emergency alarms. It has a potential to save lives and improve the lifestyle of its users

VI. References

[1] S. N. C.-C. J. K. S. Chu, "Environmental Sound Recognition With Time Frequency Audio Features," *IEEE Trans. Audio, Speech, Lang. Process,* vol. 17, 2009.

APPENDIX

I. Siren detection algorithm test results.

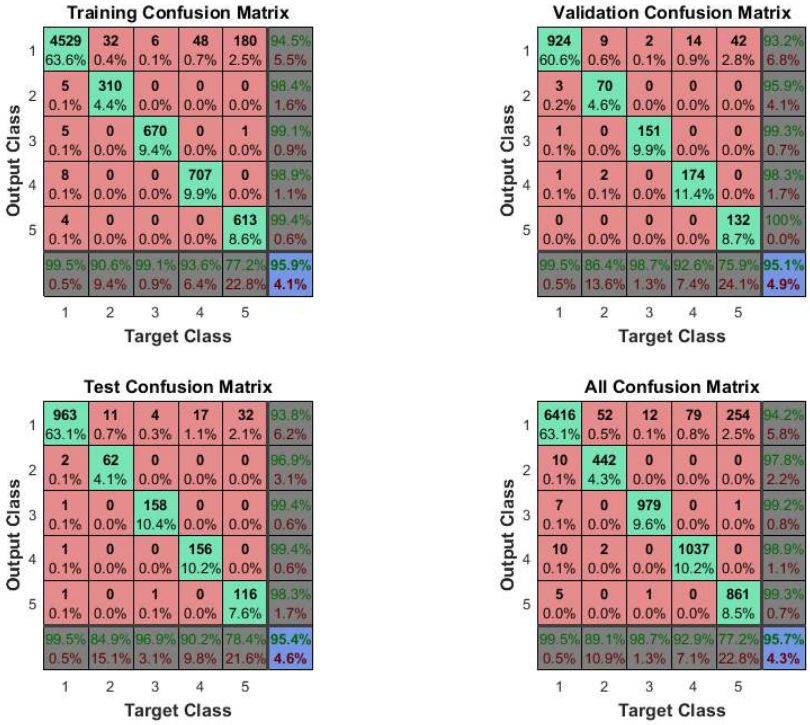

II. Wrist device hardware design block diagram

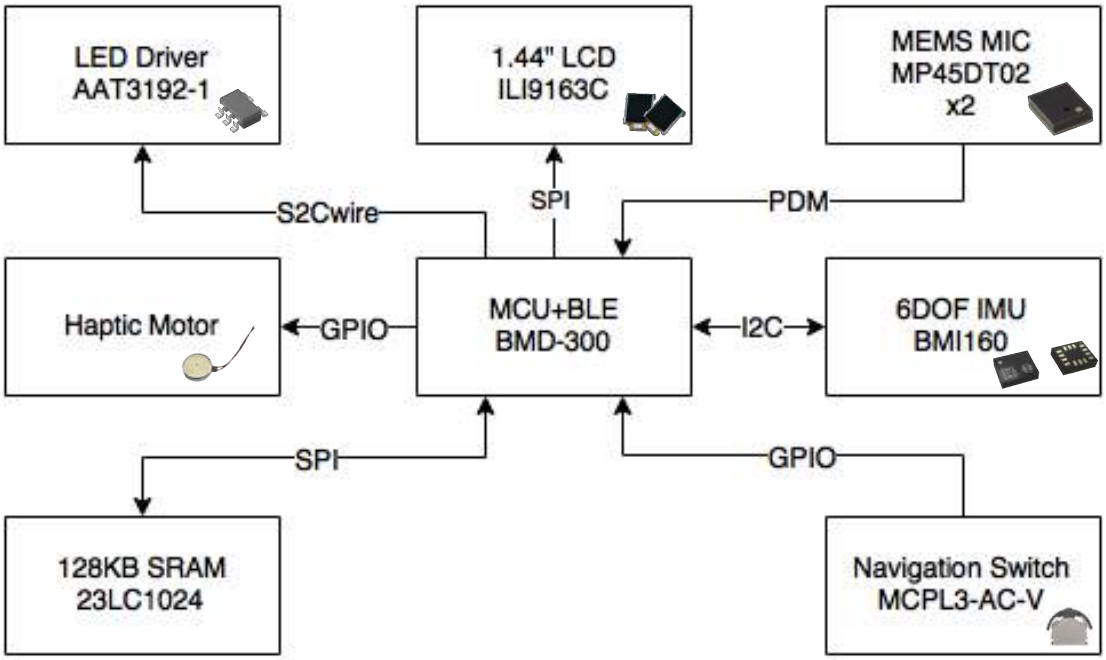

III. Wrist device hardware prototype

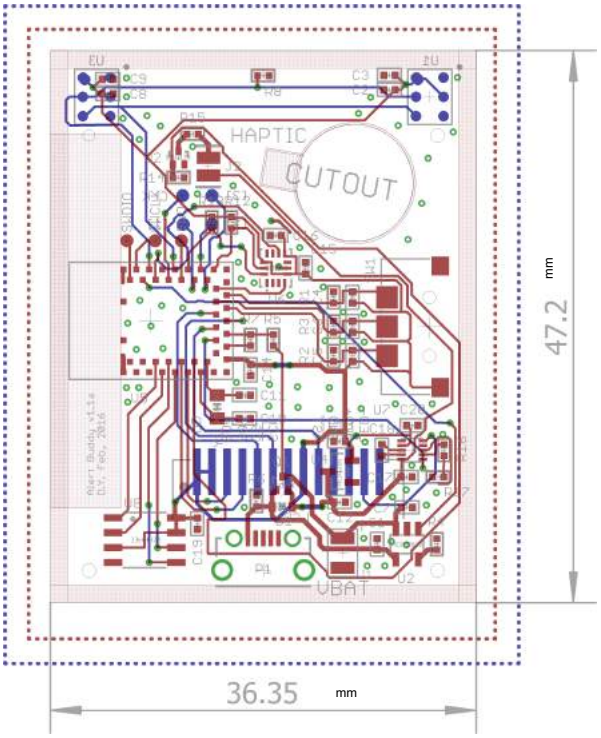

IV. Wrist device firmware design block diagram

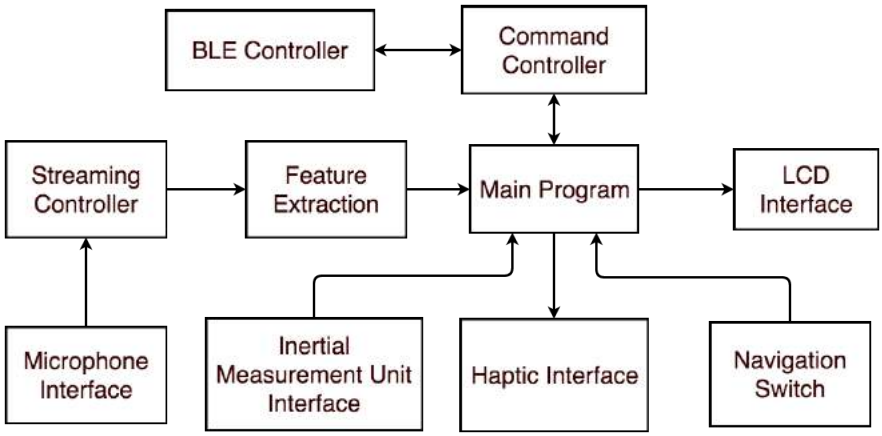

V. Mobile application screens

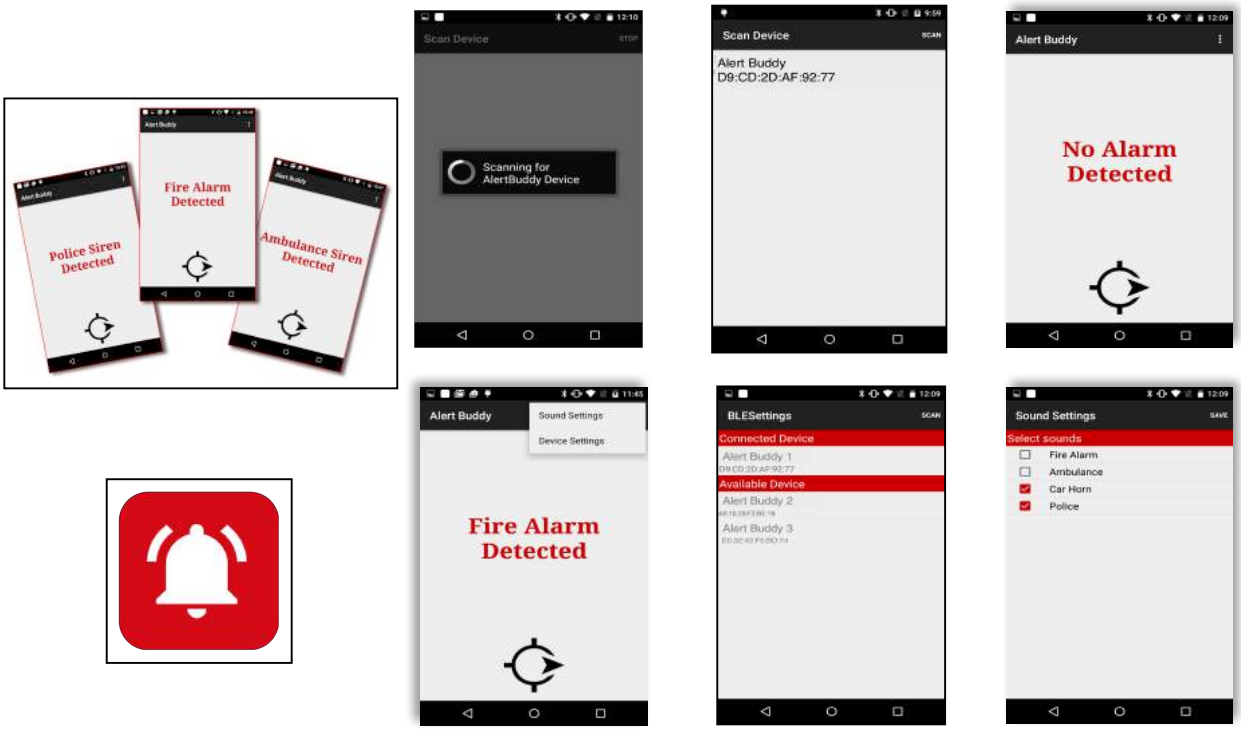

VI. MFCC Feature extraction